Antibacterial strategies to tackle wound infections

Doctoral Dissertation
Doctoral Program in Bioengineering and Medical-Surgical Sciences (31st Cycle)

Antibacterial strategies to tackle wound infections

Patrícia Varela

* * * * * *

Supervisors
Prof. Gianluca Ciardelli, Supervisor
Dr. Jochen Salber (PhD,MD), Co-Supervisor

Doctoral Examination Referees:
Prof. Lia Rimondini, Università del Piemonte Orientale
Dr. Federico Vozzi, Istituto di Fisiologica Clinica - CNR

Politecnico di Torino

April, 2019

I hereby declare that, the contents and organisation of this dissertation constitute my own original work and does not compromise in any way the rights of third parties, including those relating to the security of personal data.

…….....
Patrícia Varela
Turin, April 2019

Summary

Chronic wounds are a serious problem worldwide directly correlated with the growth of obesity and diabetes cases, and the increase of life expectancy. The major part of these wounds is infected by pathogenic bacteria. These infections associated with the perpetual inflammatory environment on the wound might become life-threatening since currently-used treatments with conventional antibiotics are failing. The usual reasons for treatment failure are related to the evolution of mechanisms of antibiotic resistance in bacteria and the formation of biofilm structures on the biotic surface, augmenting their tolerance against the antibiotic activity. Hence, drug-free antimicrobial wound products are urgently required.

For the first section of the experimental work, antimicrobial and immunomodulation properties of clinically-applied biomaterials were explored. This preparatory work allowed to understand the insufficiently explored macrophage-biomaterial interactions. Additionally, it permitted a finer selection of the bacterial strains and eukaryotic cell lines related to chronic wounds for the subsequent part of the laboratory experiments. In this second section, an extensive investigation of new antibiotic-free antibacterial polymers was performed based on polyurethane antimicrobial-peptide biomimetics.

In the wound care market, silver-containing dressings are the most commonly developed antibiotic-free antibacterial materials. Hence, for the first section of the experimental work, in chapter 2, antimicrobial, cytocompatibility and macrophage immunomodulation studies were performed with different silver-based products: Atrauman® Ag, Biatain® Alginate Ag and PolyMem WIC Silver® Non-adhesive. Biatain® Alginate Ag and PolyMem WIC Silver® Non-adhesive induced an excellent antibacterial effect in broth dilution assays. All the dressings stimulated a macrophage response in 24 hours. M0 macrophages' common response to all silver-impregnated dressings was to increase the production of the anti-inflammatory cytokine TGF-β which indicates a polarization towards tissue-healing M2-like macrophages, as it is desired in a chronic wound.

For the second section of the laboratory results, in the investigation of the antibacterial susceptibility and biological safety of antimicrobial peptide-biomimetic polyurethanes, the most promising candidate for overcoming Gram-positive bacteria known to infect wounds was selected (chapter 3) and its mechanism of action was examined (chapter 4). The chosen antimicrobial polyurethane, named NHP407-g-Poly(ILM-Br), showed rapid bactericidal capacity and prevention of biofilm formation against sensitive and drug-resistant Gram-positive

Staphylococcus aureus, *Staphylococcus epidermidis* and *Enterococcus faecalis* strains. Moreover, the determined selectivity index proved the polymer cytocompatibility on fibroblasts, keratinocytes and monocyte-derived macrophages. Through morphological characterization by scanning electron microscopy and a combination of 2D gel-based and liquid chromatography–mass spectrometry–based approaches it was possible to determine that NHP407-g-Poly(ILM-Br) is a bacterial membrane-active agent, like most of antimicrobial peptides. The newly developed antimicrobial peptide-biomimetic polyurethane NHP407-g-Poly(ILM-Br) is a very promising candidate to treat sensitive and drug-resistant Gram-positive bacteria infected wounds by mimicking the antimicrobial peptides' most common mode of action.

Acknowledgments

The present work would not be complete without the support of many people; hence I would like to start by expressing my deep gratitude to everyone that contributed to my PhD thesis project by professional and/or emotional support.

I would like to acknowledge my supervisor prof. Gianluca Ciardelli for his approachability and availability in all matters. Also, I want to express my gratitude for your unconditional support throughout the project period and for the indispensable suggestions related to the thesis' work.

To my co-supervisor Dr. med Jochen Salber, *vielen Dank* for your motivational and scientific support. My genuine appreciation for the transmitted knowledge, the important guidance received, and trust shared.

To Susanna Sartori, my dear tutor, thank you so much for your help in all situations, your kindness and contribution for enriching my work.

Thank you very much to everyone involved in the HyMedPoly EU project, for the insightful knowledge shared in our meetings and fantastic teamwork environment. Especially I want to thank Sheila, Ayesha, Alex and Jem for all the fun moments in- and outside the laboratory, shared support and friendship. As well to Subha, I learn a lot by working closely with you, thank you for all the brainstorm moments, help provided and companionship.

Many thanks to Prof. Elia Ranzato, Prof. Letizia Fracchia, Prof. Dr. med. Sören Gatermann, Prof. Dr. med. Albrecht Bufe, Prof. Julia Bandow, Dr. Inge Schmitz, Prof. Dr. Jürgen Groll for receiving me with arms wide open and letting me work in your laboratory facilities. It was a pleasure to collaborate with you and everyone in your research groups with a special thanks to Dr. Simona Martinotti, Dr. Chiara Ceresa, Ilaria Sciascia, Dr. Lennart Marlinghaus, Dr. Marcus Peters, Pascal Prochnow, Melissa Vazquez and Dr. Phillip Stahlhut for all the guidance and nice moments to remember in the laboratory.

To all my close friends, the old and the new ones gained during these three years of PhD, I want to express my gratitude for your presence in the ups and downs of the project.

To my boyfriend Jason, my partner in doing everything and nothing, I am grateful for having you in my life. Thank you for being on my side during the thesis journey and for helping me to improve it.

Finally, I want to dedicate this thesis to my mother, father and brother. Although you were far away, you gave me encouragement and love every day.

“The truth, however ugly in itself,
is always curious and beautiful
to seekers after it.”
Agatha Christie

Contents

List of tables

List of figures

Thesis goal and outline

The scope of this dissertation is to investigate unmet needs in the treatment of infection in chronic wounds, by testing the efficacy of medical devices currently used in the field and by characterising a new class of therapeutic polyurethanes under development. The outline of the present work is described on the following scheme:

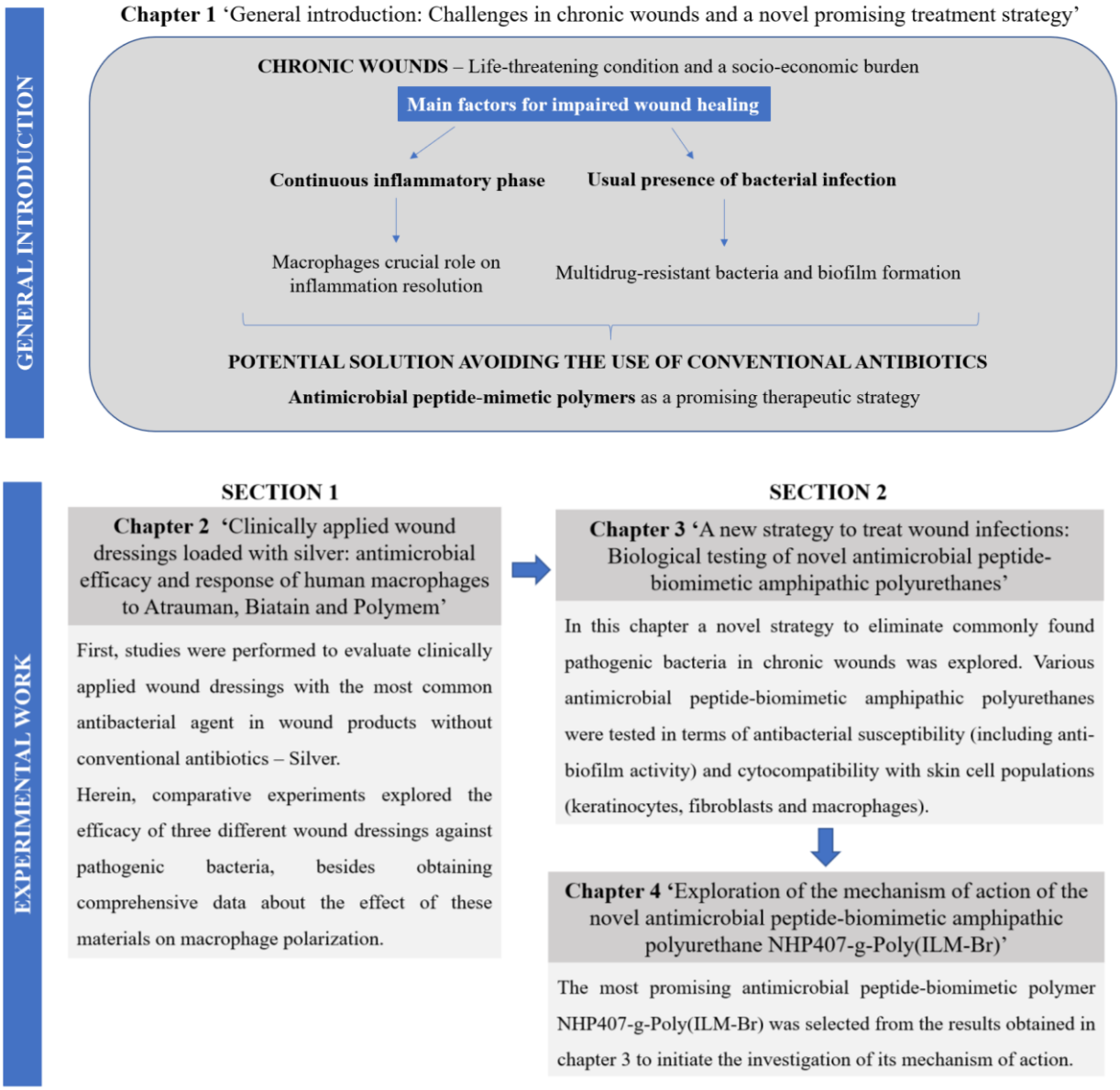

CHAPTER ONE

‘General introduction: Challenges in chronic wounds and a promising novel treatment strategy’

1.1. Chronic wounds: A brief introductory description

The complex wound healing process involves numerous populations of cells such as endothelial cells, keratinocytes, fibroblasts, neutrophils, T-lymphocytes and macrophages. Its progression, in which several processes occur simultaneously in an orderly sequence of events, is strictly regulated (1). As a consequence of an unusual progression, a chronic wound possibly will result, becoming a significant cause of morbidity and threatening the patient's quality of life. In addition, it impacts the healthcare system with high economic expenses (2). Generally, the common characteristics shared by each type of chronic wounds are: persistent excessive inflammation environment, presence of infectious microorganisms (as planktonic or sessile living), and possible existence of antibiotic-resistant pathogenic species on the wound (3,4). Collectively, these features impede the ability of dermal and epidermal cells to respond to reparative stimuli (5).

Recently a great deal of research has been directed to understand the factors that influence the healing progress, highlighting the extremely important role of macrophages. The research of clinically-applied and newly-developed antibiotic-free advanced biomedical polymers, able to play an active role in wound healing particularly by inducing antimicrobial effects, is possibly leading to an ideal therapeutic solution.

1.1.1. The never-ending torment of chronic wounds

Skin is the largest human organ that serves as our first protective barrier against any external factors and prevents excessive aqueous liquid loss. Following an injury, the skin needs to re-establish its functional capability, structural organization and restore equilibrium (homeostasis) (6). A wound is mainly characterized by modification of cells physical organization with or without destroying them. Consequently, its normal function is impaired or inhibited, whether it is part of a superficial layer such as epidermis/dermis of skin, or transitional epithelium (e.g. mucous membrane), or deep in tissue (7). Generally, cutaneous wounds can generate from a physical damage, such as mechanical trauma or thermal influences; chemical injuries caused by acids or alkaline solutions; physiological disorders or medical procedures. One common way wounds can be classified is by their duration of healing time (8). Acute wounds appear as a result of a surgical intervention, trauma or burn and heal following the phases of wound healing, in a strictly chronological order. When a wound is unsuccessful in initiating its regeneration phase after 2 to 3 weeks, and the cutaneous tissue does not recover its physiological, functional

and structural integrity within three months, it is categorized as a non-healing chronic wound (9).

Non-healing wounds are of diverse aetiologies. They are a predominant global health disorder owing to the subsequent morbidity and eventually mortality in suffering patients. Due to the magnitude of the deep impact of chronic wounds in our society, they have been portrayed as a 'silent epidemic' (10). Common examples are the diabetic foot ulcers (**figure 1.1A**), the venous leg ulcers (**figure 1.1B**) and the pressure ulcers (**figure 1.1C**) (2,9).

Figure 1.1. Representative images of the morphological aspect of chronic wounds on patients with (A) medial view of the right foot of colonized diabetic foot ulcer at the heel, (B) medial view of the dexter lower leg of an infected venous leg ulcer and (C) right ischium with a colonized pressure ulcer (2).

1.1.2. A global socio-economic burden caused by non-healing wounds

Epidemiological analyses concerning parameters related to chronic wounds are insufficient affecting the determination of the accurate costs of wound management (2). Nonetheless, it is evident that the quantity of cases of chronic wounds is ascending alarmingly in countries with high standard of hygiene/medical care (11–13). This rise is directly correlated with the increase of obese and diabetic patients and the extension of life expectancy (2).

In European countries the two most critical cases appear to be leg and foot ulcers, which affect around 1-1.4 million and 0.5-1.3 million people each year (**figure 1.2**) (14). In fact, it has been registered that the European population prevalence of chronic wounds overall, counts approximately 2 million (15).

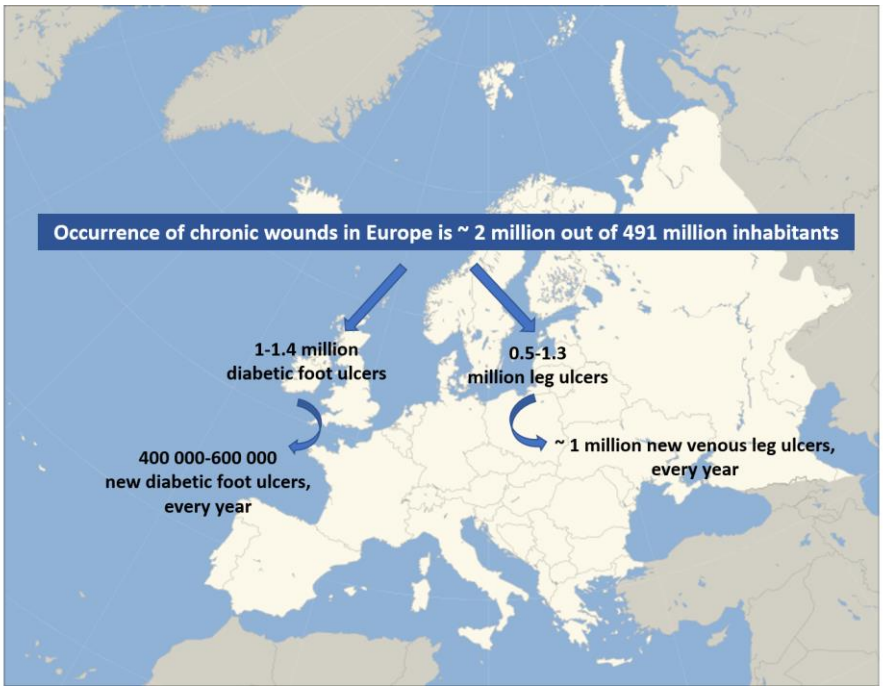

Figure 1.2. The cases of diabetic foot ulcers and leg ulcers - Annual prevalence and incidence estimation for non-healing chronic wounds in Europe. Adapted from information provided by Europe Advanced Wound Care Management (15).

Hence, the costs of prolonged and recurrent stays in the hospital, involving the consistent change of dressings and bandages, the usage of antibiotics and antiseptic products, and application of complementary advanced therapies, become a financial burden in addition to the costs of medical care provider staff involved throughout the entire procedure (9). The European Wound Management Association recently published a study in which it is reported that medical care of wounds corresponds to 2-4% of the total budget in health care (16). In Europe it was estimated that the average cost for foot ulcers is 10,000€ and 6,650€ for leg ulcers per episode. The report states, that these costs will dramatically increase if the pathophysiology of non-healing wounds will not be extensively explored and new effective therapies will not be developed (14,16).

1.2. Normal wound healing and factors that impede a proper wound remodelling

Wound healing is a complex regulated metabolic process that involves multiple cell populations. In chronological order, the four overlapping stages of normal wound healing are: haemostasis, inflammation, proliferation and remodelling (**figure 1.3**) (17,18). During

haemostasis - vasoconstriction, platelet aggregation, degranulation and fibrin production occurs. In the next stage, during the inflammation phase - neutrophils, lymphocytes and monocyte-derived macrophages infiltrate to the wound site (1). This is the phase in which any invading microorganism on the wound is eliminated (18). In overlap with inflammation, proliferation takes place, and re-epithelization, angiogenesis, collagen precursors molecules secretion and processing as a part of extracellular matrix (ECM) synthesis is observed. At last, remodelling is initiated and, during this final stage, collagen provides the matrix to sustain skin structure while vascular maturation takes place (1).

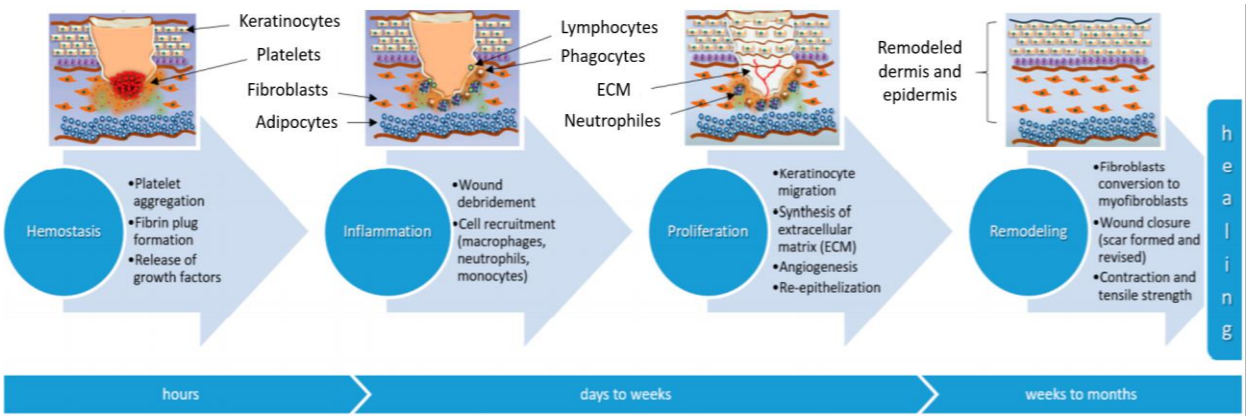

Figure 1.3. Main phases of normal wound healing and its functional processes (19).

In chronic wounds (**figure 1.4**), due to pathogenic/opportunistic infections and/or perpetual inflammatory phase, abnormalities on the complex coordinated normal wound repair occurs at least for four weeks up to several months (20). Throughout this period, fibroblasts have an abnormal morphology and a decreased proliferative capacity due to their lack of response to cytokines and growth factors that act as proliferative stimuli (21–23). Keratinocyte migration is also impacted, postponing epithelization (24). In addition, a delay on re-epithelization is caused by different cell populations at the wound site that overexpress matrix metalloproteinases (MMPs), such as matrix metalloproteinase-1 (MMP-1), inducing a continuous degradation of the ECM (25). On the other hand, synthesis of growth factors is decreased compared to the levels present in the healing of acute wounds, e.g. basic fibroblast growth factor (bFGF), vascular endothelial growth factor (VEGF) and platelet derived growth factor (PDGF) (26). In non-healing wounds, it has also been verified that the stage of angiogenesis is compromised. In fact, fibrin clots are present on the area of formation of blood vessels from the existing vasculature, blocking gas exchange preventing the formation of new vessels (27). Finally, the transition to the proliferation and remodelling stages is unsuccessful.

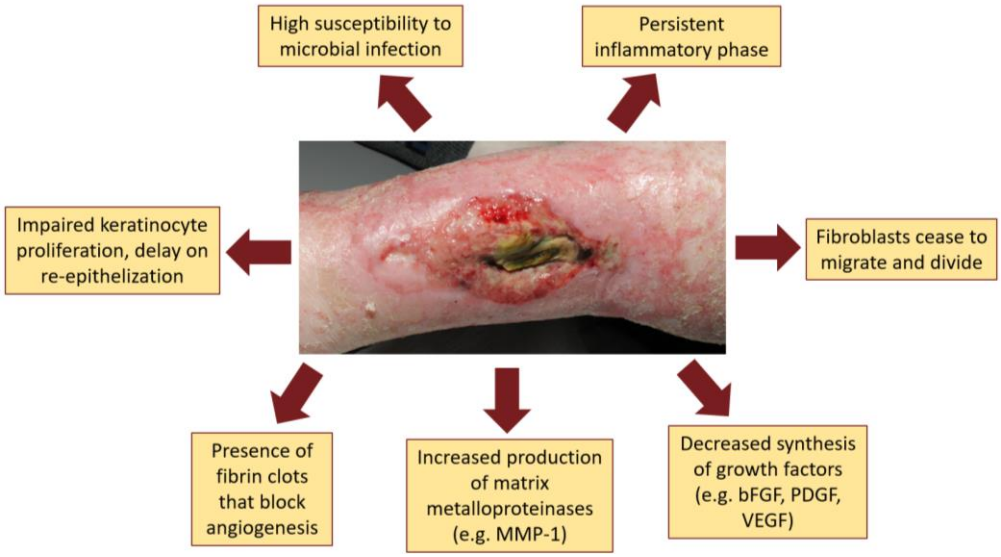

Figure 1.4. Susceptibility and dysregulated processes in the chronic wound environment (2). MMP-1, matrix metalloproteinase-1; bFGF, basic fibroblast growth factor; PDGF, platelet-derived growth factor; VEGF, vascular endothelial growth factor.

1.2.1. Bacterial infection

Chronic wounds are most frequently associated with an increased possibility of infection. These wounds are more vulnerable to microbial invasion due to their long-term loss of intact skin, that serves as a protective barrier (2). Presence of high bacterial contamination is one major cause of impaired wound healing (3). During the contamination phase, no major negative signals can be observed. Afterwards, bacterial pathogens start to proliferate, delaying wound healing and leading to a severe infection. At this stage, a continuous inflammatory environment is found in the wound (**figure 1.5**).

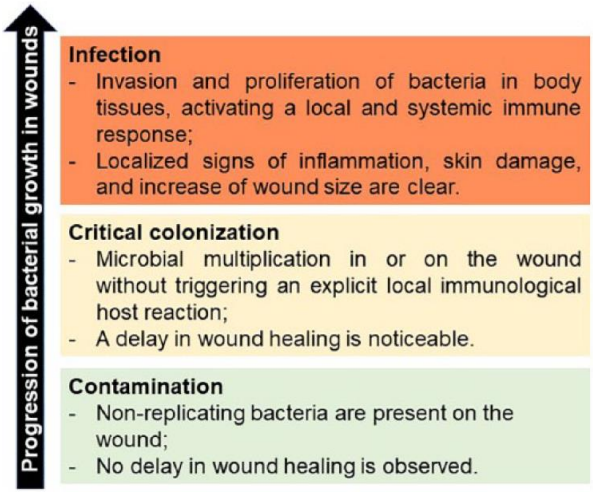

Figure 1.5. Development of bacterial growth on cutaneous wounds from contamination to infection (28).

The progression of bacterial growth in wounds is dependent on various factors. One of them is the intrinsic bacterial multiplication rate of the invading microorganisms (2). Additionally, the antimicrobial resistance (AMR) to current-clinically applied antibiotics plays an important role for the establishment of severe infection levels in chronic wounds. AMR can be found in open wounds, because the involved bacteria are already intrinsically resistant to certain antibiotics either structurally or through spontaneous mutation, or molecular mechanisms of resistance are acquired by interspecies crosstalk on the site of infection (e.g. horizontal gene transfer), providing beneficial survival skills to each other (29,30). Antibiotic resistance is a serious problem emerging worldwide (31). Its appearance is attributed to the overuse of currently-existing antibiotics, especially in inappropriate medical drug prescriptions and extensive agricultural use. In fact, there is a timeline link between the development of the antibiotic and the first reported outbreak of AMR discovery (**figure 1.6**) (32). Furthermore, the challenging pharmaceutical industry regulatory affairs are delaying the introduction of new drug developed therapies that could address the challenge of combating currently used antibiotics-resistant microorganisms (32).

The most frequently isolated bacterial species in chronic wounds is *Staphylococcus aureus*, followed by *Pseudomonas aeruginosa, Enterococcus spp.*, coagulase-negative staphylococci and anaerobic bacteria (33,34). These have been isolated from non-healing wounds as sensitive and drug-resistant variants. The Gram-positive methicillin-resistant *Staphylococcus aureus* (MRSA) species and vancomycin-resistant *Enterococcus* spp. (VRE), and the Gram-negative multidrug-resistant *Pseudomonas aeruginosa* were classified as serious threats by the center for disease control and prevention's (CDC) assessment report of current-antibacterial resistance threats due to the growing number of resistance development to many common antibiotics (35). Hence, in chronic wounds, rapidly emerging resistant bacteria is one of the main factors that contributes to the progression from a contamination to a severe infection.

Another factor that has been reported is the existence of bacteria in chronic wounds as structurally united cooperative communities. These communities are developed after microbial attachment on the biotic surface of the wound and are commonly defined as biofilms (**figure 1.7**) (36–38). The necrotic tissue and debris permit a facilitated bacterial attachment (38). In fact, more than ninety percent of chronic wounds contain biofilms which are generally polymicrobial in nature (5,39).

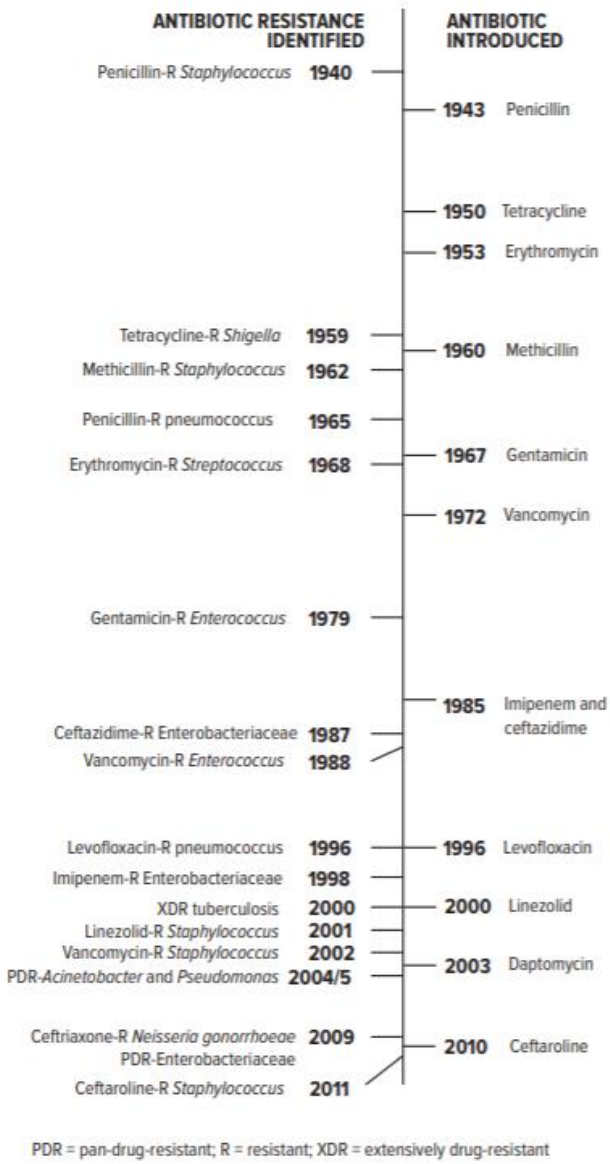

Figure 1.6. Timeline scheme of the introduction of a new antibiotic and early reports of microorganisms resistance in literature (40).

Biofilms are enclosed in a self-secreted extracellular polysaccharide matrix (EPS) (**figure 1.7**). EPS comprises plasmids, extracellular enzymes and signal molecules. The latter are used for communication among the bacteria (quorum sensing) (41). Blood components may also be found in the matrix of biofilms formed in a skin wound (42). Moreover, in these communities bacteria have a slower growth rate and the surrounding EPS matrix confers protection to bacteria against the immune system and antibiotics (42,43). Due to the restricted diffusion of the antimicrobial agents, together with the bacterial cells reduced metabolism, sessile bacterial forms within the biofilms are 10- to 1000-fold more tolerant to currently-used antibiotics than free planktonic bacteria (44).

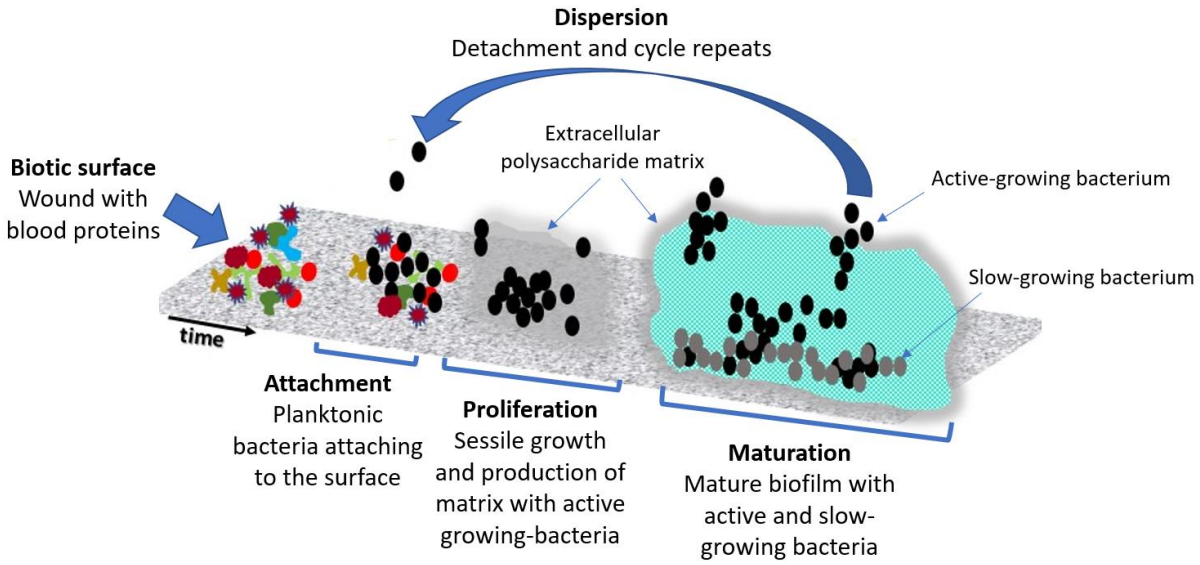

Figure 1.7. Development of biofilm formation and its main characteristics on a biotic surface (cutaneous wound). Adapted from (45).

In chronic wounds, including burns and venous/pressure ulcers, it is common to find overgranulation tissue, also recognized as hypergranulation tissue or proud flesh (46). This phenomenon is described as an excessive production of granulation tissue at the wound site beyond of what is required, overpassing the height of the wound surface resulting in an elevated tissue mass (47,48). This tissue makes the wound more vulnerable because it impedes wound healing through obstructing epithelization since it prevents the migration of cells transversely at the wound bed and surface (48,49). Dermal fibroblasts are key cells that deposit granulation tissue and produce huge amounts of extracellular matrix (ECM) (50). In non-healing wounds it is thought that these cells are unresponsive to inhibitory signal(s) arising from the keratinocytes at the basal layer of epidermis. Consequently, the process continues, leading to the hypergranulation effect (51). The disturbance of keratinocytes is associated with the presence of bacteria and/or prolonged pro-inflammatory environment. Furthermore, due to specific enzymatic activity, the wound's slightly basic pH also becomes favourable for bacterial establishment and growth (52).

Finally, a disturbance on triggering the innate immune response is advantageous for bacterial proliferation. For example, a failure of initiating the opsonization effect by an ineffective marking of pathogenic invading microorganisms with protein molecules, will affect the attraction of phagocytes (such as neutrophils and macrophages) to the location of contamination, and the successful recognition and subsequent removal of invading bacteria is hampered (43,53).

1.2.2. Perpetuation of inflammation

Inflammation is an initial key phase of the dynamic process of wound-closure. Eventually, the wound's transition to a tissue regeneration progression (correspondent to the proliferation and remodelling phases) is essential for a successful wound recovery (**figure 1.3**). During inflammation, the focus of recruited immune cell populations, such as neutrophils and macrophages is the removal of contaminating microbes (54). In the case of an incomplete microbial clearance or the activation of the immune response is compromised, more bacteria will attach and proliferate resulting in biofilm formation and a continuous immunological inflammatory process (1,2).

The overexpression of pro-inflammatory cytokines [e.g. interleukin-1 (IL-1) and interleukin-6 (IL-6)] and other signal molecules [e.g. nitric oxide synthase 2 (NOS2)] at the site of injury is directly interconnected to a disturbed innate immune response and to the presence of bacteria, creating a persistent inflammatory reaction (1,43). Dysregulated function of macrophages is the basis of alteration of the progression in skin healing, that contributes to the continuous inflammatory non-healing status of chronic skin wounds (55).

1.2.2.1. The important role of macrophages on inflammation resolution

Depending on the molecular signals present on the wound's microenvironment, in response to an injury, neutrophils and monocyte-derived macrophages arrive to the wound site with the mission of re-establishing skin integrity, joining the tissue-resident macrophages (56). The heterogenicity, plasticity and flexibility of the innate immune cell population of macrophages is a crucial characteristic in all stages of wound healing to finally reach cutaneous regeneration (57). Several published data demonstrates evidence for the key role of macrophages in scavenging, antigen presentation, phagocytosis, efferocytosis, promotion of angiogenesis and general repair (58). In addition, the shift from the inflammatory to the regenerative phase of wound closure is relying on the capacity of macrophages to phagocytise the dead cells and remaining debris at the wound site (18,59).

Simplistically, depending on the surrounding stimuli, macrophages polarize towards two phenotypic variations: classic pro-inflammatory M1 macrophages or alternative tissue-healing M2 macrophages. The first are involved in resolving infections and the second mentioned have the main functions of inflammation resolution and tissue remodelling (58,60,61). The polarization occurs through a continuous-spectrum, in which macrophages change their phenotypical and metabolic features (**figure 1.8**).

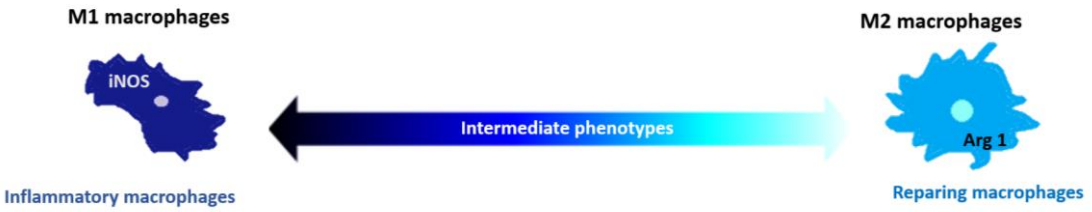

Figure 1.8. Continuous-spectrum of macrophage polarization (2). iNOS, inducible nitric oxide synthase; Arg 1, arginase 1.

During the inflammatory phase, in a normal wound-healing progression, M1 macrophages are predominant. M1-type macrophages have a crucial role in phagocytising dying or dead cells and its remnants, besides attracting other macrophage cell populations to the site of injury (62). This phenotype induces an active release of reactive oxygen species (ROS), such as superoxide anions and hydrogen peroxide (63). At the wounded location, ROS serve as chemo-attractants of monocyte cells. However, during a pathological event, the mechanism that triggers the increase of ROS production in monocytes and macrophages remains undefined (64). M1 macrophages usually produce high quantities of nitric oxide (NO) as a product of inducible nitric oxide synthase (iNOS)-mediated breakdown of arginine, which has antibacterial activity (65,66). These macrophages up-regulate major histocompatibility complexes (MHC)-II in conjunction with the co-stimulatory glycoprotein CD-86 on their membrane that is crucial for T-lymphocyte stimulation: from orchestrating infiltrated T-cells to resident T-cells of dermis and epidermis (67–70). M1 stimulation is achieved in the presence of lipopolysaccharides (LPS) of Gram-negative bacteria's outer membrane and/or interferon-Ɣ (IFN-Ɣ). Other distinctive characteristic of M1 macrophages is their high production levels of pro-inflammatory cytokines such as TNF-α and IFN-Ɣ and different interleukins - IL-1, IL-6, IL-12, IL-23 (71).

Contrarily to M1 macrophages, the M2-like phenotype appears in higher levels throughout the proliferation and remodelling stages of wound healing. M2 macrophages express on their membrane galactose receptors, mannose receptors (CD206) and haemoglobin scavenger receptors (CD163). In general, this polarization is stimulated by IL-4, IL-10 or/and IL-13 (18). Moreover, these cells constantly produce IL-4 and IL-10 that are anti-inflammatory cytokines, besides synthesizing the enzyme arginase-1 which is a key promotor of wound healing (57). Overall, M2 macrophages are responsible for promoting tissue remodelling and angiogenesis (72,73). The classification of M2-like macrophage subtypes is still under study and controversial, especially because of their plasticity in a continuous-spectrum, which makes it

difficult to divide them in a strict manner. Nevertheless, in the context of wound healing, it has been reported that M2-like macrophages can the categorized into 4 subtypes: M2a, M2b, M2c and M2d (**table 1.1**) (2,18,62,74–76).

Briefly, IL-4 and IL-13 stimulate M2a macrophages that express mannose receptors also known as CD206 on their membrane. In addition, they have profibrotic activity through secreting TGF-β and fibronectin that promotes tissue healing (71,72). M2b subtype is induced by the immune complex, for example. Through synthesizing elevated levels of the anti-inflammatory interleukin IL-10, M2b macrophages have shown a central role in reducing the inflammatory progression, although these cells still produce the pro-inflammatory cytokine TNF-α (18,57). IL-10 stimulated M2c macrophages, also secrete substantial amounts of IL-10 (77). Moreover, they produce the profibrotic factor TGF-β and have efficient phagocytic activity (78). Lastly, M2d macrophages are induced by IL-6. These cells secrete vascular endothelial growth factors (VEGF) and are pro-angiogenic (62,79).

Table 1.1. Main characteristics of M2-like macrophages subtypes (2).

			Secretion		
M2 Subtypes	**Stimulation**	**Membrane receptors**	**Cytokines**	**Chemokines**	**Signals**
M2a	IL-4, IL-13	CD163, CD206	IL-10, IL-1RA	CCL17, CCL18, CCL22, CCL24	STAT-3, Arg1, TGF-β
M2b	IC, TLR/IL-1R ligands	CD86, MHC-II	TNF-α, IL-1β, IL-6, IL-10	CCL1	SOCS3, COX-2
M2c	IL-10	CD86, CD163, CD206	IL-10	CCL16, CCL18, CXCL13	Arg 1, EGF, TGF-β, MMP-9
M2d	IL-6	CD14, CD16, CD68	TNF-α, IL-10, IL-12	CXCL10	TGF-β, VEGF

IL, interleukin; CD, cluster of differentiation; IL-1RA, IL-1 receptor antagonist; CCL, C-C motif ligand; CXCL, C-X-C motif ligand; STAT, Signal transducer and activator of transcription; EGF, epidermal growth factor; TGF, transforming growth factor; IGF, insulin-like growth factor; VEGF, vascular endothelial growth factor; Arg1, arginase; IC, immune complex; TLR, toll-like receptor; MHC, major histocompatibility complex; TNF, tumour necrosis factor; SOCS, suppressor of cytokine signalling; COX, cyclooxygenase; CCR, C-C chemokine receptor.

1.2.2.2. Phenotypical dysregulation of macrophages on chronic wounds

In chronic wounds, pro-inflammatory M1 macrophages can accumulate due to the environmental stimuli such as the presence of bacteria in planktonic or sessile living that impede the transition of M1 to M2b macrophages, in order to overcome inflammation (62). As a consequence, the wound closure will be delayed. As a proof of support, clinical research studies have shown that chronic wound fluids contain increased quantities of IL-1 and TNF-α, that are well-known pro-inflammatory molecules secreted by M1-like macrophages (80). In addition, the wound fluid includes excessive quantity of matrix metalloproteinases (MMPs) which lead to the degradation of proteins and extracellular matrix (ECM), hindering tissue regeneration (25,81).

Alteration of the typical metabolic and phenotypical profiles of M2-type macrophages is another contributing factor for delaying wound closure. In hypertrophic scars it has been reported an excessive presence of type III collagen (62,82).

Lastly, a 'simple' reduced recruitment or dysregulated differentiation of monocytes to macrophages, due to the wound environment molecular signals, is one main reason for a delayed skin wound healing.

1.3. Currently used biomedical approaches for chronic wound-care

Abnormal wound healing is rarely found on healthy individuals, but is typically associated with a health disorder, such as diabetes, cancer and/or malnutrition (20). The correct evaluation of the state of each specific wound needs to take the patient's health condition in consideration for the choice of an appropriate therapeutic treatment. A proper treatment selection is crucial to revert the non-healing state of chronic wounds. In order to achieve that, clinicians require the deepest knowledge possible about wound treatment products and techniques existing in the market. Thus, studies must obtain evidence about biocompatibility, the interaction between the wound's fluid and the wound product, possible antibacterial efficacy, the characterization of surface/chemical properties and sufficient data about its stability under diverse temperatures (83).

The use of antibiotics, a regular change of wound dressings and a debridement of necrotic tissue is currently the gold standard in wound treatment procedures (3,18). Unfortunately, failure to obtain a successful skin recovery is recurrent, after standard treatment, and the wound progresses to a severe state, while no improvement is achieved after several weeks of treatment. It may also happen that patients are hospitalised with an already established chronic wound. In

situations like these, alternative complementary advanced therapies should be selected (3). Wound care protocols state in general that the use of advanced therapies should be considered after 4 weeks of wound closure failure (3). These alternative wound care therapies imply the use of specialized procedures and products, and may include negative pressure wound therapy, acellular extracellular matrices, bioengineered skin, hyperbaric or topical oxygen treatment, and growth factors, e.g. platelet-derived growth factor (PDGF) (84). As a last resource procedure, amputation must be performed if possible.

Bandages and gauzes from natural or synthetic origin are frequently used as a first aid solution to cover and prevent contamination on wounds (85). This type of traditional dressings is deficient in important characteristics for improving wound healing: maintain the wound hydrated and participate in the wound healing process by releasing bioactive molecules. Hence, several wound products have been developed to facilitate wound healing. These 'Modern wound care products' are usually based on synthetic polymers. Often, they are bioactive through the integration of antimicrobial agents, such as antibiotics (e.g. gentamicin) or metals (e.g. silver), or by the inclusion of growth factors (86,87). In order to have a chance of continuation of normal wound healing in chronic wounds, natural or synthetic antimicrobial materials might be able to play key roles in preventing/decreasing the high bacterial contamination and stimulate an ideal tissue-healing response, leading to a proper cutaneous closure.

1.4. Antimicrobial peptides and wound healing

With the increasing prevalence of antibiotic-resistant bacterial infections and reported cases of the contribution of certain metals to the promotion of antibiotic resistance through co-selection (i.e. occurs when resistant genes to both antibiotics and metals are co-located together, or even when the efflux pump mechanism is the resistance strategy), a therapeutic gap has been opened for the rise of new antibacterial approaches, such as antimicrobial peptides (AMPs) (88,89). AMPs are interesting novel antibacterial agents, because of their broad antimicrobial spectrum and most common direct bacterial killing action by targeting the bacterial cytoplasmic membrane, inducing an irreversible damage and consequent microbial death (90). Hence, the risk of mutations leading to AMP-resistance mechanisms within the bacterial cell is low. Moreover, besides disrupting the membrane, AMPs usually have multiple modes of action such as inhibiting DNA and RNA synthesis, interference with enzymatic activity and stimulate the immune system (91). There is a big interest to explore this new class of anti-infective

therapeutics as a solution in combating difficult-to-treat slow-growing bacteria in biofilms bacteria such as reported in non-healing chronic wounds and consequently improve wound healing (92,93).

1.4.1. Antimicrobial peptides: innate immunity, structural characteristics and antibacterial action

Antimicrobial peptides are widespread in nature constituting one of the oldest evolutional host defence strategies in all living organisms (90). In literature, most reported AMPs were discovered from animals, plants, fungi and bacteria (94). Bacteria produce AMPs principally to inhibit the growth of competing microorganisms (95). For plants and invertebrates, antimicrobial peptides have an indispensable function in providing the host's defence against invading microorganisms since they lack adaptative immunity, also known as acquired immunity (96). In vertebrates, the immune system is divided into two different categories the in innate and adaptative immunity. Herein, AMPs have been reported to be part of the innate immune response (97). Humans themselves are part of the biologically classified vertebrates' group and it has been discovered that some isolated AMPs have direct participative roles in the inactivation of pathogenic microorganisms, in immunomodulation and even in controlling inflammation (98–100).

Structurally, antimicrobial peptides are quite diverse. In general, they can be classified into the following subclasses: α-helical structure (e.g. LL-37 cathelicidin); AMPs that adopt β-sheet structure (e.g. defensins); and extended coil structure (e.g. indolicidin cathelicidin) (94). Even though AMPs have structural differences, diversity of sequences and source origins, there are three characteristics that nearly all discovered AMPs have in common:

1) Amphipathicity – Antimicrobial peptides are constituted by hydrophilic and hydrophobic amino acids. The balance between hydrophobic and hydrophilic domains is very important for the antimicrobial mode of action and the hydrophilic residue is generally cationic (94,101);

2) Net positive charge – The cationic nature of AMPs arises from the presence of lysine, arginine or histidine amino acids. The net positive charge may vary from +2 to +13. There is a direct correlation between the positive charge's content of AMPs and efficient antimicrobial action (102,103);

3) Hydrophobicity level – In AMPs presence of leucine, alanine or tyrosine, for example, in the peptide sequence provides hydrophobicity features, and it should

constitute nearly 50% of the total AMP. Hydrophobicity much higher or lower than this level makes the peptide inactive (101). Hydrophobic amino acids allow the permeabilization of AMPs into the lipid bilayer membrane.

Henceforth, the fundamental amphipathic structure design for most AMPs relies on the clustering of spatially organized hydrophobic and cationic amino acids in distinct regions of the molecule (90) (**figure 1.9**). The shared features among AMPs are interconnected and a balanced amphipathicity, net charge and hydrophobicity are crucial for the AMP's mode of action. It is noteworthy to mention that despite their different amino acid sequence, comprising from 10 to 50 amino acids, the vast majority of antimicrobial peptides present a cationic character and an amphipathic structure in cell membrane interactions (104).

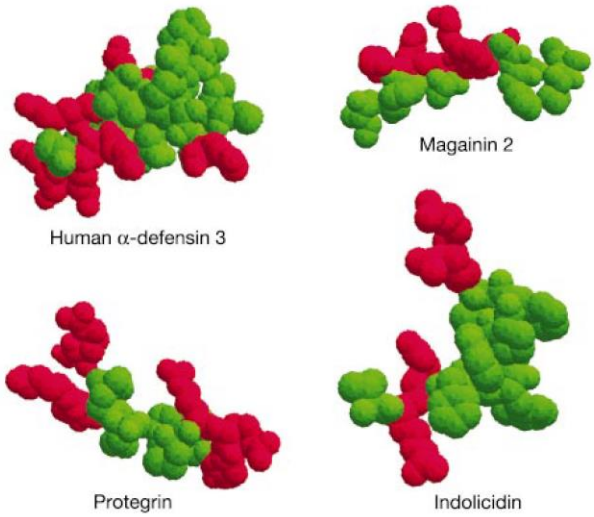

Figure 1.9. Examples of antimicrobial peptides exhibiting an amphipathic fundamental structure (90). **Red**, positively charged amino acids; **Green**, hydrophobic amino acids.

Most antimicrobial peptides induce direct killing of microorganisms by targeting the bacterial membrane (94). In fact, this mechanism was thought to be the only mode of action of AMPs years ago (90). This microbial membrane targeting can occur through:

a) the specific binding to lipid receptors;

b) the non-specific binding through electrostatic interactions between the positively charged hydrophilic amino acids and the negatively charged bacterial membrane.

The non-specific binding is frequently associated with invertebrate and vertebrate AMPs. The positive net charge of AMPs is electrostatically attracted to the negative charged bacterial membrane (105). The outer monolayer of Gram-positive and Gram-negative bacteria lipid bilayer membranes are mostly constituted by acidic phospholipids, that have negative head

groups, promoting the initial electrostatic interaction. In addition, at their surface, they are constituted by teichoic acid or lipopolysaccharides, respectively, which are also negatively charged (90,105). On the other hand, the outer leaflet of the membrane of mammalian cells is constituted by zwitterionic phospholipids, that are neutral in nature, and the lipids with negatively charged heads are facing the cytoplasm, reducing the possibility of electrostatic interaction with AMPs (106). This fundamental difference between the mammalian and the bacterial cell membrane confers a selective mode action to AMPs towards the bacterial cytoplasmic membrane (**figure 1.10**).

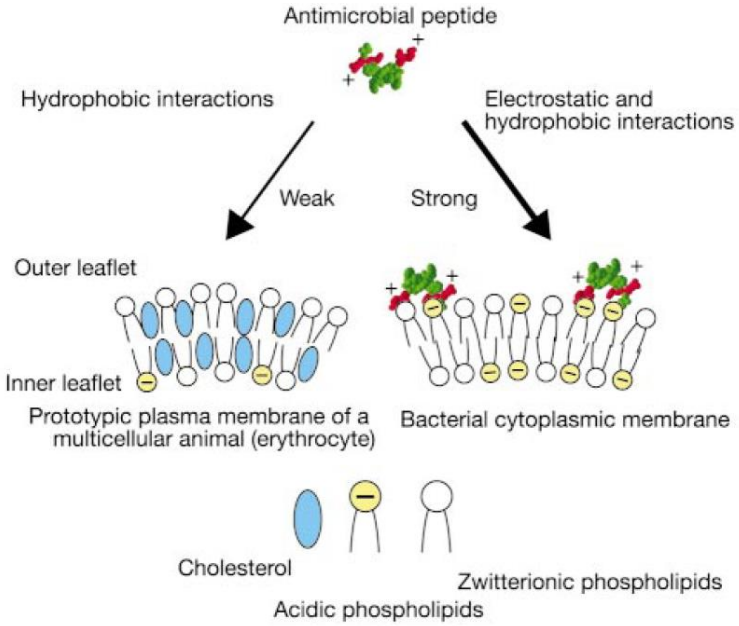

Figure 1.10. Representation of membrane target specificity of antimicrobial peptides (90).

After the initial electrostatic interaction with the bacterial membrane, the hydrophobic region of the AMPs is able to penetrate into the membrane. A pleasing scheme of this process was provided by the Shai-Matsuzaki-Huang model (90) (**figure 1.11**). Briefly, the summarized model suggests that the killing of bacteria occurs by an initial electrostatic interaction between the positive charges of AMPs with the negatively-charged bacterial outer leaflet followed by the insertion of the hydrophobic part of AMPs into the bacterial membrane occurs, moving the lipids and creating holes that will lead to the bacteria's cellular content leakage and surface tension (90,107). This model also shows that some peptides are even able to enter the cell and act intracellularly (**figure 1.11**).

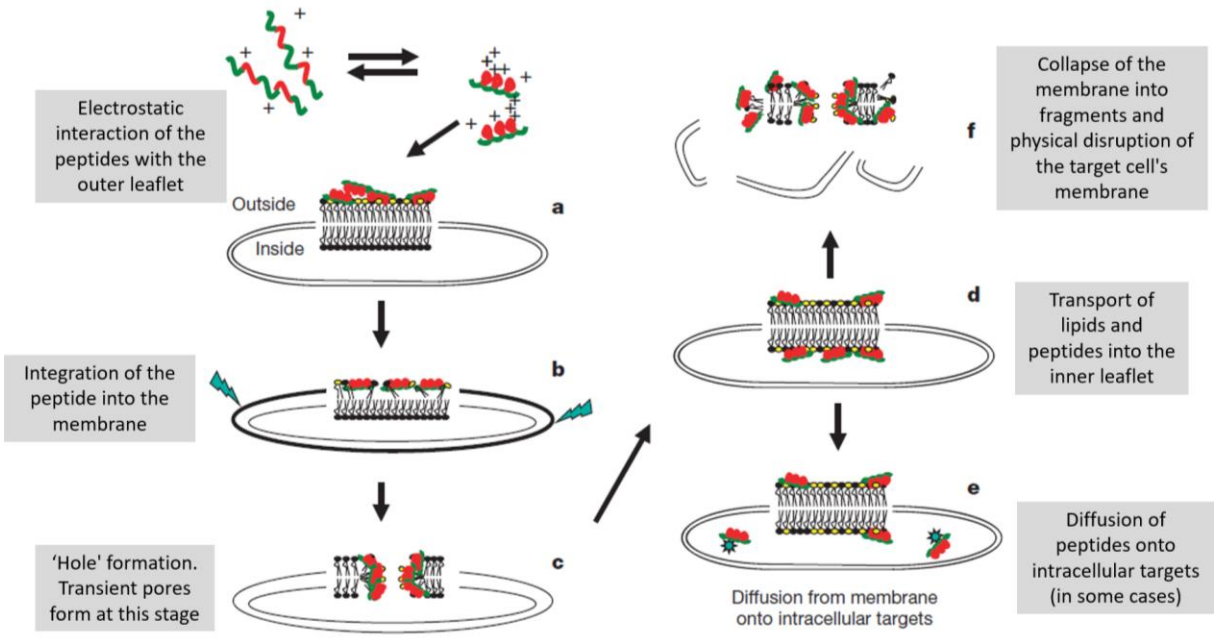

Figure 1.11. General mechanism of action of membrane targeting antimicrobial peptides following the Shai-Matsuzaki-Huang model. **Red**, hydrophilic; **Green**, hydrophobic; **Yellow**, acidic phospholipids. Adapted from (90).

According to the structure of insertion, the resulting antibacterial events can be described by prevailing classical models that are divided into three categories, that will promote membrane depolarization, leakiness and consequent bacterial death (108):

a) Barrel-stave model (**figure 1.12**) – Amphiphilic peptides attach initially to the surface of the outer membrane leaflet and are inserted vertically in the lipid bilayer forming barrel-like stable pores (109). The amphipathic structure is critical for the pore formation as the hydrophobic domains interact with the lipids of the bacterial membrane, pushing them apart. The hydrophilic regions form the lumen of the pore (110). This pore formation mechanism is considered similar to membrane protein ion channels (94).

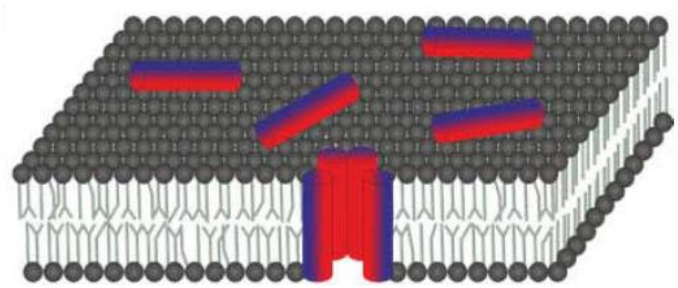

Figure 1.12. Model of interaction of antimicrobial peptides with the membrane: Barrel-stave model (111). **Red**, hydrophilic; **Blue**, hydrophobic

b) Toroidal pore model (**figure 1.13**) – In this model, after initial surface interaction, AMPs are also inserted perpendicularly into the membrane but in a less organized manner since specific peptide-peptide interactions do not occur (112). Instead, the peptides force the phospholipids of the membrane to acquire an altered alignment (local curvature), and a pore is formed by peptide parcels and lipid head groups (109). Hence, in toroidal pores the hydrophilic and hydrophobic normal alignment of lipids in the bilayer is dislocated. Moreover, as the toroidal pores are transient, some AMPs are able to translocate to the cytoplasm and target intracellular structures (113,114).

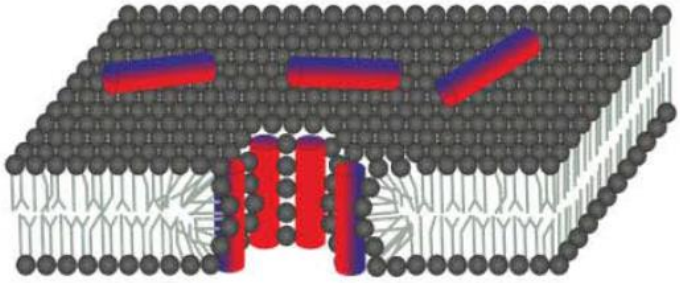

Figure 1.13. Model of interaction of antimicrobial peptides with the membrane: Toroidal pore model (111). **Red**, hydrophilic; **Blue**, hydrophobic

c) Carpet model (detergent 'like' model) (**figure 1.14**) – Basically, in this model AMPs have a detergent like behaviour and adsorb onto the lipid bilayer, reaching a concentration that covers most of its surface (carpet-like) (94). The membrane integrity is lost, and its consequent disintegration occurs by the formation of micelles from the cell lipid bilayer (detergent-like). Lipid portions are detached from the membrane, creating holes, until the point that the membrane lipid bilayer collapses, causing cell lysis. The carpet model does not necessarily require peptide-peptide interactions or the insertion of peptides into the hydrophobic transmembrane space (115).

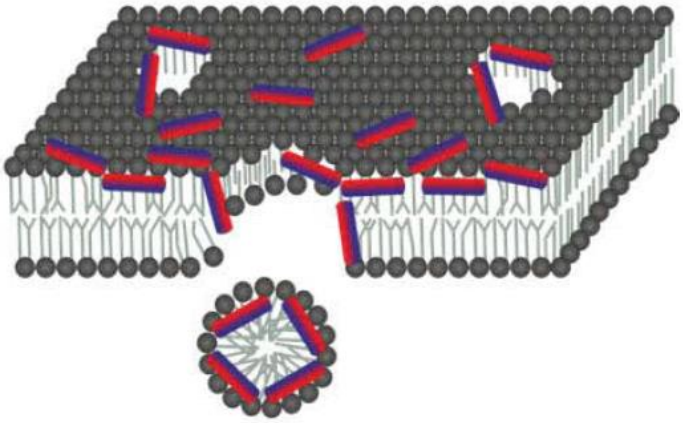

Figure 1.14. Model of interaction of antimicrobial peptides with the membrane: Carpet model (111). **Red**, hydrophilic; **Blue**, hydrophobic

Besides the previously described classical models concerning the mechanism of the AMPs action of direct killing by membrane targeting, there are other related models such as molecular electroporation, sinking raft model and interfacial activity model (94,111).

Direct killing by non-membrane targeting mechanisms have also been described for several antimicrobial peptides (110). This was revolutionary in the AMPs' studies field, in which it was believed that direct membrane targeting was the only mechanism of action of all AMPs. These AMPs have intracellular targets that will influence many processes in the cell, that are also related to membrane and cell wall stress. Cytosolic structures or metabolic pathway targets currently discovered include: the inhibition of cell wall biosynthesis, the inhibition of synthesis of nucleic acids/proteins and the interference with enzymatic activity (110,111,116,117).

In addition to AMPs' direct killing of microorganisms, it has been reported that AMPs are recruiters of immune cells contributing for the clearance of pathogenic invading microbes and controlling inflammation in an indirect way (94). Several studies have shown some AMPs' participation in the attraction and differentiation of leukocytes, the reduction of the local inflammatory environment by decreasing the secretion of pro-inflammatory cytokines/chemokines, the regulation of expression of reactive oxygen species and the stimulation of angiogenesis (98,118–121).

The independent antimicrobial action of AMPs combined with their collaborative mechanism towards immune cells suggest that antimicrobial peptides are ideal candidates for future therapeutic strategies (**figure 1.15**).

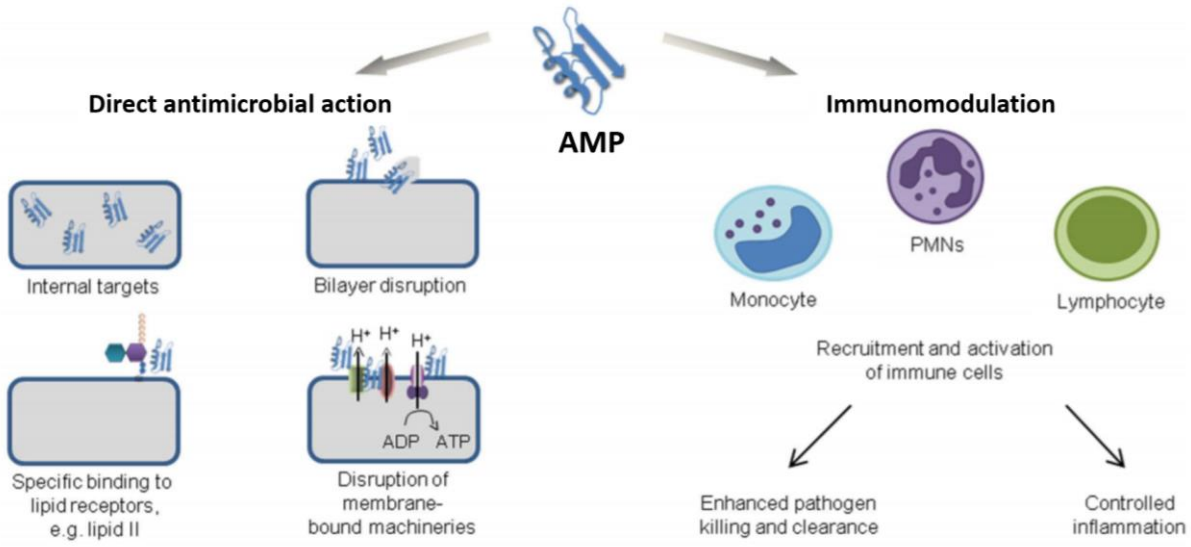

Figure 1.15. Possible antimicrobial mechanisms of action of antimicrobial peptides (122). PMN, polymorphonuclear neutrophils; ADP, adenosine diphosphate; ATP, adenosine triphosphate.

1.4.2. Potential of antimicrobial peptides in skin infections and wound healing

In response to an injury, human cells developed a collection of host defence molecules, including antimicrobial peptides, to ensure epithelial integrity. These skin AMPs have the function of inhibiting the growth of invading microorganisms and of recruiting host immune cells to the site of damage (120,123,124). Non-healing wounds, such as diabetic and foot ulcers, are often infected. As a result, the cells localized at the injury site express continuously pro-inflammatory cytokines, forcing the wound to remain in a persistent inflammatory phase of wound healing (88). In such cases, the AMPs' mode of action can present a dual beneficial outcome: neutralizes microbial pathogenicity and stimulates immune cells to help clearing infections (125). Moreover, during time the excessive pro-inflammatory molecules release will be decreased, allowing the continuation of the wound healing process. This dual result is one of the main advantages of AMPs over conventional antibiotics, confirmed in studies with *Staphylococcus aureus* and/or methicillin-resistant *S. aureus* (MRSA) infected skin models, in which the peptides tested were able to reduce the pro-inflammatory cytokines secretion, IL-6 and TNF-β, besides having direct antibacterial activity (126,127).

In addition, the AMPs' usual mode of action in targeting the membrane without involving specific-binding sites or being able to inhibit multiple structures and metabolic targets, makes bacterial resistance development much more improbable (128,129). Moreover, thanks to the same 'unspecific' mode of action, known antibiotic-resistant bacteria show sensitivity to

antimicrobial peptides (130). This is incredibly important in the context of chronic wounds, in which the colonization of drug-resistant bacteria onto skin wounds has been described (131). Even though bacteria would develop AMPs-resistance mechanisms, the AMPs immunomodulatory influence would not be affected, hence there would still be the possibility for protection against bacterial infections without possessing direct antimicrobial activity (132). This has been proven in works with *in vivo* infection models in which the peptides induced an immunomodulatory effect, acting indirectly on the microbial clearance, reducing the inflammatory environment (133,134). This AMP characteristic could be extremely helpful in chronic wounds in order to overcome the excessive persistent inflammatory phase and allow a continuation of the complex wound closure process. As previously described, macrophages have crucial roles in all stages of wound healing. In a research work with IDR-1018 antimicrobial peptides, their influence in pushing macrophages polarization to an M2-like phenotype was concluded (125). Regulation of M2 differentiation by AMPs in non-healing wounds might be a contributor to improve wound recovery, since these are anti-inflammatory tissue healing macrophages (76).

Moreover, in chronic wounds, polymicrobial infections are most commonly found. The general mechanism of bactericidal action of AMPs enables a broad-spectrum activity against Gram-positive and Gram-negative bacteria strains, including antibiotic-resistant species, facilitating wound recovery (130). Most importantly, the polymicrobial invasion of the wound site opens a way for a possible cooperation between the attacking strains leading to the formation of enclosed extracellular polymeric matrixes denominated biofilms. The bacterial population in these biofilms is heterogenic with a combination of mainly metabolically dormant and fewer active cells. As previously mentioned, biofilms work like a permeability barrier against harmful external factors. They are more difficult to eradicate, because of the higher tolerance to exogenous stresses, such as antibiotics and host defence strategies (e.g. opsonization and phagocytosis) (88). Therefore, therapies that are able to prevent the biofilm formation or lead to their destruction enhance the chance for a complete recovery of infected wounds. It has been proven that slowly and actively-growing bacteria in biofilms are killed by AMPs (135). Hence, some AMPs are bactericidal independent from the growth rate of microorganisms. A recent example is the antimicrobial peptide DRGN-1 that eradicated mixed biofilms of *Staphylococcus aureus* and *Pseudomonas aeruginosa* on murine-infected wounds, promoting wound healing (136).

Overall, it became evident that AMPs as a topical application have a lot of more advantages in the treatment of skin infections than conventional antibiotics. The benefits include their broad-

spectrum of antibacterial activity even against known antibiotic-resistant strains, their lower probability of inducing the development of resistance, their rapid action and their ability to act on metabolically-slow and -active growing bacteria (as present in biofilms). In addition to these advantages, AMPs' can have an extra indirect antimicrobial and wound healing resolution effect by activating the innate immune system (e.g. immunomodulatory activity towards macrophages), which makes them perfect candidates for infected wounds treatment.

1.4.3. Limitations of natural and synthetic antimicrobial peptides in wound context

Despite the increasing discovery of new natural AMPs in the last years and a constant development of synthetic antimicrobial peptides in research, there is a discrepancy between potential therapeutic AMPs reported in scientific articles or patents and an actual undergoing of these candidates to clinical trials (137). In the following paragraphs, the main reasons for this divergence are described:

1) High cost of production and low scalability – The major issue of the manufacturing of AMPs is the extremely high cost for their production. The well-established solid-phase peptide synthesis is currently the most used procedure for chemical synthesis of peptides, but the production is done in a relatively small scale (138,139). It has been estimated that the cost to produce 1 g of peptide by chemical synthesis reaches generally 89 to 531 euros, with various technical difficulties during the synthesis procedure, including the purification process (140,141). Moreover, new strategies must be considered for large-scale production. As an alternative to chemical synthesis, there are production systems for recombinant peptides in bacteria, yeast or mammalian cells (142). Unfortunately, the recombinant route involves an extensive and expensive research and development phase (143).

2) Regulatory challenges – The clinical development of AMPs faces many regulatory barriers during their clinical testing. During the last decades, recent initiatives have been taken by governmental and regulatory authorities to facilitate the advance of novel antibacterial agents, in response to the alarming rise of reported bacteria resistances to conventional antibiotics (144). Nevertheless, the regulatory parameters (e.g. chemistry, manufacturing, controls) for antimicrobial peptides are still complex, because of the fact that peptide therapeutics are seen as a mixture of classical small molecules (such as a

conventional antibiotic) and biological-derived agents, since they are obtained in biological systems or mimic the action of endogenous peptides/proteins (143).

3) Low physical stability under physiological conditions – Currently, the most acceptable route to administrate AMPs is local application, for example on infected wounds. This is mainly due to their short half-life in blood because they can easily be degraded by the host's proteases and peptidases (141). Even in cases of local administration, AMPs are still predisposed to the degradation by tissue proteolytic enzymes (143). Their continuous application would be expensive and could create toxic results. In addition, other factors can interfere with the antimicrobial activity of the AMPs such as the pH and the presence of salts. The latter is very important to be accessed, since salts may neutralize the cationic charge and prevent the initial electrostatic interaction with the negatively-charged bacterial surface, consequently blocking the AMPs mechanism of bactericidal action entirely (145).

Henceforth, antimicrobial peptides still present various limitations. However, in the context of wounds, the regulatory challenges are more easily overcome since the product is applied by a topical route and the physical stability of AMPs is not extensively affected. The latter was confirmed in *in vivo* infected wounds studies, in which AMPs were able to reduce or eradicate the bacterial burden, as described in section 1.4.2. Until nowadays, only few AMPs entered the market and are clinically-applied (e.g. polymyxins), but in the last years more AMPs are starting to be accepted for treatment of diabetic wounds and burned tissue in clinical trials phase III (141,143).

Thus, the major challenges to target in the market of wound products are to overcome the high cost of production, the low scalability of antimicrobial peptides and their complicated manufacturing procedure.

1.5. Synthetic antibacterial peptide-mimetic polymers: A new promising strategy to improve healing in chronic wounds

As previously described, although natural and synthetic AMPs induce an excellent antimicrobial effect (against planktonic and sessile bacteria), have immunomodulatory properties in some cases and finally promote wound healing, there are still drawbacks concerning their clinical use (section 1.4.3). In an attempt to address the AMP's high cost, low

industrial scalability, instability under physiological conditions and difficulty in manufacturing, synthetic antimicrobial peptide-mimetic polymers are on the rise. One of their major advantages is the versatility offered in polymer chemistry that permits a wider exploration of chemical and structural features in order to optimize the antibacterial potency and biocompatibility properties. Taking inspiration from nature is recognized as a promising strategy for the development of new anti-infective therapeutic agents (146,147). Despite of the great variety of antimicrobial peptides discovered in nature, the majority shares a common structure: cationic amphipathic conformation (148). Hence the design rational of these AMP-biomimetic block copolymers is built on the essential physiochemical properties of antimicrobial peptides - the cationic amphiphilic structure – which is the basis of the AMPs' bactericidal mode of action (**figure 1.16**). In fact, the structure built up by the clustering of cationic hydrophilic and hydrophobic segments into distinct domains is responsible for the interaction of AMPs with the bacterial cytoplasmic membrane and further antibacterial activity (section 1.4.1). Thus, the finality of developing AMP-biomimetic polymers is mainly to reproduce the antimicrobial mode of action of AMPs that induce their bactericidal effect through the disruption of the bacterial membrane (**figure 1.17**).

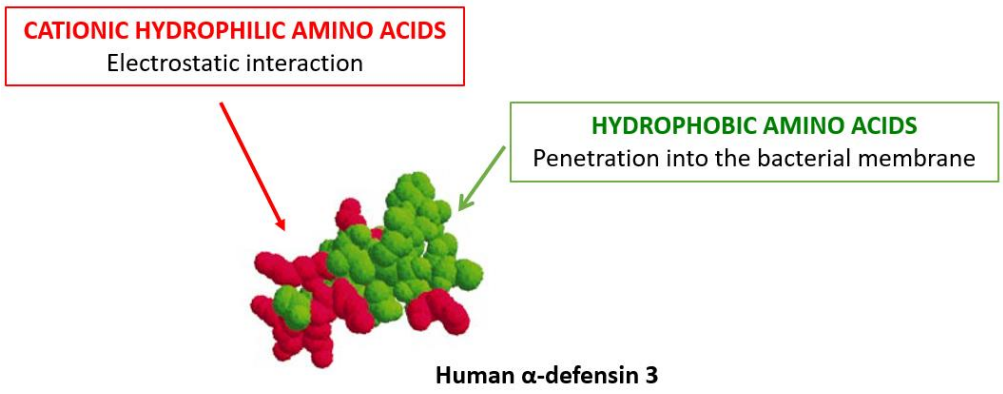

Figure 1.16. Representation of the usual amphipathic design of antimicrobial peptides and the function of each region, using Human α-defensin as example. Adapted from (90).

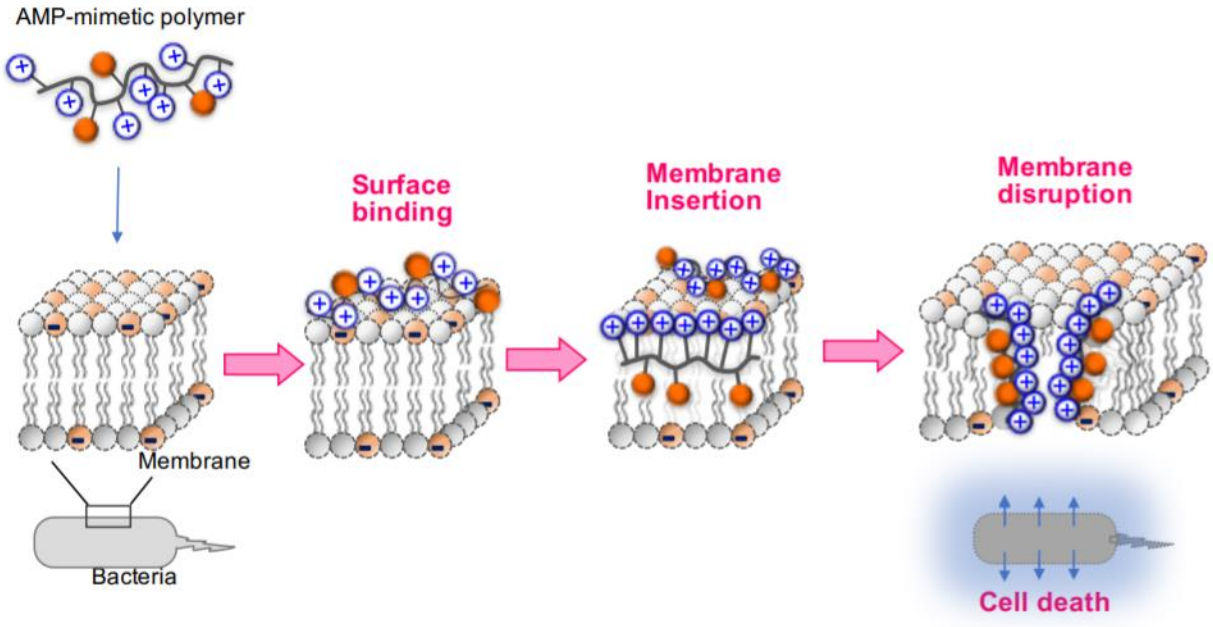

Figure 1.17. Mechanism of action of cationic amphipathic polymers (149).

AMP-mimetic antibacterial polymers that have been reported in literature are based on different polymers (150). Some examples are AMP-biomimetics based on polyacrylates, polymethacrylates, polycarbonates, and polynorbornenes (151–158). These polymer formulations have shown great efficiency in eliminating multidrug-resistant bacteria, with a special focus for MRSA, used in such studies since it is one of the most preoccupying case of antibiotic-resistant bacteria worldwide.

A deep analysis and exploration of AMP-inspired polymers has confirmed the importance of the hydrophilic/hydrophobic balance, the presence of positive charges, a general polymeric architecture and molecular weight for achieving a potent antibacterial activity and the avoidance of haemolysis or other cytotoxicity effects (159).

The strategy of using polymers as 'macromolecular agents' for treating infections is still immature. With a few exceptions, AMP-biomimetic polymers research studies are using drug-sensitive strains as testing models *in vitro*. Taking into consideration that drug-sensitive bacteria is not in general a global life-threatening issue, these studies should take a step forward and always include drug-resistant clinical isolates and evaluation of the disruptive capacity against biofilms. These inclusions would increase the relevance for clinical applications of AMP-inspired amphiphilic polymers on infected chronic wounds.

References

1. Guo S, DiPietro LA. Factors affecting wound healing. J Dent Res. 2010;89(3):219–29.
2. Varela P, Sartori S, Viebahn R, Salber J, Ciardelli G. Macrophage immunomodulation: An indispensable tool to evaluate the performance of wound dressing biomaterials. J Appl Biomater Funct Mater. 2019;17(1):1–10.
3. Frykberg RG, Banks J. Challenges in the Treatment of Chronic Wounds. Adv Wound Care. 2015;4(9):560–82.
4. Woo K, Ayello EA, Sibbald RG. The edge effect: current therapeutic options to advance the wound edge. Adv Skin Wound Care. 2007;20(2):99–117.
5. Attinger C, Wolcott R. Clinically Addressing Biofilm in Chronic Wounds. Adv Wound Care. 2012;1(3):127–32.
6. Li J, Chen J, Kirsner R. Pathophysiology of acute wound healing. Clin Dermatol. 2007;25(1):9–18.
7. Gupta B, Agarwal R, Alam MS. Textile-based smart wound dressings. Indian J Fibre Text Res. 2010;35(2):174–87.
8. Percival NJ. Classification of Wounds and their Management. Surg. 2002;20(5):114–7.
9. Lindholm C, Searle R. Wound management for the 21st century: combining effectiveness and efficiency. Int Wound J. 2016;13:5–15.
10. Sen CK, Gordillo GM, Roy S, Kirsner R, Lambert L, Hunt TK, et al. Human skin wounds: A major and snowballing threat to public health and the economy. Wound Repair Regen. 2009;17(6):763–71.
11. Heyer K, Herberger K, Protz K, Glaeske G, Augustin M. Epidemiology of chronic wounds in Germany: Analysis of statutory health insurance data. Wound Repair Regen. 2016;24(2):434–42.
12. Guest JF, Ayoub N, McIlwraith T, Uchegbu I, Gerrish A, Weidlich D, et al. Health economic burden that wounds impose on the National Health Service in the UK. BMJ Open. 2015;5(12):1–8.
13. Frenk J. Health and the economy. Harvard Int Rev. 2014;35(4):62–4.
14. Posnett J, Gottrup F, Lundgren H, Saal G. The resource impact of wounds on health-care providers in Europe. J Wound Care. 2009;18(4):154–154.
15. Europe advanced wound care management. Europe Wound Management Market - Segmented by Product, Wound Healing Therapy and Geography - Growth, Trends, and Forecast (2018 - 2023). 2018.
16. Gottrup F, Apelqvist J, Price P. Outcomes in controlled and comparative studies on non- healing wounds: J Wound Care. 2010;19(6):239–68.
17. Velnar T, Bailey T, Smrkolj V. The wound healing process: An overview of the cellular and molecular mechanisms. J Int Med Res. 2009;37(5):1528–42.
18. Krzyszczyk P, Schloss R, Palmer A, Berthiaume F. The role of macrophages in acute and chronic wound healing and interventions to promote pro-wound healing phenotypes. Front Physiol. 2018;9:1–22.

19. Gomes A, Teixeira C, Ferraz R, Prudencio C, Gomes P. Wound-healing peptides for treatment of chronic diabetic foot ulcers and other infected skin injuries. Molecules. 2017;22(10):1–18.

20. Han G, Ceilley R. Chronic Wound Healing: A Review of Current Management and Treatments. Adv Ther. 2017;34(3):599–610.

21. Cook H, Stephens P, Davies KJ, Harding KG, Thomas DW. Defective extracellular matrix reorganization by chronic wound fibroblasts is associated with alterations in TIMP-1, TIMP-2, and MMP-2 activity. J Invest Dermatol. 2000;115(2):225–33.

22. Kim BC, Kim HT, Park SH, Cha JS, Yufit T, Kim SJ, et al. Fibroblasts from chronic wounds show altered TGF-β-signaling and decreased TGF-β type II receptor expression. J Cell Physiol. 2003;195(3):331–6.

23. Cha J, Kwak T, Butmarc J, Kim TA, Yufit T, Carson P, et al. Fibroblasts from non-healing human chronic wounds show decreased expression of βig-h3, a TGF-β inducible protein. J Dermatol Sci. 2008;50(1):15–23.

24. Usui ML, Mansbridge JN, Carter WG, Fujita M, Olerud JE. Keratinocyte migration, proliferation, and differentiation in chronic ulcers from patients with diabetes and normal wounds. J Histochem Cytochem. 2008;56(7):687–96.

25. Caley MP, Martins VLC, O'Toole EA. Metalloproteinases and Wound Healing. Adv Wound Care. 2015;4(4):225–34.

26. Barrientos S, Brem H, Stojadinovic O, Medicine R, Surgery C. Clinical Application of Growth Factors and Cytokines in Wound Healing. Wound Repair Regen. 2016;22(5):569–78.

27. Kumar P, Kumar S, Udupa EP, Kumar U, Rao P, Honnegowda T. Role of angiogenesis and angiogenic factors in acute and chronic wound healing. Plast Aesthetic Res. 2015;2(5):243.

28. Gottrup F, Apelqvist J, Bjarnsholt T, Cooper R, Moore Z, Peters EJG, et al. Antimicrobials and Non-Healing Wounds. Evidence, controversies and suggestions—key messages. J Wound Care. 2014;23(10):477–82.

29. Blair JMA, Webber MA, Baylay AJ, Ogbolu DO, Piddock LJ V. Molecular mechanisms of antibiotic resistance. Nat Rev Microbiol. 2015;13(1):42–51.

30. Read AF, Woods RJ. Antibiotic resistance management. Evol Med Public Heal. 2014;2014(1):147.

31. Michael CA, Dominey-Howes D, Labbate M. The Antimicrobial Resistance Crisis: Causes, Consequences, and Management. Front Public Heal. 2014;2:145.

32. Ventola CL. The Antibiotic Resistance Crisis. Pharm Ther. 2015;40(4):277–83.

33. Ibberson CB, Stacy A, Fleming D, Dees JL, Rumbaugh K, Gilmore MS, et al. Co-infecting microorganisms dramatically alter pathogen gene essentiality during polymicrobial infection. Nat Microbiol. 2017;2:1–6.

34. Gjødsbøl K, Christensen JJ, Karlsmark T, Jørgensen B, Klein BM, Krogfelt KA. Multiple bacterial species reside in chronic wounds: A longitudinal study. Int Wound J. 2006;3(3):225–31.

35. United States Centers for Disease Control. Antibiotic resistance threats in the United

States, 2013. Current. 2013;

36. Burmølle M, Thomsen TR, Fazli M, Dige I, Christensen L, Homøe P, et al. Biofilms in chronic infections - A matter of opportunity - Monospecies biofilms in multispecies infections. FEMS Immunol Med Microbiol. 2010;59(3):324–36.

37. Leaper D, Assadian O, Edmiston CE. Approach to chronic wound infections. Br J Dermatol. 2015;173(2):351–8.

38. Zhao G, Usui ML, Lippman SI, James GA, Stewart PS, Fleckman P, et al. Biofilms and Inflammation in Chronic Wounds. Adv Wound Care. 2013;2(7):389–99.

39. Stacy A, McNally L, Darch SE, Brown SP, Whiteley M. The biogeography of polymicrobial infection. Nat Rev Microbiol. 2015;14(2):93–105.

40. Ventola C. The antibiotic resistance crisis: part 1: causes and threats. PT. 2015;40(4):277–83.

41. Sciences EH. The Extracellular Bastions of Bacteria — A Biofilm Way of Life Introduction . Biofilm Basics. Nat Educ Knowl. 2013;4:1–10.

42. Donlan RM, Costerton JW. Biofilms: survival mechanisms of clinically relevant microorganisms. Clin Microbiol Rev. 2002;15(2):167–93.

43. Hampton S. Bacteria and wound healing. J Community Nurs. 2007;21(10):32–40.

44. Potera C. Antibiotic resistance: Biofilm Dispersing Agent Rejuvenates Older Antibiotics. Environ Health Perspect. 2010;118(7):A288.

45. Idrees A, Varela P, Ruini F, Vasquez JM, Salber J, Greiser U, et al. Drug-free antibacterial polymers for biomedical applications. Biomed Sci Eng. 2018;2(1).

46. Jaeger M, Harats M, Kornhaber R, Aviv U, Zerach A, Haik J. Treatment of hypergranulation tissue in burn wounds with topical steroid dressings: A case series. Int Med Case Rep J. 2016;9:241–5.

47. McShane DB, Bellet JS. Treatment of hypergranulation tissue with high potency topical corticosteroids in children. Pediatr Dermatol. 2012;29(5):675–8.

48. Vuolo J. Hypergranulation: exploring possible management options. Br J Nurs. 2010;19(2):4–8.

49. Widgerow AD, Leak K. Hypergranulation tissue: evolution, control and potential elimination. Wound Heal South Africa. 2010;3(2):7–9.

50. Caldeira J, Sousa A, Sousa DM, Barros D. Extracellular matrix constitution and function for tissue regeneration and repair. In: Peptides and Proteins as Biomaterials for Tissue Regeneration and Repair. 2018. p. 29–72.

51. Werner S, Krieg T, Smola H. Keratinocyte-fibroblast interactions in wound healing. J Invest Dermatol. 2007;127(5):998–1008.

52. Schreml S, Szeimies RM, Karrer S, Heinlin J, Landthaler M, Babilas P. The impact of the pH value on skin integrity and cutaneous wound healing. J Eur Acad Dermatology Venereol. 2010;24(4):373–8.

53. Hiemstra P, Daha M. Opsonization. Encycl Immunol. 1998;1885–8.

54. Grice EA, Segre JA. Interaction of the microbiome with the innate immune response in

chronic wounds. Adv Exp Med Biol. 2012;946:55–68.

55. Koh TJ, DiPietro LA. Inflammation and wound healing: the role of the macrophage. Expert Rev Mol Med. 2011;13:1–12.

56. Minutti CM, Knipper JA, Allen JE, Zaiss DMW. Tissue-specific contribution of macrophages to wound healing. Semin Cell Dev Biol. 2017;61:3–11.

57. Ogle ME, Segar CE, Sridhar S, Botchwey EA. Monocytes and macrophages in tissue repair: Implications for immunoregenerative biomaterial design. Exp Biol Med. 2016;241(10):1084–97.

58. Das A, Sinha M, Datta S, Abas M, Chaffee S, Sen CK, et al. Monocyte and Macrophage Plasticity in Tissue Repair and Regeneration. Am J Pathol. 2015;185(10):2596–606.

59. Khanna S, Biswas S, Shang Y, Collard E, Azad A, Kauh C, et al. Macrophage dysfunction impairs resolution of inflammation in the wounds of diabetic mice. PLoS One. 2010;5(3):e9539.

60. Biswas SK, Mantovani A. Orchestration of metabolism by macrophages. Cell Metab. 2012;15(4):432–7.

61. Das A, Datta S, Roche E, Chaffee S, Jose E, Shi L, et al. Novel mechanisms of Collagenase Santyl Ointment (CSO) in wound macrophage polarization and resolution of wound inflammation. Sci Rep. 2018;8(1):1–14.

62. Hesketh M, Sahin KB, West ZE, Murray RZ. Macrophage phenotypes regulate scar formation and chronic wound healing. Int J Mol Sci. 2017;18(7):1–10.

63. Bae YS, Lee JH, Choi SH, Kim S, Almazan F, Witztum JL, et al. Macrophages generate reactive oxygen species in response to minimally oxidized LDL: TLR4- and Syk-dependent activation of Nox2. Circ Res. 2009;104(2):210–8.

64. Tan HY, Wang N, Li S, Hong M, Wang X, Feng Y. The Reactive Oxygen Species in Macrophage Polarization: Reflecting Its Dual Role in Progression and Treatment of Human Diseases. Oxid Med Cell Longev. 2016;2016:1–16.

65. Schairer DO, Chouake JS, Nosanchuk JD, Friedman AJ. The potential of nitric oxide releasing therapies as antimicrobial agents. Virulence. 2012;3(3):271–9.

66. Martinez F, Sica A, Mantovani A, Locati M. Macrophage activation and polarization. Front Biosci. 2008;13:453–61.

67. Balbo P, Silvestri M, Rossi GA, Crimi E, Burastero SE. Differential role of CD80 and CD86 on alveolar macrophages in the presentation of allergen to T lymphocytes in asthma. Clin Exp Allergy. 2001;31(4):625–36.

68. Porta C, Riboldi E, Ippolito A, Sica A. Molecular and epigenetic basis of macrophage polarized activation. Semin Immunol. 2015;27(4):237–48.

69. Cruz MS, Diamond A, Russell A, Jameson JM. Human αβ and γδ T cells in skin immunity and disease. Front Immunol. 2018;9(1304):1–13.

70. Jameson J. A Role for Skin gamma delta T Cells in Wound Repair. Science (80-). 2002;296(5568):747–9.

71. Novak ML, Koh TJ. Macrophage phenotypes during tissue repair. J Leukoc Biol.

2013;93(6):875–81.

72. Gordon S, Martinez FO. Alternative activation of macrophages: mechanism and functions. Immunity. 2010;32(5):593–604.

73. Bruno A, Pagani A, Pulze L, Albini A, Dallaglio K, Noonan DM, et al. Orchestration of Angiogenesis by Immune Cells. Front Oncol. 2014;4(131).

74. Roszer T. Understanding the mysterious M2 macrophage through activation markers and effector mechanisms. Mediators Inflamm. 2015;2015:1–16.

75. Rees PA, Greaves NS, Baguneid M, Bayat A. Chemokines in Wound Healing and as Potential Therapeutic Targets for Reducing Cutaneous Scarring. Adv Wound Care. 2015;4(11):687–703.

76. Ferrante CJ, Leibovich SJ. Regulation of Macrophage Polarization and Wound Healing. Adv Wound Care. 2012;1(1):10–6.

77. Mantovani A, Sica A, Sozzani S, Allavena P, Vecchi A, Locati M. The chemokine system in diverse forms of macrophage activation and polarization. Trends Immunol. 2004;25(12):677–86.

78. Zizzo G, Hilliard BA, Monestier M, Cohen PL. Efficient Clearance of Early Apoptotic Cells by Human Macrophages Requires M2c Polarization and MerTK Induction. J Immunol. 2012;189(7):3508–20.

79. Wang Q, Ni H, Lan L, Wei X, Xiang R, Wang Y. Fra-1 protooncogene regulates IL-6 expression in macrophages and promotes the generation of M2d macrophages. Cell Res. 2010;20(6):701–12.

80. MacLeod AS, Mansbridge JN. The Innate Immune System in Acute and Chronic Wounds. Adv Wound Care. 2016;5(2):65–78.

81. Newby AC. Metalloproteinase expression in monocytes and macrophages and its relationship to atherosclerotic plaque instability. Arterioscler Thromb Vasc Biol. 2008;28(12):2108–14.

82. Gauglitz G, Korting H, Pavicic T, Ruzicka T, Jeschke M. Hypertrophic scarring and keloids: pathomechanisms and current and emerging treatment strategies. Mol Med. 2011;17(1–2):113–25.

83. National Institute for Health and Care Excellence. Chronic wounds: advanced wound dressings and antimicrobial dressings | Key-points-from-the-evidence | Advice | NICE. 2016;(March):1–43.

84. Shankaran V, Brooks M, Mostow E. Advanced therapies for chronic wounds: NPWT, engineered skin, growth factors, extracellular matrices. Dermatol Ther. 2013;26(3):215–21.

85. Bharambe S V., Darekar AB, Saudagar RB. Wound healing dressings and drug delivery systems: A review. Int J Pharm Technol. 2013;5(3):2764–86.

86. Simões D, Miguel SP, Ribeiro MP, Coutinho P, Mendonça AG, Correia IJ. Recent advances on antimicrobial wound dressing: A review. Eur J Pharm Biopharm. 2018;127:130–41.

87. Tonda-Turo C, Ruini F, Ceresa C, Gentile P, Varela P, Ferreira AM, et al. Nanostructured scaffold with biomimetic and antibacterial properties for wound

healing produced by 'green electrospinning.' Colloids Surfaces B Biointerfaces. 2018;172:233–43.

88. Pfalzgraff A, Brandenburg K, Weindl G. Antimicrobial peptides and their therapeutic potential for bacterial skin infections and wounds. Front Pharmacol. 2018;9(281):1–23.

89. Pal C, Asiani K, Arya S, Rensing C, Stekel DJ, Larsson DGJ, et al. Metal Resistance and Its Association With Antibiotic Resistance. In: Advances in Microbial Physiology. 2017. p. 261–313.

90. Zasloff M. Antimicrobial peptides of multicellular organisms. Nature. 2002;415(6870):389–95.

91. Lewies A, Du Plessis LH, Wentzel JF. Antimicrobial Peptides: the Achilles' Heel of Antibiotic Resistance? Probiotics Antimicrob Proteins. 2018;1–12.

92. Fjell CD, Hiss JA, Hancock REW, Schneider G. Designing antimicrobial peptides: Form follows function. Nat Rev Drug Discov. 2012;11(1):37–51.

93. Joo HS, Fu CI, Otto M. Bacterial strategies of resistance to antimicrobial peptides. Philos Trans R Soc B Biol Sci. 2016;371(1695).

94. Kumar P, Kizhakkedathu JN, Straus SK. Antimicrobial peptides: Diversity, mechanism of action and strategies to improve the activity and biocompatibility in vivo. Biomolecules. 2018;8(4):1–24.

95. Hassan M, Kjos M, Nes IF, Diep DB, Lotfipour F. Natural antimicrobial peptides from bacteria: Characteristics and potential applications to fight against antibiotic resistance. J Appl Microbiol. 2012;113(4):723–36.

96. Su Z, Zhang Q, Huang Y, Xiang Q, Li Y. Overview on the recent study of antimicrobial peptides: Origins, functions, relative mechanisms and application. Peptides. 2012;37(2):207–15.

97. Ganz T. The Role of Antimicrobial Peptides in Innate Immunity. Integr Comp Biol. 2006;43(2):300–4.

98. Hilchie AL, Wuerth K, Hancock REW. Immune modulation by multifaceted cationic host defense (antimicrobial) peptides. Nat Chem Biol. 2013;9(12):761–8.

99. Hancock REW, Haney EF, Gill EE. The immunology of host defence peptides: Beyond antimicrobial activity. Nat Rev Immunol. 2016;16(5):321–34.

100. Brown KL, Hancock REW. Cationic host defense (antimicrobial) peptides. Curr Opin Immunol. 2006;18(1):24–30.

101. Chen Y, Guarnieri MT, Vasil AI, Vasil ML, Mant CT, Hodges RS. Role of peptide hydrophobicity in the mechanism of action of α-helical antimicrobial peptides. Antimicrob Agents Chemother. 2007;51(4):1398–406.

102. Gagnon MC, Strandberg E, Grau-Campistany A, Wadhwani P, Reichert J, Bürck J, et al. Influence of the Length and Charge on the Activity of α-Helical Amphipathic Antimicrobial Peptides. Biochemistry. 2017;56(11):1680–95.

103. Jiang Z, Vasil AI, Hale JD, Hancock REW, Vasil ML, Hodges RS. Effects of net charge and the number of positively charged residues on the biological activity of amphipathic α-helical cationic antimicrobial peptides. Biopolym - Pept Sci Sect. 2008;90(3):369–83.

104. Mangoni ML, Shai Y. Short native antimicrobial peptides and engineered ultrashort lipopeptides: Similarities and differences in cell specificities and modes of action. Cell Mol Life Sci. 2011;68(13):2267–80.

105. Shai Y. Mode of action of membrane active antimicrobial peptides. Biopolym - Pept Sci Sect. 2002;66(4):236–48.

106. Guilhelmelli F, Vilela N, Albuquerque P, Derengowski L da S, Silva-Pereira I, Kyaw CM. Antibiotic development challenges: The various mechanisms of action of antimicrobial peptides and of bacterial resistance. Front Microbiol. 2013;4(353).

107. Chen L, Gao L, Fang W, Golubovic L. How the Antimicrobial Peptides Kill Bacteria: Computational Physics Insights. Commun Comput Phys. 2012;11(03):709–25.

108. Gomes P, Martins MCL, Montelaro RC, Costa F, Carvalho IF. Covalent immobilization of antimicrobial peptides (AMPs) onto biomaterial surfaces. Acta Biomater. 2010;7(4):1431–40.

109. Melo MN, Ferre R, Castanho MARB. Antimicrobial peptides: Linking partition, activity and high membrane-bound concentrations. Nat Rev Microbiol. 2009;7(3):245–50.

110. Brogden KA. Antimicrobial peptides: Pore formers or metabolic inhibitors in bacteria? Nat Rev Microbiol. 2005;3(3):238–50.

111. Wenzel M. Bacterial response to membrane - active peptide antibiotics. Ruhr University Bochum; 2013.

112. Wimley WC. Describing the mechanism of antimicrobial peptide action with the interfacial activity model. ACS Chem Biol. 2010;5(10):905–17.

113. Van 'T Hof W, Veerman ECI, Heimerhorst EJ, Nieuw Amerongen A V. Antimicrobial peptides: Properties and applicability. Biol Chem. 2001;382(4):597–619.

114. Uematsu N, Matsuzaki K. Polar angle as a determinant of amphipathic α-helix-lipid interactions: A model peptide study. Biophys J. 2000;79(4):2075–83.

115. Yeaman MR. Mechanisms of Antimicrobial Peptide Action and Resistance. Pharmacol Rev. 2003;55(1):27–55.

116. Wenzel M, Kohl B, Münch D, Raatschen N, Albada HB, Hamoen L, et al. Proteomic response of Bacillus subtilis to lantibiotics reflects differences in interaction with the cytoplasmic membrane. Antimicrob Agents Chemother. 2012;56(11):5749–57.

117. Wenzel M, Chiriac AI, Otto A, Zweytick D, May C, Schumacher C, et al. Small cationic antimicrobial peptides delocalize peripheral membrane proteins. Proc Natl Acad Sci USA. 2014;111(14):E1409–18.

118. Nijnik A, Hancock R. Host defence peptides: antimicrobial and immunomodulatory activity and potential applications for tackling antibiotic-resistant infections. Emerg Health Threats J. 2012;2(1):7078.

119. Afacan NJ, Yeung ATY, Pena OM, Hancock REW. Therapeutic potential of host defense peptides in antibiotic-resistant infections. Curr Pharm Des. 2012;18(6):807–19.

120. Lai Y, Gallo RL. AMPed up immunity: how antimicrobial peptides have multiple roles in immune defense. Trends Immunol. 2009;30(3):131–41.

121. Hancock REW, Nijnik A, Philpott DJ. Modulating immunity as a therapy for bacterial infections. Nat Rev Microbiol. 2012;10(4):243–54.

122. Ulm H, Wilmes M, Shai Y, Sahl H-G. Antimicrobial Host Defensins – Specific Antibiotic Activities and Innate Defense Modulation. Front Immunol. 2012;3:249.

123. Nakatsuji T, Gallo RL. Antimicrobial peptides: Old molecules with new ideas. J Invest Dermatol. 2012;132(3):887–95.

124. Conlon JM. Host-defense peptides of the skin with therapeutic potential: From hagfish to human. Peptides. 2015;67:29–38.

125. Mansour SC, De La Fuente-Núñez C, Hancock REW. Peptide IDR-1018: Modulating the immune system and targeting bacterial biofilms to treat antibiotic-resistant bacterial infections. J Pept Sci. 2015;21(5):323–9.

126. Thangamani S, Nepal M, Chmielewski J, Seleem M. Antibacterial activity and therapeutic efficacy of Fl-P(R)P(R)P(L)-5, a cationic amphiphilic polyproline helix, in a mouse model of staphylococcal skin infection. Drug Des Devel Ther. 2015;9:5749–54.

127. Mohamed MF, Abdelkhalek A, Seleem MN. Evaluation of short synthetic antimicrobial peptides for treatment of drug-resistant and intracellular Staphylococcus aureus. Sci Rep. 2016;6:29707.

128. Marr AK, Gooderham WJ, Hancock RE. Antibacterial peptides for therapeutic use: obstacles and realistic outlook. Curr Opin Pharmacol. 2006;6(5):468–72.

129. Won H-S, Kim J-H, Lee B-J, Seo M-D, Mishig-Ochir T. Antimicrobial Peptides for Therapeutic Applications: A Review. Molecules. 2012;17(10):12276–86.

130. Lázár V, Martins A, Spohn R, Daruka L, Grézal G, Fekete G, et al. Antibiotic-resistant bacteria show widespread collateral sensitivity to antimicrobial peptides. Nat Microbiol. 2018;3(6):718–31.

131. Hill KE, Wilson MJ, Howard AJ, Thomas DW, Howell-Jones RS, Price PE. A review of the microbiology, antibiotic usage and resistance in chronic skin wounds. J Antimicrob Chemother. 2005;55(2):143–9.

132. Näslund Salomonsson E, Nilsson E, Björn C, Mahlapuu M, Johansson A-L, Noppa L, et al. Efficacy and safety profile of the novel antimicrobial peptide PXL150 in a mouse model of infected burn wounds. Int J Antimicrob Agents. 2015;45(5):519–24.

133. Nijnik A, Madera L, Ma S, Waldbrook M, Elliott MR, Easton DM. Synthetic Cationic Peptide IDR-1002 Provides Protection against Bacterial Infections through Chemokine Induction and Enhanced Leukocyte Recruitment. J Immunol. 2010;184(5):2539–50.

134. Scott MG, Dullaghan E, Mookherjee N, Glavas N, Waldbrook M, Thompson A. An anti-infective peptide that selectively modulates the innate immune response. Nat Biotechnol. 2007;25(4):465–72.

135. Jorge P, Lourenço A, Pereira MO. New trends in peptide-based anti-biofilm strategies: a review of recent achievements and bioinformatic approaches. Biofouling. 2012;28(10):1033–61.

136. M.C. Chung E, Dean SN, Propst CN, van Hoek ML, Bishop BM. Komodo dragon-inspired synthetic peptide DRGN-1 promotes wound-healing of a mixed-biofilm

infected wound. npj Biofilms Microbiomes. 2017;3(9).

137. Kosikowska P, Lesner A. Antimicrobial peptides (AMPs) as drug candidates: a patent review (2003–2015). Expert Opin Ther Pat. 2016;26(6):689–702.

138. Amblard M, Fehrentz JA, Martinez J, Subra G. Methods and protocols of modern solid phase peptide synthesis. Mol Biotechnol. 2006;33(3):239–54.

139. Chan WC, White PD. Solid Phase Peptide Synthesis — A Practical Approach. Vol. 12, Reactive Polymers. 2003. 310 p.

140. Hancock REW, Sahl HG. Antimicrobial and host-defense peptides as new anti-infective therapeutic strategies. Nat Biotechnol. 2006;24(12):1551–7.

141. Kang S-J, Park SJ, Mishig-Ochir T, Lee B-J. Antimicrobial peptides: therapeutic potentials. Expert Rev Anti Infect Ther. 2014;12(12):1477–86.

142. Yi T, Sun S, Huang Y, Chen Y. Prokaryotic expression and mechanism of action of aα-helical antimicrobial peptide A20L using fusion tags. BMC Biotechnol. 2015;15(1):69.

143. Mahlapuu M, Håkansson J, Ringstad L, Björn C. Antimicrobial Peptides: An Emerging Category of Therapeutic Agents. Front Cell Infect Microbiol. 2016;6:194.

144. Fox JL. Antimicrobial peptides stage a comeback. Nat Biotechnol. 2013;31(5):379–82.

145. Tam JP, Lu YA, Yang JL. Correlations of cationic charges with salt sensitivity and microbial specificity of cystine-stabilized β-strand antimicrobial peptides. J Biol Chem. 2002;277(52):50450–6.

146. Ergene C, Yasuhara K, Palermo EF. Biomimetic antimicrobial polymers: Recent advances in molecular design. Polym Chem. 2018;9(18):2407–27.

147. Sartori S, Chiono V, Tonda-Turo C, Mattu C, Ciardelli G. Biomimetic polyurethanes in nano and regenerative medicine. J Mater Chem B. 2014;2(32):5128–44.

148. Sovadinova I, Palermo EF, Urban M, Mpiga P, Caputo GA, Kuroda K. Activity and Mechanism of Antimicrobial Peptide-Mimetic Amphiphilic Polymethacrylate Derivatives. Polymers (Basel). 2011;3(3):1512–32.

149. Takahashi H, Caputo GA, Vemparala S, Kuroda K. Synthetic Random Copolymers as a Molecular Platform to Mimic Host-Defense Antimicrobial Peptides. Bioconjug Chem. 2017;28(5):1340–50.

150. Sgolastra F, Deronde BM, Sarapas JM, Som A, Tew GN. Designing mimics of membrane active proteins. Acc Chem Res. 2013;46(12):2977–87.

151. Punia A, He E, Lee K, Banerjee P, Yang NL. Cationic amphiphilic non-hemolytic polyacrylates with superior antibacterial activity. Chem Commun. 2014;50(53):7071–4.

152. Punia A, Debata PR, Banerjee P, Yang NL. Structure-property relationships of antibacterial amphiphilic polymers derived from 2-aminoethyl acrylate. RSC Adv. 2015;5(115):95300–6.

153. Colak S, Nelson CF, Nusslein K, Tew GN. Hydrophilic modifications of an amphiphilic polynorbornene and the effects on its hemolytic and antibacterial activity. Biomacromolecules. 2009;10(2):353–9.

154. Lienkamp K, Madkour AE, Musante A, Nelson CF, Nüsslein K, Tew GN. Antimicrobial polymers prepared by ROMP with unprecedented selectivity: A molecular construction kit approach. J Am Chem Soc. 2008;130(30):9836–43.

155. Tan JPK, Gao S, Hedrick JL, Zhang Y, Guo XD, Li L, et al. Biodegradable nanostructures with selective lysis of microbial membranes. Nat Chem. 2011;3(5):409–14.

156. Ong ZY, Coady DJ, Yang C, Hedrick JL, Yang Y-Y, Qiao Y. Highly dynamic biodegradable micelles capable of lysing Gram-positive and Gram-negative bacterial membrane. Biomaterials. 2011;33(4):1146–53.

157. Nimmagadda A, Liu X, Teng P, Su M, Li Y, Qiao Q, et al. Polycarbonates with Potent and Selective Antimicrobial Activity toward Gram-Positive Bacteria. Biomacromolecules. 2017;18(1):87–95.

158. Li L, Chin W, Zhong G, Dong H, Xu L, Cheng J, et al. Biodegradable Antimicrobial Polycarbonates with In Vivo Efficacy against Multidrug-Resistant MRSA Systemic Infection. Adv Healthc Mater. 2015;4(14):2128–36.

159. Konai MM, Bhattacharjee B, Ghosh S, Haldar J. Recent Progress in Polymer Research to Tackle Infections and Antimicrobial Resistance. Biomacromolecules. 2018;19(6):1888–917.

*"*Part of the work described in chapter one has been previously published in
Varela, P., Sartori, S., Viebahn, R., Salber, J. & Ciardelli, G. (2019) *'Macrophage immunomodulation: An indispensable tool to evaluate the performance of wound dressing biomaterials'* Journal of Applied Biomaterials & Functional Materials
DOI: 10.1177/2280800019830355*"*

CHAPTER TWO

‘Clinically applied wound dressings loaded with silver: Antimicrobial efficacy and response of human macrophages to Atrauman, Biatain and Polymem’

Graphical abstract

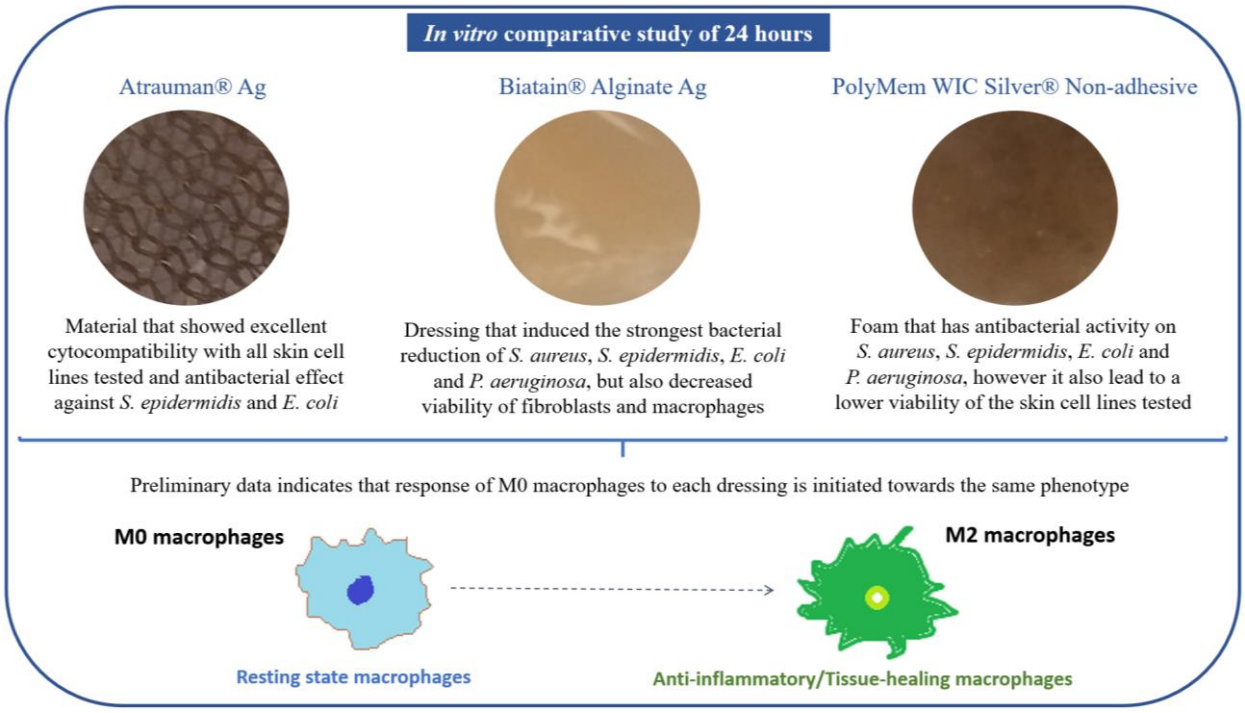

Abstract

A high number of wound infections is a serious problem worldwide. To reverse this trend, many wound dressings with antimicrobial properties have been developed. Considering the increasing presence of conventional antibiotic-resistant microorganisms, product developers have been focussing their effort in introducing antibiotic-free antibacterial wound dressings to the market, with silver being the most common incorporated antimicrobial agent. However, more information about the microbial and eukaryotic cells' response to these dressings is needed for a proper selection of antimicrobial dressings for each infected wound case. In particular, one insufficiently explored parameter is their effect on the immunomodulation of macrophages, that are a crucial wound repair participating immune cell population, that plays a key role in the transition of the inflammation to the proliferation phase of wound healing.

Three different clinically applied antimicrobial wound dressings, that have silver impregnated, were selected for this study: Atrauman® Ag, Biatain® Alginate Ag and PolyMem WIC Silver® Non-adhesive. Antimicrobial susceptibility tests (disk diffusion and broth dilution), cell viability evaluation (CellTiter-Blue®) and experiments to determine macrophage polarization (e.g. flow cytometry, ELISA and glucose uptake) were performed after 24 hours of incubation. Among all materials, Biatain® Alginate Ag induced the most evident bactericidal effect on Gram-positive and Gram-negative bacteria tested, followed by PolyMem WIC Silver® Non-adhesive, but did not show good cytocompatibility *in vitro*. While Atrauman® Ag showed excellent cytocompatibility results on L929 fibroblasts, HaCaT keratinocytes and THP-1 derived macrophages, but no significant antimicrobial activity was observed. Overall, it was confirmed that macrophages initiate, in fact, an alteration of their metabolism and phenotype in response to wound dressings of different composition in a short period of contact (24 hours). M0 resting state macrophages common response to all silver-containing dressings used in this study was to increase the production of the anti-inflammatory cytokine TGF-β, which indicates an acquisition of M2-like macrophages characteristics.

2.1. Introduction

Numerous wound dressing products exist on the market (1). Clinicians are daily faced with the extreme difficult challenge of selecting the most appropriate dressing for each specific case, by doing a comprehensive assessment of the wound status and collecting clinical data of the patient's physical features (2). The market has been developing dressings with antimicrobial properties in accordance with the prevalent high number of skin and soft skin infection cases

(also known as acute bacterial skin and skin structure infections) of inpatient and outpatient health care (3,4). In particular, antibiotic-free antibacterial wound dressings are on the rise, in accordance with the constantly increasing number of bacterial species isolated from non-healing wounds that are resistant to commonly used antibiotics in the hospital setting (5). Among the available products, silver-based wound dressings definitely dominate the market, due to the silver's broad antimicrobial activity against more than 600 clinically isolated strains of non- and more importantly drug-resistant bacteria (3,6,7). With a few exceptions, the antimicrobial principle of these silver dressings relies on the release of silver ions (Ag^+) that induce the antimicrobial activity. Silver ions are antibacterial through various mechanisms of action such as their interaction with the bacterial membrane, destabilizing the phospholipidic layer or leading to a decrease of adenosine triphosphate (ATP) levels, their induction of an increased production of reactive oxygen species (ROS) and their interaction with cytosolic components as enzymes and nucleic acids (8). However, these dressings are not sufficiently explored, especially concerning the effects on immunomodulation of macrophages, a crucial wound healing participating immune cell population (9). Acquisition of data on macrophage-biomaterial interactions is decisive to have a more complete assessment of the characteristics of each wound matrix and could lead to the selection of the most appropriate material to prevent or reduce local infection. Wound healing is a highly complex regulated process. The optimal wound healing stages in chronological order go through haemostasis, inflammation, proliferation and remodelling phases (9,10). During this process, macrophages are playing key roles through their plasticity in a continuous spectrum by shifting from a predominant M1 pro-inflammatory population to an anti-inflammatory/tissue-remodelling M2 phenotype, with some populations sharing characteristics of M1 and M2 macrophages (11). A very important function of macrophages is their intervention in the transition of inflammatory to proliferation phase of wound healing (12). After an injury, during the early stages of repair in cutaneous healing, M1 macrophages are more frequently found (13). They are specialized in phagocytising dead cells and their components, besides attracting other macrophages to the damage location (14). M1 macrophages are known for being antigen presenting cells and for producing the antibacterial oxidative metabolite nitric oxide (NO), which is an antimicrobial agent. Their metabolism is activated towards the production of high levels of pro-inflammatory cytokines such as IFN-Ɣ, IL-1, IL-6 and TNF- α (15,16). Typically, M1 macrophages present augmented levels of major histocompatibility complex (MHC) cell surface receptors, known as HLA-DR, and the chemokine receptors CD197 that bind CCL19 and CCL21 (17).

In contrast, M2-like macrophages appear in higher quantity during proliferation and remodelling phases of the wound healing process. Different from M1 macrophages, M2-like macrophages express high levels of galactose receptors, mannose receptors (CD206) and haemoglobin scavenger receptors (CD163) (11,15). Moreover, these cells constantly produce anti-inflammatory cytokines such as IL-4 and IL-10, and the growth factor TGF-β that has the important function of inducing proliferation of human fibroblasts, leading to remodelling of the new extracellular matrix for an optimal wound closure (18,19).

Unfortunately, in infected wounds a transition from inflammatory to proliferation/remodelling phases is not achieved and a persistent inflammation environment is sensed (14). In such cases, it is needed to avoid external factors, such as biomaterials composition, which would prompt this unfavourable environment. Hence it is pivotal to evaluate the immunomodulatory effect that different types of commercially available products induce.

In this chapter, research activities were carried out to explore the antimicrobial efficacy of silver containing biomaterials that are used on infected wounds, with a major focus on the response of macrophages to the material, that currently is an insufficiently understood parameter. A comparative test of the matrix without and with the antimicrobial agent (silver) is also included.

2.2. Material and Methods

2.2.1. Wound dressing materials

The commercially available wound dressings for this research work were selected according to the most applied products in clinical set-ups at the University Medical Centre (UMC) of Bochum in Germany. The selected dressings have the same active component – silver ions – being released in different concentrations/time and from diverse systems: metallic silver, patented ion silver complex salt (patent EP1654013B1, registered by Coloplast) or nanocrystalline silver particles. The characteristics of the chosen untreated wound dressings and their correspondent dressings incorporated with a specific type of silver are described in **table 2.1**. Before starting the biological experiments, disks were cut out of the wound dressings in a non-sterile environment and afterwards were sterilized under Ultra-violet light for 20 minutes, since it is a simple and non-expensive technique extensively used in the area of medical research, and has a strong antimicrobial activity (20).

Table 2.1. Selected commercially available wound dressing products (adapted from the informative documents provided by the suppliers).

Name of Product	Base constitution	Quantity and Type of silver	Other characteristics
Atrauman®	Polyester mesh	Not present	Porous structure (1 mm pore size) and impregnated with neutral ointment that contains fatty acids to promote wound closure
Atrauman® Ag	Polyamide mesh	300 - 500 μg/cm^2 of unreactive metallic silver Ag(0) that in aqueous or moist environment is rapidly ionised to silver ions Ag^+	Impregnated with ointment made of ester mixture of natural and vegetable fatty acids (Macrogol 2000)
Biatain® Alginate	Dressing consisting of 85% alginate and 15% carboxymethyl cellulose	Not present	High dressing integrity and calcium ions are released from the dressing inducing a haemostatic effect
Biatain® Alginate Ag		950 μg/cm^2 of inorganic salt that releases ionic silver Ag^+ in the presence of wound exudate	Highly absorbent, and provides a haemostatic effect
PolyMem® WIC Non-adhesive	Polyurethane foam	Not present	Contains a humectant (glycerol) that avoids the dressing to dry and to adhere to the wound bed, a non-ionic surfactant (poloxamer 188) that facilitates wound cleansing, and a starch copolymer to enhance the fluid handling properties of the foam
PolyMem WIC Silver® Non-adhesive		124 μg/cm^2 of nanocrystalline silver particles that release clusters of extremely small and highly reactive silver particles, and silver ions, in wound fluid taken up by the dressing	

2.2.2. Culture conditions of bacterial and eukaryotic cell lines

Four bacterial strains known to infect open wounds were selected for this work. All strains were obtained from the American Type Culture Collection (ATCC). Two of them are Gram-positive – *Staphylococcus aureus subsp. aureus* Rosenbach (ATCC® 29213™) and *Staphylococcus epidermidis* (Winslow and Winslow) Evans (ATCC® 12228™) – and the others are Gram-negative bacteria – *Escherichia coli* (Migula) Castellani and Chalmers (ATCC® 25922™) and *Pseudomonas aeruginosa* (Schroeter) Migula (ATCC® 27853™). For all experiments, bacterial cells were grown at 37°C for 18h on blood agar plates (mixture of nutrient agar with 5% sheep blood pH ~7.4).

Fibroblasts, keratinocytes and monocyte-derived macrophages, which are cell populations that constitute skin, were used to evaluate the effects of the dressings on 2D cell culture layers of mammalian cells. For all cell lines, the cell number was determined on a Neubauer counting chamber in the presence of 0.4% trypan blue (Gibco) to exclude non-viable cells.

Murine fibroblasts L929 cell line (German Collection of Microorganisms and Cell Cultures – DSMZ) was cultured in RPMI 1640 medium with stable glutamine (PAN Biotech), supplemented with 10% heat-inactivated Fetal bovine serum - FBS (PAN Biotech), and 100 U/mL penicillin - 0.1 mg/mL streptomycin (PAN Biotech). Cells were maintained in T75 vented cap culture flasks (ThermoFisher Scientific) at 37°C in an atmosphere containing 5% CO_2, by sub-passage with 0.25% Trypsin 1 mM EDTA (PAN Biotech) at each 2-3 days.

The keratinocyte immortalized cell line HaCaT (Deutsches Krebsforschungszentrum - DKFZ, Heidelberg) was expanded in 4.5 g/L glucose Dulbecco's Modified Eagle Medium – high glucose DMEM (ThermoFisher Scientific) completed with 10% heat-inactivated Fetal bovine serum (FBS) (PAN Biotech), and 100 U/mL penicillin - 0.1 mg/mL streptomycin (PAN Biotech) in T75 vented cap culture flasks (ThermoFisher Scientific) at 37°C and 5% CO_2.. The detachment of adhered cells was performed with TrypLE Express (ThermoFisher Scientific). The splitting ratio was from 1:5 to 1:10.

Human monocytic cell line THP-1 (ATCC) was grown at 37°C and 5% CO_2 in vertically positioned T75 vented cap culture flasks (ThermoFisher Scientific) in the exact same complete RPMI 1640 medium as previously described for L929 cells. Additional medium was added or renewed every 2 – 3 days when the maximum cell concentration was reached – $8x10^5$ cells/mL. To induce THP-1 monocyte differentiation to M0 macrophages, monocytes were first seeded on cell culture treated 24-well plates (density of 10^6 cells/mL) in the presence of 200 ng/mL of phorbol 12-myristate-13-acetate (PMA) (Sigma Aldrich) for 24 hours (37°C, 5% CO_2). Afterwards the medium was replaced to complete RPMI and cells were again incubated for 48 hours before any further experiment.

2.2.3. Antibacterial susceptibility tests

2.2.3.1.Disk diffusion

The European Committee on Antimicrobial Susceptibility Testing (EUCAST) guidelines were followed for this experiment (21). Briefly, well-isolated colonies were selected and immersed in 2 mL of 0.9% NaCl. Density was adjusted to MacFarland 0.5 turbidity standard (corresponds to ~$1\text{-}2x10^8$ colony forming units per millilitre - CFU/mL). With a sterile swab the inoculum was spread evenly on Mueller-Hinton agar plates.

Afterwards, the disks obtained from the antimicrobial dressing materials with 1 cm diameter size were carefully placed on the agar plates. As a first control, disks of untreated materials were placed on the agar to observe if there is not a bacterial growth inhibition without the

antibacterial agent. A second control was included in the tests with specific antibiotics known to inhibit the strains growth in order to validate the assay: 1 µg oxacillin for *S. aureus* and *S. epidermidis*, and 300 µg streptomycin for *E. coli* and *P. aeruginosa*. Plates were incubated at 37°C for 16-20 hours (in duplicates). Photographs were acquired with a Panasonic Lumix DMC-FZ100 digital camera.

2.2.3.2.Colonies count to determine bacterial reduction in broth medium

In order to determine the bacterial reduction in the presence of the material, the broth microdilution method was performed following the EUCAST recommendation to use the ISO 20776-1:2006 standard, with some modifications. The dressing material was cut to circles of 6.5 mm diameter that were placed in duplicates on the bottom of 96-well plates. Colonies selected from an overnight culture grown on blood agar plates were inserted in a tube with 2 mL 0.9% saline solution NaCl. Turbidity was adjusted to MacFarland 0.5 and the inoculum was diluted 400-fold in Mueller-Hinton broth (~$3.75x10^5$ CFU/ml). 100 µL of the bacteria suspension was added on the material on each well. The plate was incubated for 24h at 37°C. After this period, the turbidity of the well was visualized to determine if the material had sufficient concentration of antibacterial agent to inhibit the growth (minimal inhibitory concentration – MIC) of each bacteria strain. Following to the broth MIC test, the entire volume of the well was spread evenly on blood agar plates. These plates were incubated from 16 to 20 hours at 37°C and the colony forming units (CFU) were counted and compared to the initial CFU/mL.

2.2.4. Cytocompatibility test on different cell populations of skin

In a sterile flat bottom 24-well plate, $5x10^4$ cells per well for L929 fibroblasts and $5x10^5$ cells per well for HaCaT keratinocytes were cultured and incubated at 37ºC and 5% CO_2 for 24 hours to allow cell adherence. In the case of THP-1 monocytes, the period of incubation was longer due to the induced stimulation for its differentiation into M0 macrophages as previously described in point 2.2.2. After this time, the medium of the wells was renewed, and the sterilized materials (6.5 mm diameter) were added in triplicates on top of the cells on each well. The plate was kept in a humidified incubator (37ºC and 5% CO_2) for 24 hours. Afterwards, CellTiter-Blue® viability assay was performed following the provider instructions. Briefly, the CellTiter-Blue® is based on the conversion of resazurin (a redox dye) to resorufin (a fluorescent end-product) by living cells. After 2h of incubation with CellTiter-Blue reagent, the fluorescence intensity was quantified on a black 96 well-plate by measuring the fluorescence at 590 nm, after

excitation at 560 nm in a Tecan microplate reader Infinite® 200 PRO. As positive control a lysis solution of 9% Triton® X-100 (Promega) was added to the cells, and as negative control, cells were plated on the Tissue Culture Polystyrene (TCPS). This procedure was adapted from the ISO norm 10993-5:2009 (22).

2.2.5. Evaluation of the effects of the materials on macrophages

2.2.5.1.Morphological evaluation

Bright field images were acquired on an Olympus IX51 microscope with a magnification of 200× to observe the morphological characteristics of monocyte-derived macrophages after being exposed to the material for 24 hours.

2.2.5.2.Flow cytometry analysis

Analysis of the phenotypical characteristics of macrophages in the presence of wound dressings for 24 hours was performed by flow cytometry (Partec, Münster, Germany).

For direct labelling of cells, all fluorescein-isothiocyanate (FITC)- or phycoerythrin (PE)-conjugated anti-human monoclonal antibodies (Biolegend UK Ltd) were diluted 1:25 and incubated for 30 minutes at 4°C. The following antibodies were added to cells suspended in 1.5% paraformaldehyde (PFA): FITC-labeled mouse anti-human CD197 (clone G043H7), PE-labeled mouse anti-human HLA-DR (clone L243), PE-labeled mouse anti-human CD163 (clone GHI/61) and FITC-labeled mouse anti-human CD206 (clone 15-2). As autofluorescence control, unstained M0 macrophages were used. Data was analysed with FloMax software version 2.3 (Partec).

2.2.5.3. Quantification of cytokine production (ELISA)

Legend Max™ ELISA kits with pre-coated plates (BioLegend UK Ltd) were used to measure the pro-inflammatory cytokine IL-1β and anti-inflammatory cytokines, IL-10 and TGF-β, present in the cell culture supernatant of the different conditions tested following the manufacturer's procedure.

2.2.5.4. Nitric oxide detection

Nitrate/Nitrite Colometric assay kit (Cayman Chemical, Biomol GmbH, Germany) was used to quantify the concentration of total NO products (nitrate NO_3^- + nitrite NO_2^-) in the supernatant

that was produced by macrophages in the presence of 6 different materials for 24 hours. The method was according to manufacturer's instructions.

2.2.5.5. Glucose uptake

After 24 hours in the presence of the unloaded and antibacterial loaded dressing materials, the glucose uptake by macrophages was evaluated. After washing the wells of the 24-well plates with PBS, RPMI 1640 medium without glucose (Gibco™) supplemented with 100 µM of fluorescent d-glucose analog 2-[*N*-(7-nitrobenz-2-oxa-1,3-diazol-4-yl) amino]-2-deoxy-d-glucose (2-NBDG) (Cayman Chemical, Biomol GmbH, Germany) was added. The plates were incubated at 37°C for 60 minutes in the dark. The supernatant was removed and the wells were washed once with PBS. Accutase (PAN Biotech) was added to induce the detachment of the cells and the content of the wells was transferred to a black 96-well plate to read fluorescence (excitation 465/emission 540 nm) in a Tecan microplate reader Infinite® 200 PRO.

2.2.6. Statistical analysis

All data was first expressed as mean ± standard deviation of at least two independent assays in triplicate. The statistical analysis was performed with the GraphPad Prism 5.00.288 software by one-way analysis of variance (ANOVA) followed by Bonferroni's multiple comparison test. Statistically significant values are represented as * $p < 0.05$, ** $p < 0.01$ and *** $p < 0.001$.

2.3. Results and discussion

2.3.1. Antibacterial susceptibility to the clinically used antimicrobial wound dressings

The antibacterial efficacy of the 3 selected wound dressings was evaluated on four bacterial strains typically found in wound infections (*S.aureus*, *S.epidermidis*, *E.coli* and *P. aeruginosa*). As a first assessment of the antibacterial capacity of the materials, disk diffusion was performed. As expected, no bacterial inhibition was observed with the untreated materials (**figure 2.1, A, C and E**). The inhibition of growth or killing of bacteria depends on the method applied, the solution/agar used and the incubation time period, besides depending on the strains used and the specific characteristics of each material. In our evaluation, it was observed that only Biatain Alginate Ag was able to inhibit the growth of the 4 strains tested (**figure 2.1, table 2.2**). Atrauman Ag and PolyMem WIC Silver induced an inhibition zone against *S. epidermidis* only (**figure 2.1 and table 2.2**). The latter material was studied before against *S. aureus* and *P.*

aeruginosa and the same lack of antibacterial effect was observed on the agar disk diffusion test (23).

All materials have the antibacterial inhibition by the release of silver ions in common, that occurs optimally in contact with a moist or liquid environment, such as the exudate of wounds provide. However, these ions have a different origin for each material, and the basis polymer and quantity of silver is also diverse. It seems that in a short period of time, the Ag^+ generated from the inorganic salt used in Biatain Alginate Ag, diffuses quicker than the one originated by the metallic silver incorporated into Atrauman Ag and the silver ions and particles that are formed from the nanocrystalline silver of PolyMem WIC Silver. Moreover, it is important to take into consideration that among all dressings Biatain Alginate Ag is the material with most silver per cm^2 (0.95 mg/cm^2) (24).

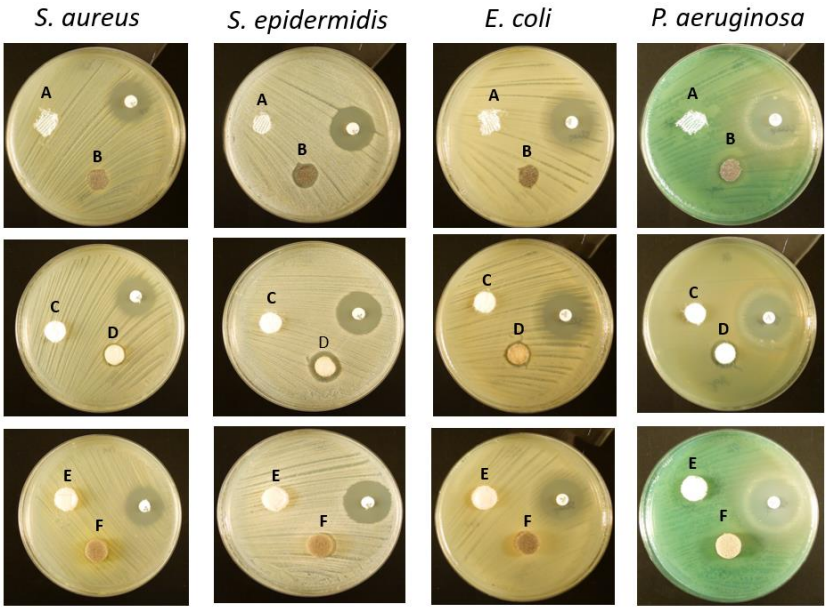

Figure 2.1. Representative images of the antibacterial susceptibility to the wound dressings by the disk diffusion method. A – Atrauman; B – Atrauman Ag; C – Biatain Alginate; D – Biatain Alginate Ag; E – PolyMem WIC; F – PolyMem WIC Silver. The antibiotic disks were oxacillin (*S. aureus* and *S. epidermidis*) and streptomycin (*E. coli* and *P. aeruginosa*).

Table 2.2. Diameter of the Halo of bacterial growth inhibition induced by the placed antibacterial commercial wound dressings.

Dressing material	Diameter of the inhibition zone (mm)			
	S.aureus	***S.epidermidis***	***E.coli***	***P. aeruginosa***
Atrauman® Ag	-	13.5 ± 0.5	-	-
Biatain® Alginate Ag	12.5 ± 0.5	16.5 ± 0.5	13.0 ± 0	15.5 ± 0.5
PolyMem WIC Silver®	-	12.5 ± 0.5	-	-

Average ± Standard deviation

Another antibacterial method was performed as complement to the disk diffusion results. In this method, the dressings were completely submersed in Mueller-Hinton broth with a more liquid environment than disk diffusion and differences on the antibacterial properties were clearly observed. Moreover, with the colony forming units (CFU) counted after 24 hours, it was possible to determine the exact reduction of CFU/mL provoked by each antimicrobial dressing. Atrauman Ag seems to prevent the continuous growth of *S. epidermidis* and *E. coli* (**figure 2.2**). In case of *E. coli* this effect was not observed on the disk diffusion test, probably because the agar is not sufficiently moist to induce the release of enough quantity of silver ions. As observed in disk diffusion, no antibacterial effect was detected against *S. aureus* and *P. aeruginosa* (**figure 2.1**). These results are not in accordance with previous studies performed by the material developers, that observed bacterial reductions of all strains within 24 hours. However, their antibacterial evaluation method was entirely different from the ones applied in the present study. The EUCAST guidelines followed here were performed to have uniformity in all tests with the different wound dressings, whereas in the other study the standard method 2180 of the American Society for Testing Materials was used, in which the melted agar was inoculated with the different bacterial strains and then dispersed onto the dressing to be examined (25). In the latter method, bacteria are 'forced' to grow on the silver dressing creating an enclosed environment in which the thin agar inoculated layer is in closer contact with the wound dressing. This might be an explanation for the different results, because in both methods bacteria are still growing on an optimal surface (MHB agar) or in a nutritious medium (MHB broth), giving space to avoid the antibacterial effect from the Atrauman Ag dressing *in vitro*. It is also important to notice that metallic silver is relatively inert and releases biocidal Ag^+ ions when interacting with moisture and wound fluid on skin, which have different constituents than the ones existing on MHB (26). This can be a factor that influenced the release of silver ions. Biatain Alginate Ag was able to induce 80 to 99% reduction of CFU/mL on all strains tested, showing significantly different values of CFU in the presence of this material versus the initial bacterial concentration (**figure 2.2**). This result, in combination with the disk diffusion, proves that due to the higher concentration of the ionic silver complex in the dressing and its type of silver system, Biatain Alginate Ag allows a rapid dissociation of the inorganic salt in contact with a aqueous environment releasing Ag^+ ions more effectively in the first 24 hours than the other dressings.

PolyMem WIC Silver showed efficient antibacterial properties in a liquid medium, in comparison with the disk agar diffusion method. Here a significant reduction of bacterial CFU against *S. epidermidis* and both Gram-negative strains was determined. For *S. aureus* this

dressing seems to induce a bacteriostatic effect (**figure 2.2**). Thus, the release of clusters of reactive small particles and silver ions from the nanocrystalline silver seems to be very reduced on agar. Moreover, Boonkaew *et al.* observed a zone of inhibition against *Staphylococcus aureus* if the material is pre-activated in 0.85% saline solution by inducing its swelling, before it is placed on the agar plate (27). Hence, it becomes clear that the fluid taken up by this polyurethane foam plays a major role in unleashing the antimicrobial power of nanocrystalline silver. During the course of experiments, among all the dressings tested, it was noted that PolyMem and PolyMem WIC Silver were highly absorbent, entrapping a part of the liquid medium in its foam. This was also observed by Burd *et al.*, in which this absorbency capacity was associated with the very low release of silver ions measurement but still a great antibacterial effect was determined. This result lead the authors to conclude that PolyMem WIC silver dressing induces its antibacterial effect mainly by 'soaking' the pathogenic bacteria and its contaminants into the foam structure and induce its 'killing' internally (28). In addition, the same authors stated that this could be a benefit, because it will decrease the possibility for toxicity on the healthy wound cells (28).

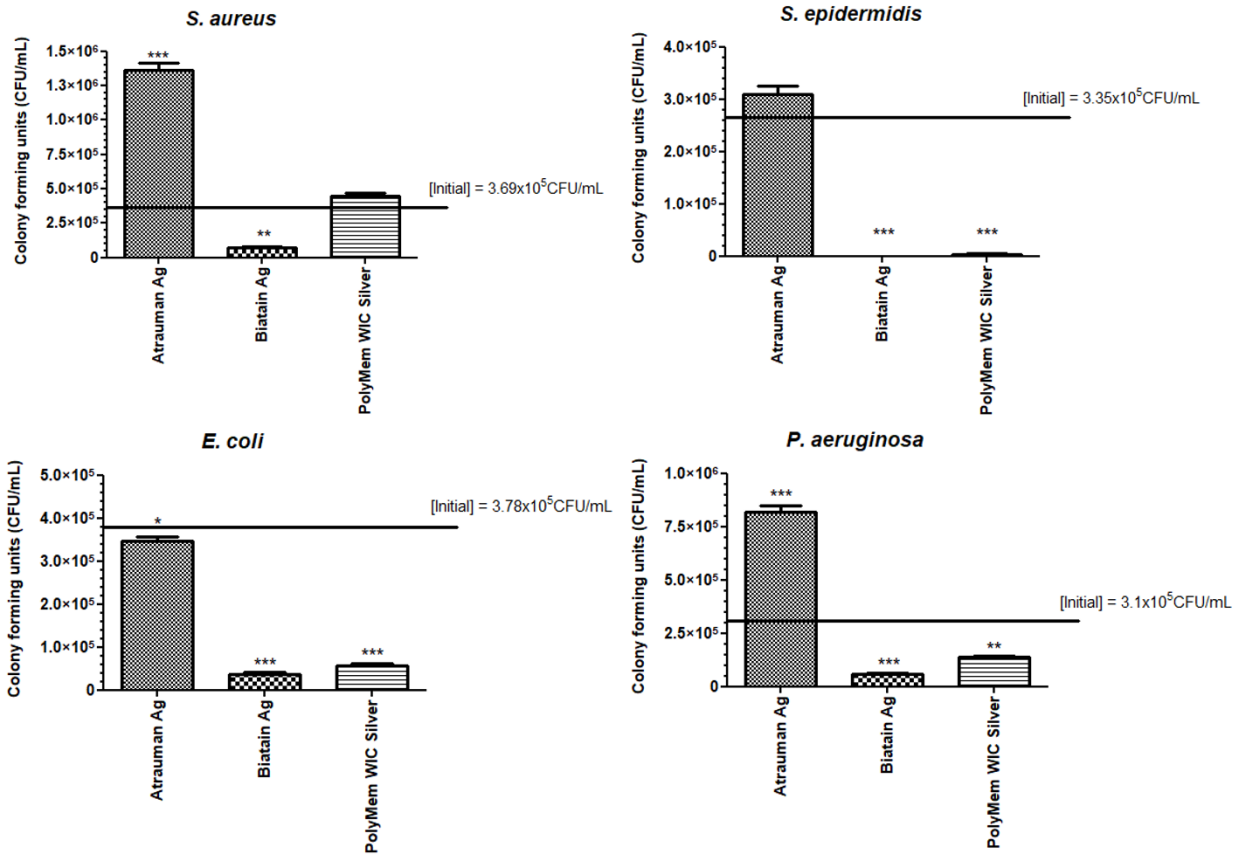

Figure 2.2. Bacterial growth or reduction (in reference to the initial inoculum) in the presence of the antibacterial materials for 24 hours assessed by counting the colony forming units/mL. p values were determined for all groups versus initial CFU/mL. Statistical significance is presented as following * $p \leq 0.05$, ** $p \leq 0.01$ and *** $p \leq 0.001$.

2.3.2. Bioevaluation of the cytocompatibility of the wound dressings

To perform a preliminary direct contact assessment of the biomaterial compatibility *in vitro* on 2D-cell cultures, three cell populations that are involved in wound regeneration were selected: fibroblasts, keratinocytes and monocyte-derived macrophages.

Among the 6 types of materials, Atrauman and Atrauman Ag showed an excellent cytocompatibility to the three different cell lines (**figure 2.3**).

The high concentration of silver complex salt in Biatain Alginate Ag leads to the release of the active component's Ag^+ ions, that turned out to be cytotoxic to the populations tested. The lower cell viability can be ascribed to the incorporated Ag^+ ions due to the statistical difference observed in comparison with silver-free Biatain Alginate, which showed an optimal cell viability (≥ 70%) (22).

In principle, it was expected that all materials without antimicrobial agents would be cytocompatible, but surprisingly PolyMem WIC induced a reduction of cell viability by more than 30%, which is considered a cytotoxic effect by the ISO norm 10993-part 5 (22). PolyMem WIC foam is constituted by a polyurethane foam sheet bonded to a semipermeable polyurethane film. It contains a non-ionic surfactant, copolymer Poloxamer 188 which works as a wound cleanser, and a humectant (glycerol) that gives moisturizing properties to the dressing when adhered to the wound bed (29). Both components are soluble in wound fluid or skin moisture. Taking in consideration the multiple components in PolyMem that work with the wound environment to promote healing, design of *in vitro* tests for PolyMem dressings are challenging in terms of providing a setting in which the dressing performs optimally. Our selection of performing a direct contact test, that requires the presence of the dressing inside the well of the 24-well cell culture plates, was based on having a standard method to be applied to all dressings under study and have a comparative platform. It is possible that the soaking of the cell culture medium inside the foam lead to a decrease of the necessary nutrients (e.g. ions, growth factors, proteins) for an optimal cell growth. In combination with nanocrystalline silver, a higher reduction of cell viability was observed, showing significant values of *** $p \leq 0.001$ for L929 fibroblasts and * $p \leq 0.05$ for HaCaT keratinocytes (**figure 2.3**).

Toxicity of PolyMem Silver and Biatain Alginate Ag has been reported before, on *in vitro* indirect contact studies on diabetic fibroblasts, in which the authors registered a decrease in cell viability of more than 50% (30). Moreover, cytotoxicity of PolyMem Ag has been described in Yunoki and collaborators research article, in which the authors attribute the negative effect on mammalian cells to the uptake of silver clusters of large size by endocytosis (23).

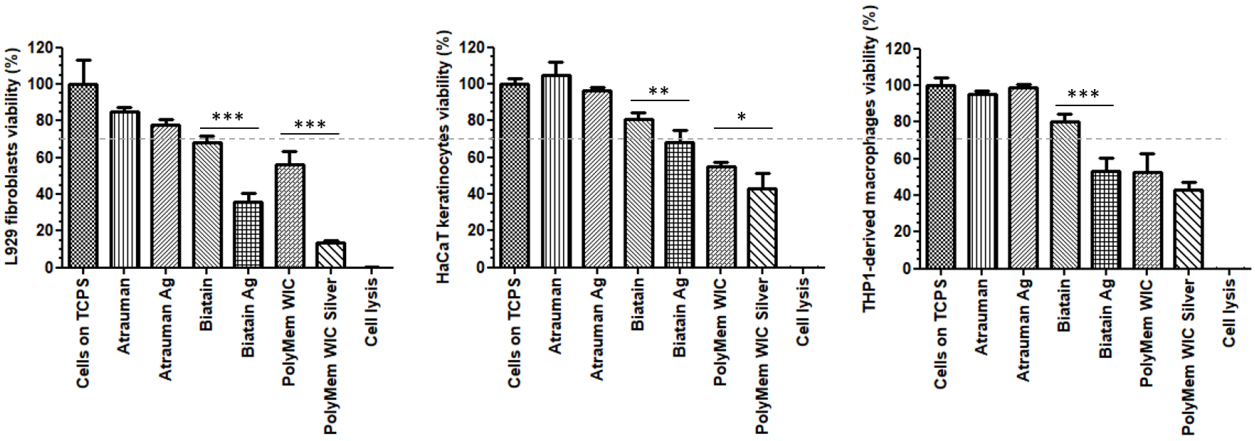

Figure 2.3. Cell viability in the presence of unloaded and silver loaded dressing materials for 24 hours. The dashed line represents 70% viability. The negative control are the cells seeded directly on tissue culture polystyrene (Cells on TCPS) and the positive control are dead cells that were lysed with 9% Triton® X-100 at the endpoint of the assay (Cell lysis). p statistical significance values (* $p \leq 0.05$, ** $p \leq 0.01$ and *** $p \leq 0.001$) were determined for unloaded vs respective silver containing material.

2.3.3. Response of monocyte-derived macrophages to wound dressings: Phenotypical and metabolic characterization of macrophages after being exposed to the materials for one day period of contact

After incubating M0 macrophages with the 6 different wound dressings, our intention was to determine which metabolic choices, that lead to their activation status and function, were undertaken by macrophages in the short time of 24 hours. Therefore, the phenotypical and metabolic profile of the monocyte-derived macrophages were analysed after an incubation with the material on top of the cell layer for 24 hours.

For phenotypical characterization, besides obtaining bright field images, macrophages were stained with cell surface markers CD197/HLA-DR and CD163/CD206 that are typically expressed by M1 and M2, respectively, and were analysed by flow cytometry. For further characterization, metabolic changes were analysed in terms of cytokine production (IL-1β, IL-10 and TGF- β), nitric oxide (NO) release and glucose uptake.

All dressings influenced macrophage immunomodulation, except for the silver-free Atrauman in which cell morphology, markers expressed on the membrane and levels of signals production were very similar to the M0 macrophages (**figure 2.4, 2.5 and 2.6**). Hence, this material seems to be inert in terms of immunomodulatory properties. In case of silver-containing Atrauman, the slight decrease of NO production and the significant increase of the anti-inflammatory TGF-β cytokine on the THP-1 derived macrophages supernatant shows that this dressing is stimulating the macrophages to polarize towards a M2-like state (**figure 2.6**). In this case, it

seems that the effect comes from the Ag^+ ions released by the matrix that have been reported to have anti-inflammatory properties (31–35).

The bright field microscopic images show generally a more elongated cell morphology in comparison with the M0 macrophages for the Biatain Alginate dressings (**figure 2.4 E and F**). Both silver-free Biatain Alginate and Biatain Alginate Ag raised the levels of TGF-β demonstrating their ability of inducing the production of this specific anti-inflammatory cytokine (**figure 2.6**). Interestingly, Biatain Alginate alone also induced the production of pro-inflammatory molecules and expression of a M1-associated marker. Indeed, a slightly higher IL-1β concentration, augmented expression of HLA-DR and significantly more nitric oxide concentration in the supernatant in comparison with M0 macrophages was detected (**figure 2.5 and 2.6**). Biatain Alginate consists of 85% alginate and 15% carboxymethylcellulose. Although, the information about the origin of the alginate is not openly available, it was previously reported that alginate isolated from *Sargassum vulgare* has pro-inflammatory activity (36). Hence, the M1 characteristics observed on macrophages in the presence of Biatain might be a consequence of the contact with alginate. However, macrophages in the presence of Biatain Alginate Ag decreased the NO levels and a significant increase of single positive $CD206^+$ cells and double positive $CD163^+/CD206^+$ on the membrane of macrophages was determined (**figure 2.5 and 2.6**). It is well observed on **figure 2.5 B**, that the previously mentioned markers are less in the correspondent quadrants of the plot for a representative sample of M0 macrophages population. Hence, the combination of the matrix properties (consists in alginate and carboxymethylcellulose) with the ionic silver complex salt has a clear action in initiating the immunomodulation of macrophages towards the M2-state, possibly to M2a or M2c which are both pro-angiogenic subtypes that show similar characteristics (14,15). PolyMem alone induced a slight increase of populations that express HLA-DR and double CD197/HLA-DR markers that are considered pro-inflammatory receptors (**figure 2.5**). A significant increase in the production of IL-1β, IL-10 and TGF- β was observed additionally (**figure 2.6**). The polarization of macrophages involves plasticity in a continuous spectrum. Hence, in this case, macrophages might be shifting from a M1- to M2-state or be part of a mixed activation of M1/M2 phenotypes population (37,38). One proof of these theories are the two different shapes of cell morphology observed in **figure 2.4 G** that shows more rounded cells than stretched ones.

In comparison to the respective silver-free foam, the macrophages in contact with PolyMem WIC Silver maintain the induction of high TGF-β production but typical cell surface markers of M1 and pro-inflammatory cytokines are not detected anymore (**figure 2.5 C and 2.6**). This

proves once again the anti-inflammatory properties of silver ions and particles. From the microscopic images, it is observable the presence of some stretched shape macrophages which is one phenotypical characteristic of M2-like macrophages (**figure 2.4 H**) (39).

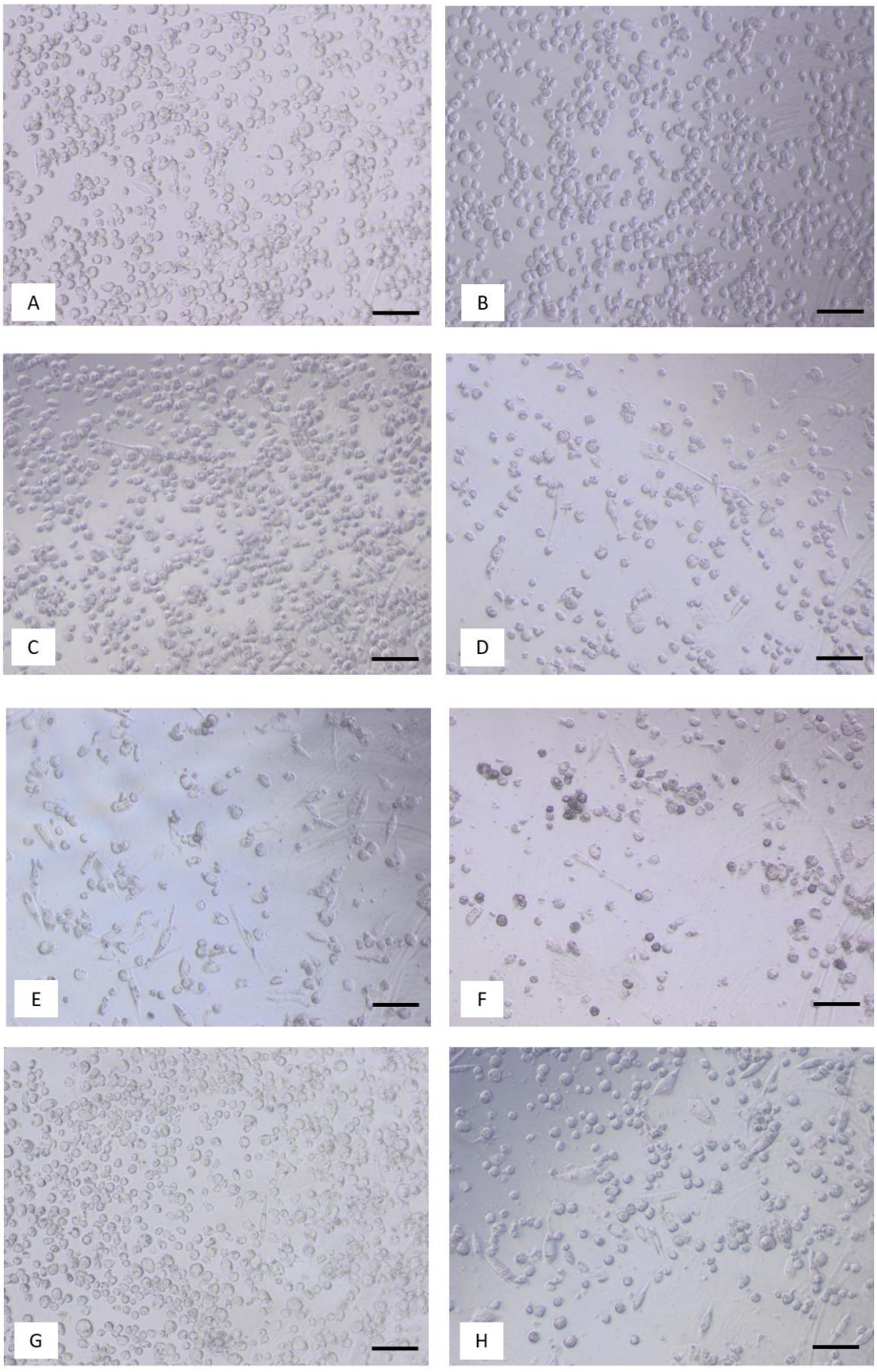

Figure 2.4. Bright field images of macrophages after 24 hours of exposure to silver-free and silver-containing wound dressings. A, B – M0 macrophages; C – Atrauman; D – Atrauman Ag; E – Biatain Alginate; F – Biatain Alginate Ag; G – PolyMem WIC; H – PolyMem WIC Silver. Bar represents 100 μm.

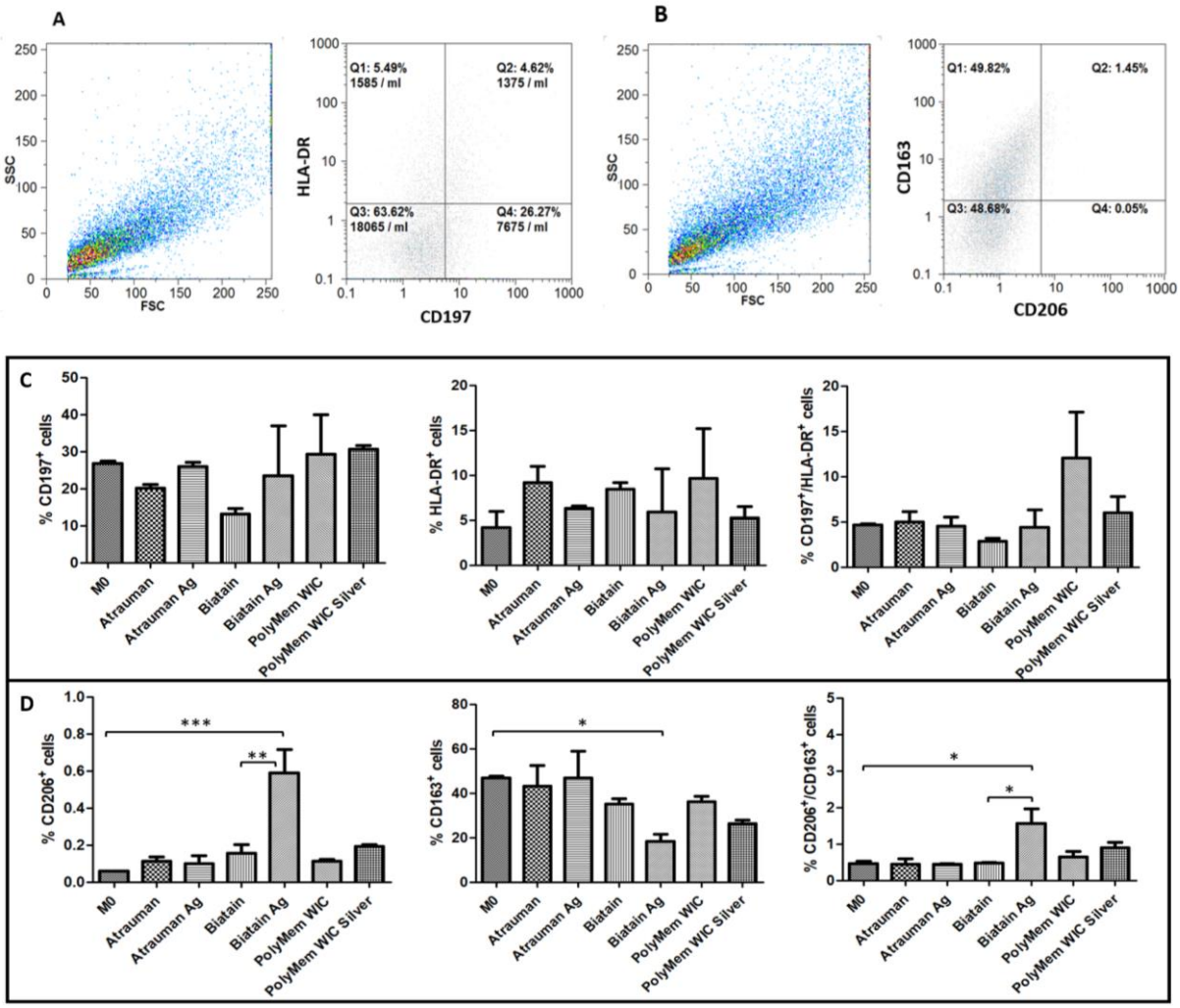

Figure 2.5. Surface markers for phenotypical characterization of macrophage populations. A,B - Representative dot plots from Flow cytometry of M0 macrophages; C - Percentage of single positive CD197 cells, single positive HLA-DR and double positive $CD197^{+}$/HLA-DR. D - Percentage of single positive CD206 cells, single positive CD163 and double positive $CD206^{+}/CD163^{+}$. p values (* $p \leq 0.05$, ** $p \leq 0.01$ and *** $p \leq 0.001$) were determined for M0 vs all materials and unloaded vs respective silver containing material.

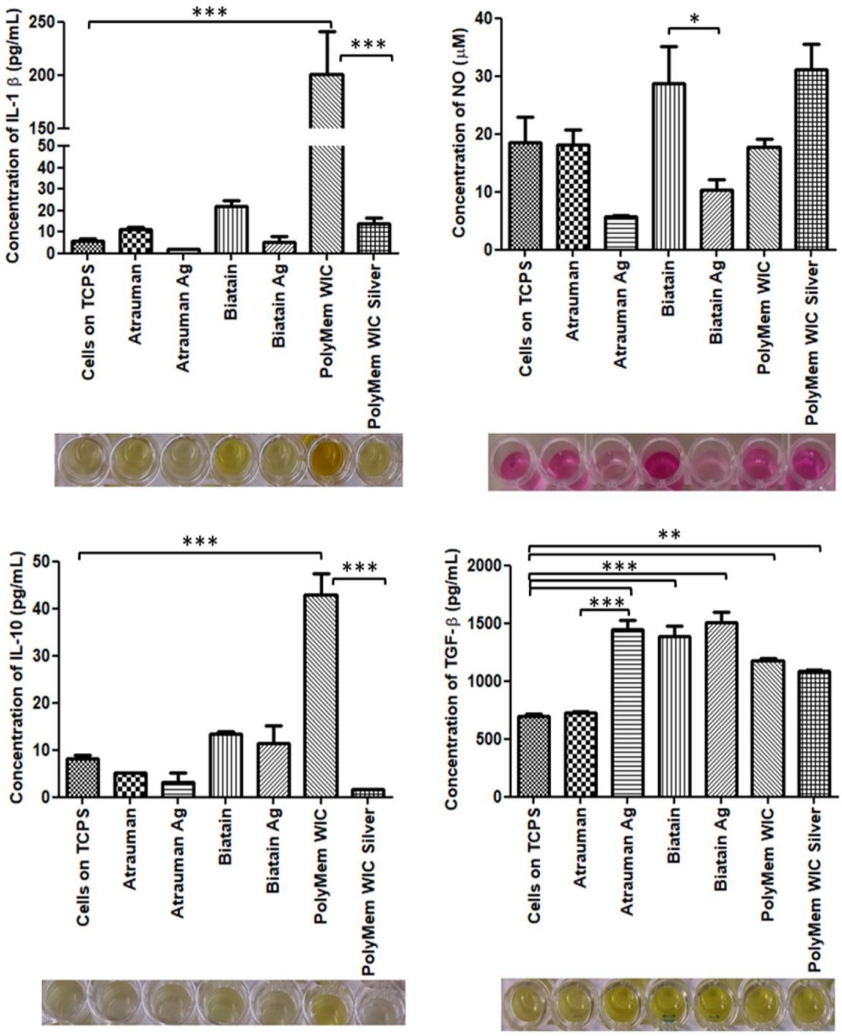

Figure 2.6. Concentration of produced pro-inflammatory and anti-inflammatory signals by macrophages in the presence of different commercially available materials for 24 hours.
p values (* $p \leq 0.05$, ** $p \leq 0.01$ and *** $p \leq 0.001$) were determined for Cells on TCPS (M0 macrophages) vs all materials and untreated vs respective silver containing dressing.

The glucose uptake by macrophages exposed to unloaded versus respective silver containing dressings increased significantly in all conditions compared to M0 resting state macrophages, with exception of Atrauman Ag. Still it is clear that macrophages consume slightly less glucose in the presence of the silver containing materials, demonstrating that these macrophages are polarizing on a continuous spectrum towards M2-macrophages (**figure 2.7**). An increased expression of glucose transporters (mainly GLUT1) on the membrane and higher rates of consumption of glucose by pro-inflammatory M1 macrophages has been reported, due to their metabolic adaptation in which they perform fermentation of glucose to obtain a rapid production of energy (40). The most significant increase of glucose consumption occurred to macrophages that were previously exposed to PolyMem WIC, the same dressing that provoked

the highest secretion of the pro-inflammatory cytokine IL-1β (**figure 2.6 and 2.7**). This observation supports that under the influence of this dressing indeed there is a part of the M0 population that shows characteristics of M1-like state macrophages.

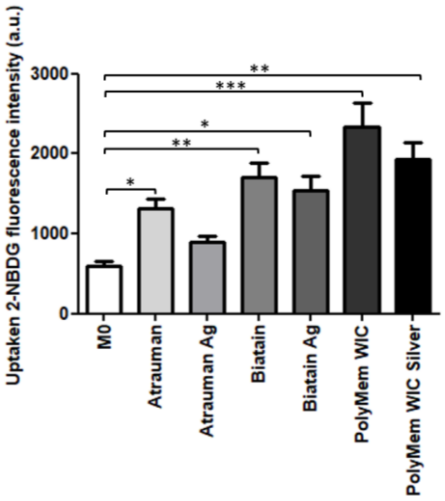

Figure 2.7. Glucose consumption by monocyte-derived macrophages after exposure to the materials during 24 hours. 2-NBDG, fluorescent d-glucose analog. Statistical determination of * $p \leq 0.05$, ** $p \leq 0.01$ and *** $p \leq 0.001$ for Cells on TCPS (M0 macrophages) vs all materials, and untreated vs respective silver containing dressing.

2.4. Conclusion

Microbial contamination of wounds is a significant contributor for the delay of wound healing (41). The usage of antimicrobial wound dressings has been increased in hospitals as a common practice for prevention of infections or the reduction of bacterial burden in the wound environment. Incorporation of silver as an antimicrobial agent that is not a conventional systemic antibiotic treatment in such matrixes is one of the most common strategies. In the last years many clinical cases were reported, in which currently-used antibiotics failed in their bactericidal or bacteriostatic effect, due to the evolution and propagation of multidrug-resistant species (42). Out of the three antimicrobial wound dressings selected for this study, Biatain Alginate Ag was the one able to decrease significantly the number of Gram-positive (*S. aureus* and *S. epidermidis*) and Gram-negative (*E. coli* and *P. aeruginosa*) bacteria in 24 hours. However, in a direct contact test, it also provoked a cytotoxic outcome on fibroblasts and monocyte-derived macrophages, reducing the viability about 50%. Nevertheless, this material is clearly stimulating the polarization of M0 macrophages to the M2-state since an increase of expression of membrane M2 markers $CD163^{+}$/$CD206^{+}$ and production of TGF-β was verified.

With a rapid killing of microorganisms and shifting macrophages to a tissue-healing population, Biatain Alginate Ag seems promising for regressing the inflammatory perpetual state on chronic wounds which would impulse a proper cutaneous closure.

Atrauman and Atrauman Ag showed excellent cytocompatibility features on the cell lines used in this work. One specific observation was that Atrauman itself seems to be inert in inducing any alteration to the macrophages phenotype for a period of 24 hours. This can be an advantage in clinical situations that no interference with the natural wound healing is demanded, such as acute wounds that eventually recover naturally and a dressing is just necessary to protect the wound from external factors. The presence of metallic silver influenced the production of TGF-β to a significant extent, which shows that silver is in fact stimulating the macrophages to secrete this anti-inflammatory signal.

PolyMem WIC alone is stimulating macrophages to obtain pro-inflammatory and tissue-healing characteristics. This observation is not in accordance with the product description on the company website, in which it is strongly defined that PolyMem WIC (that contains glycerol and poloxamer 188) is an anti-inflammatory dressing. As published by Szél *et al*., glycerol is a polyol with anti-inflammatory properties (43). Additionally, the anti-inflammatory effect induced by the non-ionic block copolymer surfactant Poloxamer 188 has also been confirmed (44). Hence it becomes clear that the increase on the production of the anti-inflammatory cytokines IL-10 and TGF-β is due to stimulation by glycerol and poloxamer 188, both present in this product. The reason concerning the increase on IL-1β secretion and expression of typical pro-inflammatory membrane markers is not yet fully understood and it needs to be further investigated. It cannot be ruled out to be an artefact of the experimental design. Nonetheless, a significant drop on IL-1β production was observed when the macrophages were in the presence of PolyMem WIC with the nanocrystalline silver particles, proving once again the anti-inflammatory impact induced by silver ions and particles. This antimicrobial dressing has also shown a great antibacterial effect against the most common strains found in infected wounds, but it brought a toxic effect to the 2D cell culture of fibroblasts, keratinocytes and monocyte-derived macrophages.

All silver-containing dressings tested induced a significant increase of TGF-β secretion, which has profibrotic activities and is associated to M2a and M2c subsets of M2 macrophages (45). Profibrotic action means that it promotes fibrosis which involves the overgrowth of an organ or tissue during a reparative process, by deposition of ECM components such as collagen (46).

Although this study gives great indications about the response of macrophages to different biomaterials, the macrophages used were in a resting state (M0 macrophages), hence in future

studies it is necessary to investigate the immunomodulatory effects of these same dressings on macrophages polarized to the M1 pro-inflammatory state due to the fact that in the wound environment this macrophage phenotype is predominant. It would be interesting to explore the same features with monocytes isolated from donors' blood, to have an *in vitro* set closer to human circumstances. However, the main advantage of using a cell line such as THP-1 human monocytes is that the origin of cells is consistent in every assay, meaning less variability in the results obtained. Hence, these cells are a great tool to give insights of immunomodulation owed by biomaterial-macrophages interactions.

Concerning the experimental design, a main challenge was found. It was difficult to find a common experimental setting *in vitro* that fits perfectly for the specific characteristics of all dressings, more noticeable by the unique property of soaking the surrounding medium and induce killing of bacteria mostly internally by PolyMem WIC. The application of the exact same antimicrobial, cytocompatibility and immunomodulation assessment procedures was supported by the fact that this is a comparative study, therefore the dressings had to be tested in common standard conditions. In addition, there was a decrease of viability of monocyte-derived macrophages in the presence of Biatain Alginate Ag, PolyMem WIC and PolyMem WIC silver after 24 hours. This may have influenced the results of the measured concentrations of pro-inflammatory and anti-inflammatory molecules, and the uptake of glucose. Nevertheless, in comparison with M0 macrophages, secretion of IL-1β, IL-10 and TGF-β increased significantly in macrophages in contact with PolyMem WIC. Also, for Biatain Alginate Ag and PolyMem WIC silver the production of TGF-β was significantly higher than the M0 state, and the glucose uptake was increased in cells at the presence of the three wound dressings. Hence, although a smaller number of cells existed attached to the bottom of the wells by the endpoint of the assay, it was still detected higher concentrations of secreted cytokines in the supernatant and more glucose uptake.

In conclusion, the main finding of this work is that macrophages start to change their metabolism and phenotype in response to wound dressings of different composition in a short one-day period. Moreover, silver has shown to possess anti-inflammatory properties. The other major final remark from this research work is, that it is clear that even with commercially-available and clinically-applied products the balance between antibacterial activity versus cytotoxicity *in vitro*, and stimulation of an optimal wound environment towards cutaneous-healing remains a significant challenge.

References

1. Dhivya S, Padma VV, Santhini E. Wound dressings - A review. Biomed. 2015;5(4):24–8.
2. Baranoski S, Ayello EA. Wound dressings: An evolving art and science. Adv Ski Wound Care. 2012;25(2):87–92.
3. Simões D, Miguel SP, Ribeiro MP, Coutinho P, Mendonça AG, Correia IJ. Recent advances on antimicrobial wound dressing: A review. Eur J Pharm Biopharm. 2018;127:130–41.
4. Burnham JP, Kirby JP, Kollef MH. Diagnosis and management of skin and soft tissue infections in the intensive care unit: a review. Intensive Care Med. 2016;42(12):1899–911.
5. Piddock LJ V. Understanding drug resistance will improve the treatment of bacterial infections. Nat Rev Microbiol. 2017;15(11):639–40.
6. Nam G, Rangasamy S, Purushothaman B, Song JM. The Application of Bactericidal Silver Nanoparticles in Wound Treatment. Nanomater Nanotechnol. 2015;5:23.
7. Zewde B, Ambaye A, Stubbs Iii J, Raghavan D. A review of stabilized silver nanoparticles – Synthesis, biological properties, characterization, and potential areas of applications. JSM Nanotechnol Nanomed. 2016;4(2):1043.
8. Sütterlin S, Tano E, Bergsten A, Tallberg AB, Melhus Å. Effects of silver-based wound dressings on the bacterial flora in chronic leg ulcers and its susceptibility in vitro to silver. Acta Derm Venereol. 2012;92(1):34–9.
9. Krzyszczyk P, Schloss R, Palmer A, Berthiaume F. The role of macrophages in acute and chronic wound healing and interventions to promote pro-wound healing phenotypes. Front Physiol. 2018;9:1–22.
10. Velnar T, Bailey T, Smrkolj V. The wound healing process: An overview of the cellular and molecular mechanisms. J Int Med Res. 2009;37(5):1528–42.
11. Ferrante CJ, Leibovich SJ. Regulation of Macrophage Polarization and Wound Healing. Adv Wound Care. 2012;1(1):10–6.
12. Landén NX, Li D, Ståhle M. Transition from inflammation to proliferation: a critical step during wound healing. Cell Mol Life Sci. 2016;73(20):3861–85.
13. Sindrilaru A, Scharffetter-Kochanek K. Disclosure of the Culprits: Macrophages—Versatile Regulators of Wound Healing. Adv Wound Care. 2013;2(7):357–68.
14. Hesketh M, Sahin KB, West ZE, Murray RZ. Macrophage phenotypes regulate scar formation and chronic wound healing. Int J Mol Sci. 2017;18(7):1–10.
15. Novak ML, Koh TJ. Macrophage phenotypes during tissue repair. J Leukoc Biol. 2013;93(6):875–81.
16. Schairer DO, Chouake JS, Nosanchuk JD, Friedman AJ. The potential of nitric oxide releasing therapies as antimicrobial agents. Virulence. 2012;3(3):271–9.
17. Yamane K, Leung KP. Rabbit M1 and M2 macrophages can be induced by human recombinant GM-CSF and M-CSF. FEBS Open Bio. 2016;6(9):945–53.

18. Berg C, Trofast C, Bengtsson T. Platelets induce reactive oxygen species-dependent growth of human skin fibroblasts. Eur J Cell Biol. 2003;82(11):565–71.

19. Ogle ME, Segar CE, Sridhar S, Botchwey EA. Monocytes and macrophages in tissue repair: Implications for immunoregenerative biomaterial design. Exp Biol Med. 2016;241(10):1084–97.

20. Valente TAM, Silva DM, Gomes PS, Fernandes MH, Santos JD, Sencadas V. Effect of sterilization methods on electrospun poly(lactic acid) (PLA) fiber alignment for biomedical applications. ACS Appl Mater Interfaces. 2016;8(5):3241–9.

21. Matuschek E, Brown DFJ, Kahlmeter G. Development of the EUCAST disk diffusion antimicrobial susceptibility testing method and its implementation in routine microbiology laboratories. Clin Microbiol Infect. 2014;20(4):255–66.

22. International Organization for Standardization. ISO 10993-5 Biological evaluation of medical devices - Part 5: Tests for in vitro cytotoxicity. International Standard. 2009.

23. Yunoki S, Kohta M, Ohyabu Y, Iwasaki T. In vitro parallel evaluation of antibacterial activity and cytotoxicity of commercially available silver-containing wound dressings. Plast Surg Nurs. 2015;35(4):203–11.

24. Coloplast CC. Biatain Ag Non-Adhesive [Internet]. 2015 [cited 2018 Sep 1]. p. 2–4. Available from: https://www.coloplast.us/Global/US/Wound Care/New MSDS Sheets - Wound 6-2017/Biatain(R) Ag Non-Adhesive Foam Dressing.pdf

25. Ziegler K, Görl R, Effing J, Ellermann J, Mappes M, Otten S, et al. Reduced cellular toxicity of a new silver-containing antimicrobial dressing and clinical performance in non-healing wounds. Skin Pharmacol Physiol. 2006;19(3):140–6.

26. Qin Y. Antimicrobial textile dressings in managing wound infection. In: Advanced Textiles for Wound Care. 2009. p. 179–97.

27. Boonkaew B, Kempf M, Kimble R, Supaphol P, Cuttle L. Antimicrobial efficacy of a novel silver hydrogel dressing compared to two common silver burn wound dressings: Acticoat^{TM} and PolyMem Silver ®. Burns. 2014;40(1):89–96.

28. Burd A, Kwok CH, Hung SC, Chan HS, Gu H, Lam WK, et al. A comparative study of the cytotoxicity of silver-based dressings in monolayer cell, tissue explant, and animal models. Wound Repair Regen. 2007;15(1):94–104.

29. Schulz A, Depner C, Lefering R, Kricheldorff J, Kästner S, Fuchs PC, et al. A prospective clinical trial comparing Biobrane® Dressilk® and PolyMem® dressings on partial-thickness skin graft donor sites. Burns. 2016;42(2):345–55.

30. Zou SB, Yoon WY, Han SK, Jeong SH, Cui ZJ, Kim WK. Cytotoxicity of silver dressings on diabetic fibroblasts. Int Wound J. 2013;10(3):306–12.

31. Wilkinson LJ, White RJ, Chipman JK. Silver and nanoparticles of silver in wound dressings: a review of efficacy and safety. J Wound Care. 2011;20(11):543–9.

32. Rosique RG, Rosique MJ, Farina Junior JA. Curbing Inflammation in Skin Wound Healing: A Review. Int J Inflam. 2015;1–9.

33. Hermans MH. Silver-containing dressings and the need for evidence. Am J Nurs. 2006;106(12):60–8.

34. Lansdown ABG. Silver I: its antibacterial properties and mechanism of action. J Wound Care. 2014;11(4):125–30.

35. Leaper DJ. Silver dressings: Their role in wound management. Int Wound J. 2006;3(4):282–311.

36. Lins KOAL, Vale ML, Ribeiro RA, Costa-Lotufo L V. Proinflammatory activity of an alginate isolated from Sargassum vulgare. Carbohydr Polym. 2013;92(1):414–20.

37. Bosurgi L, Manfredi AA, Rovere-Querini P. Macrophages in injured skeletal muscle: A perpetuum mobile causing and limiting fibrosis, prompting or restricting resolution and regeneration. Vol. 2, Frontiers in Immunology. 2011.

38. Dalmas E, Clément K, Guerre-Millo M. Defining macrophage phenotype and function in adipose tissue. Trends Immunol. 2011;32(7):307–14.

39. Sridharan R, Cameron AR, Kelly DJ, Kearney CJ, O'Brien FJ. Biomaterial based modulation of macrophage polarization: A review and suggested design principles. Mater Today. 2015;18(6):313–25.

40. Freemerman AJ, Johnson AR, Sacks GN, Milner JJ, Kirk EL, Troester MA, et al. Metabolic reprogramming of macrophages: Glucose transporter 1 (GLUT1)-mediated glucose metabolism drives a proinflammatory phenotype. J Biol Chem. 2014;289(11):7884–96.

41. Leaper D, Assadian O, Edmiston CE. Approach to chronic wound infections. Br J Dermatol. 2015;173(2):351–8.

42. Blair JMA, Webber MA, Baylay AJ, Ogbolu DO, Piddock LJ V. Molecular mechanisms of antibiotic resistance. Nat Rev Microbiol. 2015;13(1):42–51.

43. Szél E, Polyánka H, Szabõ K, Hartmann P, Degovics D, Balázs B, et al. Anti-irritant and anti-inflammatory effects of glycerol and xylitol in sodium lauryl sulphate-induced acute irritation. J Eur Acad Dermatology Venereol. 2015;29(12):2333–41.

44. Harting MT, Jimenez F, Kozar RA, Moore FA, Mercer DW, Hunter RL, et al. Effects of poloxamer 188 on human PMN cells. Surgery. 2008;144(2):198–203.

45. Lu J, Cao Q, Zheng D, Sun Y, Wang C, Yu X, et al. Discrete functions of M 2a and M 2c macrophage subsets determine their relative efficacy in treating chronic kidney disease. Kidney Int. 2013;84(4):745–55.

46. Wynn TA. Cellular and molecular mechanisms of fibrosis. J Pathol. 2008;214(2):199–210.

CHAPTER THREE

‘A new strategy to treat wound infections: Biological testing of novel antimicrobial peptide-biomimetic amphipathic polyurethanes’

Graphical abstract

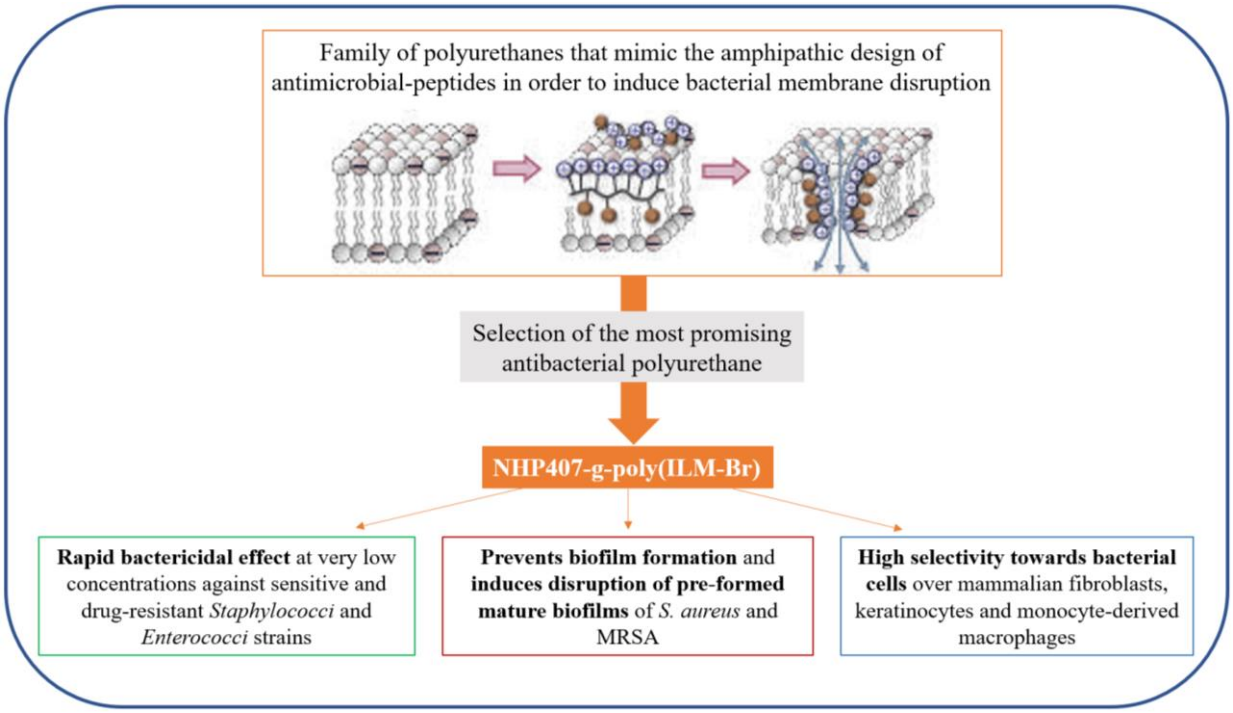

Abstract

Antibiotic-resistant pathogenic bacteria have been isolated from chronic wounds and are one of the main factors for delaying wound healing. Concomitant with the increasing resistance to conventional antibiotics, it is urgently needed to develop new therapeutic strategies without currently-used drugs to tackle antimicrobial-resistant bacteria, prevent biofilm formation and cause its disruption. Inspiration on the fundamental structure of host-defence antimicrobial peptides (AMPs) is a promising approach in the design of innovative therapeutic materials. Hence, in this work newly synthesized AMP-biomimetic amphipathic polyurethanes (PUs) were evaluated as a strategy to tackle biofilm and planktonic multidrug-resistant bacteria often colonising chronic wounds. Their rational design was based on the amphipathic cationic structure existing on most AMPs to reproduce the membrane-disruptive mechanism.

Antibacterial susceptibility assays and cytocompatibility experiments were performed to select the most potent AMP-biomimetic amphipathic polyurethane.

An efficient newly synthesized antibacterial PU based polymeric system in combating planktonic and biofilm Gram-positive sensitive and drug-resistant bacteria was revealed, the NHP407-g-Poly(ILM-Br). This PU induced a rapid bactericidal effect on planktonic Gram-positive bacteria and it was able to prevent biofilm formation for a period of 72 hours. Moreover, in higher concentrations it was able to disrupt Gram-positive mature biofilms of both drug-sensitive and -resistant bacteria. The cell viability of L929 murine fibroblasts, HaCaT human keratinocytes and THP-1 monocyte-derived human macrophages was optimal in the presence of lower concentrations that are active against Staphylococcal bacteria (13 μg/mL). Hence, a promising therapeutic AMP-biomimetic amphipathic polyurethane was identified to overcome Gram-positive bacteria responsible for wound infections.

3.1. Introduction

Antibiotic resistance crisis is a life-threatening problem in modern society worldwide (1). Especially in wounds, antibiotic-resistant pathogenic bacteria have been isolated and are the root factor for impeding a proper wound healing (2). These evolved antimicrobial-resistant strains survive in wounds as planktonic or sessile forms (3). The sessile form comes from the ability of microorganisms to attach on abiotic and biotic surfaces, forming a protected community denominated biofilm (4). In fact, more than 90% of chronic wounds contain biofilms which are generally polymicrobial in nature (5,6). Studies have shown that the most commonly pathogenic isolates from chronic wounds are *Staphylococcus aureus* and

Pseudomonas aeruginosa (7,8). Due to the rapidly increasing resistance towards conventional antibiotics, our society is now entering the post-antibiotic era: a lot of effort is focused on the development of new therapeutic strategies without currently used antibiotics to tackle antimicrobial-resistant bacteria, prevent biofilm formation and/or cause its disruption.

Biomimetic of the fundamental structure of host-defence antimicrobial peptides (AMPs) is an attractive approach. Besides being an excellent choice to develop novel candidates as strong antibacterial agents, by using polymer-based synthetic mimics of AMPs it is also possible to overcome the high economical production costs of natural and synthetic AMPs (9,10). Moreover, based on reported cases concerning the short-period of activity and cell toxicity of low molecular weight agents, a more valuable prospect is open for innovative efficient antimicrobial therapies by using polymers (11). AMPs are produced in all living organisms, including humans in which they are synthesized by eukaryotic cells as part of the innate immune response (first line of defence) to invading pathogens (12–14). They have a broad antimicrobial spectrum. Although no common structure has been identified, most of AMPs are amphiphilic, presenting a clustering of cationic and hydrophobic amino acid residues (12). An outstanding characteristic of these peptides is their higher selectivity towards the bacterial cytoplasmatic membrane due to the electrostatic interaction between the cationic groups with the acidic phospholipids of bacteria, binding to the lipid bilayer. Most commonly after this initial interaction, the hydrophobic region of the peptide gets inserted into the cell membrane, presses the lipids apart and forms pores on the membrane. Consequently, the bacterial cytoplasmatic membrane becomes disrupted, leading to bacterial death (10,12,13). Besides creating direct stress on the bacterial membrane, other additional mechanisms of action have been described for the antibacterial action of AMPs, such as their interference with cell wall synthesis and inhibition of cytoplasmatic components (15,16). Regardless of the mechanism of action, the initial electrostatic interaction with the bacterial cytoplasmic membrane is essential for the antibacterial activity (16). Although bacteria are able to develop resistance to AMPs, reported cases are rare due to the varied possible mechanisms of action and the main mode of action of disrupting the membrane that is not easily avoided (11). Especially the latter bactericidal mode of action makes AMPs a desirable solution to combat slow-growing bacteria, such as the ones existing in biofilms (17).

Hence, to efficiently mimic an AMP, it is very important to obtain a hydrophobic-hydrophilic balance in the polymeric backbone and that the cationic region is crucial for a strong interaction with the bacterial membrane. Studies have been proving that long polymeric systems with

positive charges have an immeasurable antibacterial potential by penetrating the bacteria cell wall (10,11,16,18–20).

In this work, newly synthesized AMP-biomimetic amphipathic polyurethanes (PUs) with intrinsic antimicrobial properties were explored as a strategy to tackle biofilm and planktonic multidrug-resistant bacteria existing on chronic wounds. Their rational design was not based on the secondary structures of AMPs such as α-helices, but instead they were designed to mimic the fundamental amphipathic cationic structure of AMPs to reproduce the membrane-disruptive mechanism. Most of this library of newly synthesized PUs was produced with polyionic-based block copolymers. Polyionic liquids (PILs) are cationic polymeric systems that are very versatile and have been explored for their unique physicochemical properties and efficient antimicrobial action (21).

Henceforth, this research work aims to explore the antibacterial and cytocompatibility effect of amphipathic polyurethanes in dispersion as a future easy to handle therapeutic products to apply directly on infected wounds.

3.2. Material and Methods

3.2.1. Polymers – Novel amphipathic polyurethanes

The library of amphiphilic PUs tested were synthesized in professor Gianluca Ciardelli's group 'Materials in Biotechnology and Biomedical Lab' at Politecnico di Torino and were kindly provided by an Early Stage Researcher of the HyMedPoly project (Purkayastha *et al*., unpublished). The polyurethane backbone and monomers used for the synthesis of the different groups of polymeric systems are represented in **figure 3.1**.

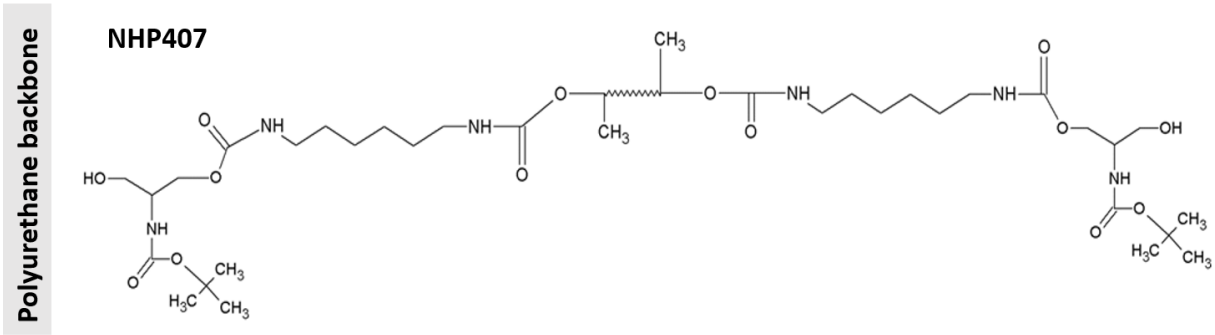

(first part of **figure 3.1** – description on next page)

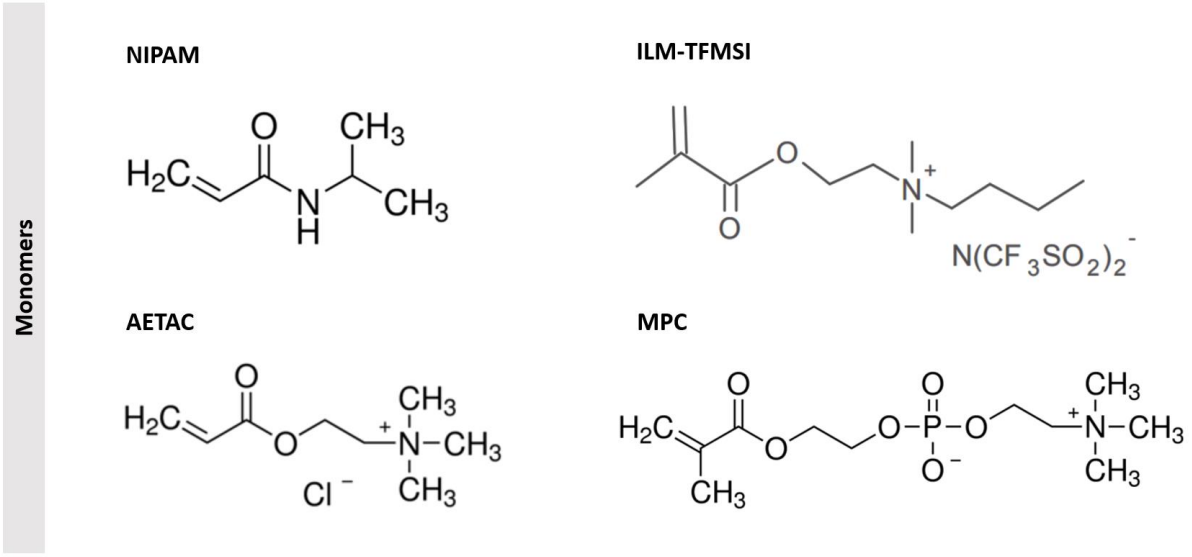

Figure 3.1. Acronym and chemical structure representation of the polyurethane backbone and the monomers used to produce newly synthesized amphipathic polyurethanes. NIPAM, N-isopropylacrylamide; ILM-TFMSI, N,N,N,N-Butyldimethylmethacryloyloxyethylammonium bis(trifluoromethanesulfonyl)imide; AETAC, 2-(Acryloyloxy)ethyl trimethylammonium chloride; MPC, Methacryloyloxyethyl phosphorylcholine.

All synthesized PUs have a common backbone, the amphiphilic Poloxamer-based poly(ether urethane) (PEU) that was produced by a two-step process in inert gas atmosphere using anhydrous 1,2-dichloroethane (DCE) as solvent. In a first step, Poloxamer P407 (P407) as macrodiol was reacted with 1,6-hexamethylene diisocyanate (HDI) in the presence of a catalyst (dibutyltin dilaurate) to form a pre-polymer. P407 belongs to the poloxamers family and is a thermoresponsive non-ionic triblock copolymer consisting in a central block of poly(propylene) oxide (PPO) flanked by two blocks of poly(ethylene oxide) (PEO) (22,23). Then, in the second step, N-Boc serinol was added as a chain extender and the reaction was stopped with methanol. The synthesized PEU has the acronym NHP407, in which N refers to the chain extender, H to HDI and P407 to the macrodiol (24). After these steps, trifluoroacetic acid was used to remove the Boc protecting group from amino groups. Subsequently, the grafting of further monomers was performed from the polyurethane main chain NHP407 by ceric ammonium nitrate (CAN) initiated redox reaction in aqueous phase. The tested copolymers can be divided into 3 groups:

a) Middle block: Poly(N-isopropylacrylamide) (PNIPAM)

The thermoresponsive NIPAM (Sigma-Aldrich) was grafted from the NHP407 (PU backbone), forming the NHP407-g-PNIPAM. Then, hydrophilic monomers were added: in one case the cationic liquid 2-(Acryloyloxy)ethyl trimethylammonium chloride (AETAC) (Sigma-Aldrich),

in the other the zwitterionic substance Methacryloyloxyethyl phosphorylcholine (MPC) (Sigma-Aldrich). Two different polymers were obtained: NHP407-g-[poly(NIPAM)-b-poly(AETAC)] and NHP407-g-[poly(NIPAM)-b-poly(MPC)]. These synthesized PUs were dialyzed against deionized water and freeze-dried. The freeze-dried polymers were prepared in purified H_2O for biological testing.

b) Middle block: Poly[N,N,N,N-Butyldimethylmethacryloyloxyethylammonium bis(trifluoromethanesulfonyl)imide] [Poly(ILM-TFMSI)]

The ionic liquid ILM-TFMSI (Solvionic) was grafted from the PU backbone (NHP407). Afterwards, a hydrophilic monomer, either cationic AETAC or zwitterionic MPC was sequentially added and polymerized to the Poly(ILM-TFMSI) block. Therefore, the polymers will be further denominated as NHP407-g-[poly(ILM-TFMSI)-b-poly(AETAC)] and NHP407-g-[poly(ILM-TFMSI)-b-poly(MPC)]. The synthesized PUs were dialyzed against deionized water and subsequently freeze-dried. In this case, the freeze-dried polymeric systems were prepared in purified water and dimethyl sulfoxide (DMSO) (Sigma-Aldrich) for the biological tests.

c) Functionalization of NHP407-g-Poly(ILM-TFMSI)

The ionic liquid ILM-TFMSI was grafted from the PU backbone being designated as NHP407-g-Poly(ILM-TFMSI). Next, the hydrophobic bis(trifluoromethanesulfonyl)imide anionic counter ions ($N(CF_3SO_2)_2^-$ or TFMSI) were mainly exchanged for hydrophilic bromide ions (Br^-) in methanol forming a more hydrophilic system NHP407-g-Poly(ILM-Br). The counter ion exchanged polymers were separated, dialyzed against deionized water and freeze-dried. As in point b), these polymers were also prepared in purified water and DMSO for antibacterial testing.

3.2.2. Preparation of monomers and polymers for biological assays

The monomers NIPAM, ILM-TFMSI, AETAC and MPC were used following manufacturer's recommendations. As mentioned above, the amphiphilic PUs were prepared in specific conditions to be tested on biological assays (described on **table 3.1**). Some polymeric systems were prepared in purified H_2O and DMSO to investigate the role played by ionic dissociation in the antibacterial activity.

Table 3.1. Parameters for the preparation of the newly synthesized amphiphilic polyurethanes. RT, room temperature.

	Polyurethane	Stock concentration (mg/ml)	Medium	Time of stirring (days)	Conditions used for stirring
Common PU backbone	NHP407	50	H_2O	1	5 hours with ice around and then continue at RT
Group 1	NHP407-g-[poly(NIPAM)-b-poly(AETAC)]	50	H_2O	3	5 hours with ice around and then continue at RT
	NHP407-g-[poly(NIPAM)-b-poly(MPC)]	50	H_2O	3	5 hours with ice around and then continue at RT
Group 2	NHP407-g-[poly(ILM-TFMSI)-b-poly(AETAC)] (Preparation A)	50	DMSO	1	RT
	NHP407-g-[poly(ILM-TFMSI)-b-poly(AETAC)] (Preparation B)	10	H_2O	7	RT (ultrasonication in case of aggregation)
	NHP407-g-[poly(ILM-TFMSI)-b-poly(MPC)] (Preparation A)	50	DMSO	1	RT
	NHP407-g-[poly(ILM-TFMSI)-b-poly(MPC)] (Preparation B)	10	H_2O	7	RT (ultrasonication in case of aggregation)
Group 3	NHP407-g-Poly(ILM-TFMSI) (Preparation A)	50	DMSO	3	RT
	NHP407-g-Poly(ILM-TFMSI) (Preparation B)	15.2	H_2O	8	5 hours with ice around and then continue at RT (ultrasonication every day in case of aggregation)
	NHP407-g-Poly(ILM-Br) (Preparation A)	50	DMSO	3	RT
	NHP407-g-Poly(ILM-Br) (Preparation B)	50	H_2O	7	5 hours with ice around and then continue at RT

3.2.3. Antimicrobial susceptibility testing against planktonic bacteria

The Minimum inhibitory concentration (MIC) and the Minimum bactericidal concentration (MBC) were determined for each monomer/polymer against either ATCC bacterial strains that are susceptible to known antibiotics or bacterial clinically-isolated species that are drug-resistant. The drug-sensitive strains used were: *Staphylococcus aureus subsp. aureus* Rosenbach (ATCC® 29213™), *Staphylococcus epidermidis* (Winslow and Winslow) Evans (ATCC® 12228™), *Enterococcus faecalis* (Andrewes and Horder) Schleifer and Kilpper-Bälz

(ATCC® 29212™), *Escherichia coli* (Migula) Castellani and Chalmers (ATCC® 25922™), *Pseudomonas aeruginosa* (Schroeter) Migula (ATCC® 27853™) and *Klebsiella pneumoniae subsp. pneumoniae* (Schroeter) Trevisan (ATCC® 15380™). The Gram-positive drug-resistant isolates used were the following: Methicillin-resistant *Staphylococcus aureus* (MRSA), Macrolide-lincosamide-streptogramin B and Methicillin (MLS Mec A+) antibiotic-resistant *Staphylococcus epidermidis* (ARSE) and Vancomycin-resistant Enterococci (VRE). For all experiments, bacterial cells were grown at 37°C for 18 hours on blood agar plates (mixture of nutrient agar with 5% sheep blood pH ~7.4).

The MIC values were determined using the broth microdilution method following ISO 20776-1:2006 standard as recommended by EUCAST. After the preparation of a series of dilutions for each monomer/polymer in Mueller-Hinton broth (MHB) and the addition of pre-inoculated bacterial selected colonies from an overnight culture that were inserted in a tube with 2 mL 0.9% NaCl, then turbidity was adjusted to MacFarland 0.5 and the inoculum was diluted in order to have a final concentration in the well of ~3.75×10^5 CFU/mL, the 96-well plates were incubated for 18-22 hours at 37ºC. The lowest concentration that inhibits visible bacterial growth was considered the MIC. In parallel to the MIC test, optical density readings were done at 600 nm in a microplate spectrophotometer (Thermo Scientific Multiskan GO - Thermo Fisher Scientific) as a function of time - 0, 2, 4, 6, 8, 22 and 24 hours. The control was broth containing only bacterial cells.

Following to the broth dilution MIC test, the entire volume (100 µL) of the MIC wells and 3 concentrations above were spread on blood agar plates. The plates were incubated overnight at 37ºC. Colony forming units (CFU) were counted. The MBC value corresponds to the lowest concentration of polymer with which 0 CFU/mL were visualized, meaning that 99.9% killing occurred.

3.2.4. Bactericidal effect after 30 and 90 minutes

In order to evaluate the efficacy of the polyurethane grafted block-copolymers to induce a bactericidal effect in a short time, the percentage of bacterial killing was determined after 30 and 90 minutes in contact with the PUs.

For this experiment, the concentrations tested were 0.5 × MBC, 1 × MBC and 2 × MBC against ~ 3.75×10^5 CFU/mL Gram-positive bacteria *S. aureus* (ATCC® 29213™), *S. epidermidis* (ATCC® 12228™) and *E. faecalis* (ATCC® 29212™), and their correspondent drug-resistant isolates. After bacteria were exposed to the polymers in 96 well-plates for 30 and 90 minutes,

the entire volume of the well (100 μL) was spread on blood agar plates and incubated overnight. On the next day, colony forming units (CFU) were counted and compared with the initial CFU/mL of control plates (originated from bacteria in broth only), to determine the percentage of bacterial reduction.

3.2.5. Biofilm prevention capacity

On sterile cell culture treated flat bottom 96 well-plates, a serial dilution of the PU was added in cation-adjusted MHB (50 μL). Then, colonies isolated from an overnight culture grown on blood agar plates were selected and diluted in order to add ~10^6 CFU/ml per well (50 μL). Plates were sealed and incubated at 37°C for 24, 48 and 72 hours. After each incubation time the supernatant was removed and the biomass of the biofilm formed on the bottom of each well was quantified by safranin staining (25). Briefly, after fixing the biofilm with 100% ethanol, 0.1% safranin (Merck) was added for 5 minutes in order to stain the bacterial DNA (chromosome and plasmids). The biofilm was washed with phosphate buffered saline (PBS) (pH=7.4) (PAN Biotech). In the end it was resuspended in 1% sodium dodecyl sulphate (SDS) (Sigma Aldrich). Biofilm biomass was quantified by reading the absorbance at 490 nm in a microplate reader using a microplate spectrophotometer, Thermo Scientific Multiskan GO, Thermo Fisher Scientific.

3.2.6. Antimicrobial susceptibility testing against sessile bacteria (pre-formed biofilms)

Bacteria isolated colonies were suspended in 0.9% NaCl saline solution with a sterile loop. The turbidity was adjusted to McFarland 0.5 with a densitometer (approx. 10^8 CFU/ml). After that, a dilution of 100-fold in cation-adjusted Mueller-Hinton broth (approx. 10^6 CFU/ml) was performed. 100 μl of the bacteria suspension was distributed per well on the sterile cell culture treated flat-bottom 96 well-plates. These plates were sealed and incubated at 37 °C for 24, 48 or 72 hours. After the incubation time period, the supernatant was removed and 100 μL of different concentrations of polymer diluted in cation-adjusted Mueller-Hinton broth was added per well. Plates were sealed and incubated at 37 °C for 24 hours. Then the supernatant was discarded and the remaining biofilm biomass on the bottom of the well was quantified with safranin staining as described in point 3.2.5.

3.2.7. Eukaryotic cell culture conditions

To evaluate the cytotoxicity of the PU grafted block copolymers on mammalian cells, a murine fibroblasts cell line (L929) was first used as a counter-screen for non-selective inhibitors. The L929 cells (German Collection of Microorganisms and Cell Cultures – DSMZ) were cultured in RPMI 1640 medium (PAN Biotech), supplemented with 10% heat-inactivated Fetal bovine serum (FBS) (PAN Biotech), 100 U/mL penicillin and 0.1 mg/mL streptomycin (PAN Biotech). The cells were maintained in T75 vented cap culture flasks (Thermo Fischer) at 37ºC in an atmosphere containing 5% CO_2, by sub-passage at each 2-3 days.

In case an excellent cytocompatibility on L929 was observed (percentage of cell viability higher than 70% with concentrations of polymer higher than 1 mg/mL) or if the polymer showed a selectivity index (SI)[1] higher than 1 on most of the non- and drug-resistant strains, other skin cells were included in the assays. The half minimal inhibitory concentration (IC_{50}) value was determined by linear regression analysis.

Keratinocytes and monocyte-derived macrophages are cell populations also present in skin. The keratinocyte immortalized cell line HaCaT was obtained from the Deutsche Krebsforschungszentrum - DKFZ, Heidelberg. It was grown in T75 vented cap culture flasks (ThermoFisher Scientific) at 37°C, 5% CO_2, supplemented with 4.5 g/L glucose Dulbecco's Modified Eagle Medium – high glucose DMEM (ThermoFisher Scientific), 10% heat-inactivated FBS (PAN Biotech), and 100 U/mL penicillin - 0.1 mg/mL streptomycin (PAN Biotech). Cell detachment was done with TrypLE Express (ThermoFisher Scientific) and the splitting ratio was from 1:5 to 1:10.

The human monocytic cell line THP-1 (ATCC) was grown at 37°C and 5% CO_2 in vertically positioned T75 vented cap culture flasks (ThermoFisher Scientific) in the exact same complete RPMI 1640 medium as previously described for L929 cells. Medium was added or renewed every 2 or 3 days.

To induce its differentiation to macrophages, THP-1 were first seeded on cell culture treated 24-well plates with a density of 10^6 cells/mL in the presence of 200 ng/mL of phorbol 12-myristate-13-acetate (PMA) (Sigma Aldrich) for 24 hours at 37°C, 5% CO_2. Afterwards the medium was replaced with complete RPMI and cells were again incubated for 48 hours before any further experiment.

---

[1] The selectivity index (SI) was calculated as follows:

$$\textbf{Selectivity index (SI)} = \frac{\text{Half maximal inhibitory concentration on fibroblasts } (IC_{50})}{\text{Minimal inhibitory concentration on bacteria (MIC)}}$$

3.2.8. Cell compatibility tests

In a sterile flat bottom tissue-culture polystyrene (TCPS) 96-well plate, 5×10^4 cells/well (in case of L929 fibroblasts) and 5×10^5 cells/well (for HaCaT keratinocytes) were cultured and incubated at 37ºC, 5% CO_2 for 24 hours to allow cell adherence. In the case of THP-1 monocytes, the period of incubation was longer due to the induced stimulation for its differentiation into M0 macrophages as previously described in point 3.2.7. After this time, a serial dilution of PUs was added in each well with a final volume of 100 µL and the plate was kept in a humidified incubator for 1 day. Afterwards, observation of cell morphology by acquisition of bright field images was performed. In addition, cell viability/toxicity assays were also done: CellTiter-Blue® Cell Viability Assay (Promega), CytoTox-ONE™ Homogeneous Membrane Integrity Assay (Promega) and Live/Dead Fixable Staining Kit (PromoCell).

Briefly, CellTiter-Blue® is based on the capacity of alive cells to convert a resazurin into a fluorescent end-product (resorufin). After 2 hours of incubation with CellTiter-Blue reagent, the fluorescence intensity was quantified on black 96 well-plates by measuring the fluorescence at 590 nm, after excitation at 560 nm, in a microplate reader (Tecan plate reader Infinite® 200 PRO).

With the supernatant obtained in the end time of the previous described cell viability assay, the CytoTox-ONE™ evaluation was performed. This fluorometric assay estimates the quantity of nonviable cells. The measurement is done by detecting lactate dehydrogenase released from damaged membrane cells with a coupled enzymatic evaluation that results in the conversion of resazurin into resorufin (fluorescent product). The control for this assay was cell lysis done by the addition of 2 µL 9% Triton® X-100 (Promega) lysis buffer. On a black 96 well-plate the fluorescence intensity was read at 590 nm after excitation at 560 nm (Tecan plate reader Infinite® 200 PRO).

The Live/Dead staining kit associated with the microscopy observation on an Olympus IX51 microscope, allowed the analysis of viable/dying cells and their morphology. For this assay two fluorescent-based dyes were used: Calcein-AM and Ethidium homodimer III. Calcein-AM is a cell-permeant dye that enters viable cells and is hydrolysed by intracellular esterases converted the green-fluorescent calcein. The ethidium homodimer III membrane-impermeable fluorescent dye binds to DNA and is used to detect dead and dying cells. The dyes were prepared in PBS. The images were obtained under an Olympus IX51 inverted fluorescence microscope with the filters TRITC and FITC and a magnification of 100x.

3.2.9. Statistical analysis

In overall, data is expressed in Average ± Standard deviation of two or three independent experiments, each in triplicates. Statistical analysis was performed with the GraphPad Prism 5.00.288 software using One-way analysis of variance (ANOVA) with Dunnett's post-test in order to compare all columns with column control. Statistically significant values are as follows: *p ≤ 0.05, **p ≤ 0.01, ***p ≤ 0.001.

3.2.10. Workflow

Depending on the results obtained on the MIC against drug-susceptible bacteria found on skin wounds and cytocompatibility on L929 fibroblasts, different approaches for the polymeric systems under study were engaged. On the diagram below it is represented a comprehensive workflow in order to figure out which is the most promising newly synthesized amphipathic polyurethane for solving two key problems of infected chronic wounds: (1) presence of drug-resistant bacteria and (2) biofilm formation:

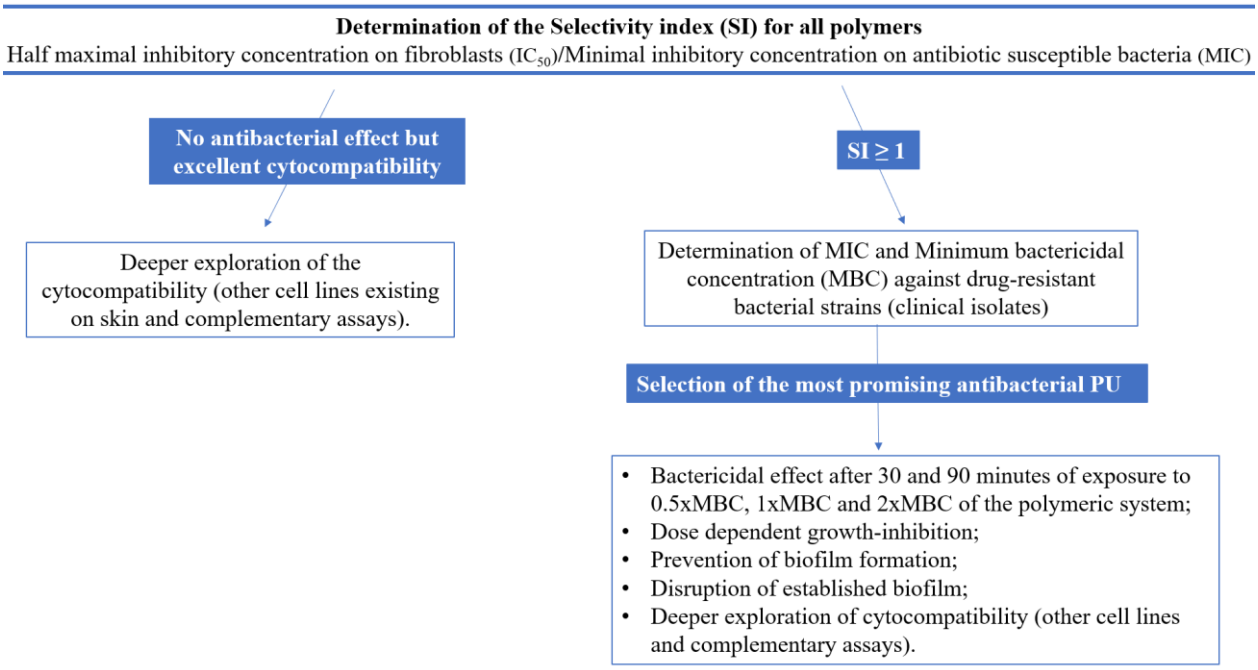

3.3. Results and discussion

3.3.1. Screening of the newly synthesized block copolymers on antibiotic sensitive-bacteria and its cytocompatibility

In order to perform the first screening and reduce the vast library of newly synthesized AMP-biomimetic amphipathic polyurethanes, the antimicrobial evaluation was done on drug-sensitive strains. The cytocompatibility was evaluated on L929 mouse fibroblasts as it is one cell line recommended by ISO 10993-5:2009 for cytotoxicity tests (26).

The polyurethane backbone NHP407 used for the synthesis of all polymers only induces a pronounced negative effect on cell viability at high concentrations (~ 5 mg/mL), hence it is a safe polyurethane with good cytocompatibility with L929 fibroblasts (**table 3.2**). Moreover, it did not induce bacterial growth inhibition, therefore the antibacterial effect observed by other newly synthesized block copolymers derive from their specific characteristics and not from this backbone.

NHP407-g-[poly(NIPAM)-b-poly(AETAC)] showed a bactericidal effect against *S. aureus* and *S. epidermidis* with low concentrations of 62.5 and 14.6 μg/mL respectively. Growth inhibition results on *E. faecalis*, *P. aeruginosa* and *K. pneumoniae* were also observed without a bactericidal effect until a maximum concentration of 2 mg/mL. Thus, it seems that this block copolymer is bacteriostatic against these strains. There was a selectivity index higher than 1 for both Staphylococci species under study and for the Gram-negative *K. pneumoniae*, but the latter did not induce a bactericidal impact (**table 3.2**). The monomers NIPAM and AETAC were able to inhibit the multiplication of the four strains of bacteria tested – *S. aureus*, *S. epidermidis*, *E. coli*, *P. aeruginosa* - but only achieved this with very high concentrations in the range of 3.75 to 15 mg/mL in the case of AETAC and a MIC of 12.5 to 50 mg/mL by testing NIPAM (**table 3.3**). These results prove that the antibacterial effect obtained by the block copolymer is ascribed to its entire cationic amphipathic structure.

In case of NHP407-g-[poly(NIPAM)-b-poly(MPC)] it was observed that it did not induce any inhibitory effect against all drug-sensitive species tested (**table 3.2**). It should be observed that in NHP407-g-[poly(NIPAM)-b-poly(MPC)] the ionic block is the poly(MPC), which contains the zwitterionic phosphorylcholine group, that comprises both anionic and cationic units. This confirms the importance of the dissociation of polycation and anion (exposing a free polycationic chain) in the polymeric system for an initial electrostatic interaction with the bacteria surface, and subsequent possibility for pore formations on the membrane. Interestingly,

a higher half maximal inhibitory concentration (IC_{50}) was determined with this polymer than with its original backbone NHP407, meaning that NHP407-g-[poly(NIPAM)-b-poly(MPC)] has a better cytocompatibility with L929 fibroblasts (**table 3.2**). In principle, poly(MPC) has the ability to penetrate the eukaryotic cell membrane without apparent destabilisation, hence it is highly cytocompatible (27). The 2-methacryloyloxyethyl phosphorylcholine (MPC) is a synthetic molecule developed to mimic the molecular structure of phosphatidylcholine - which is a constituent of eukaryotic plasma membranes (28). MPC was selected as a component of this polymer mainly because it was reported that the zwitterionic phosphorylcholine group in the side chain of MPC provides biologically inert functions to material surfaces, subsequently it is efficient in preventing bacteria adhesion and biofilm formation (27). In theory, bacteria would not be able to adhere to this material if it was tested as a mesh, such as an electrospun nanofiber, but the microdilution antibacterial assay was performed with the material as amphipathic PU in suspension. Even the MPC alone on Gram-positive and Gram-negative bacteria did not influence their growth (**table 3.3**). The choice of testing all these newly synthesized PUs as dispersion, was motivated by their possible application in transdermal delivery, considering that in chronic wounds it is very common that the pathogenic bacteria are also localized in deep tissue layers (29,30). Nevertheless, due to its excellent cytocompatibility with fibroblasts, a deeper biological characterization of this polymer will be explored further ahead in this chapter.

The cationic hydrophobic ionic liquid ILM-TFMSI is constituted by bis(trifluoromethanesulfonyl)imide anionic counter ions ($N(CF_3SO_2)_2^-$ or TFMSI). Counter ion is the designation given to the smaller of two ions which neutralizes the bulky polymerizable unit (31). In accordance to Zhao and collaborators, protic (e.g. H_2O) and aprotic (e.g. DMSO) solvents cause a different effect on the nature of solvation of ionic liquids (ILs) (32). The same authors reported that anions of the ILs had a strong interaction preferentially with H_2O molecules than with DMSO, which lead to the generation of more free cations and anions. However, the ILs in DMSO tended to become solvent-surrounded ion pairs resulting in a small quantity of free ions. Hence, there is a complete dissociation of cations and anions in H_2O, likely to pave the way for a stronger electrostatic interaction between the cationic polymerizable unit with the negatively charged head groups of acidic phospholipids on the bacterial cytoplasmic membrane, eventually inducing its disruption. Taking these findings in consideration, block copolymers constituted with ILM-TFMSI were tested in water and DMSO. NHP407-g-[poly(ILM-TFMSI)-b-poly(AETAC)] was efficient in killing 99.9% of *S. aureus* and *S. epidermidis* with concentrations between 3.91 – 28.64 µg/mL (**table 3.2**). No major

differences were found on the minimum bactericidal concentrations of NHP407-g-[poly(ILM-TFMSI)-b-poly(AETAC)] prepared in DMSO in comparison with H_2O. The reason for this observation, might be the fact that both preparations A and B are finally analysed in an aqueous environment, the Mueller-Hinton broth. Thus, the exposed positive charge of the polycation comes mainly from the dissociation between the poly(AETAC) with its hydrophilic counter ion - chloride anion (Cl^-) - that will go through dissociation in a high extent as soon it is in contact with water due to its hydrophilic properties.

Similarly to the previously described polymer, NHP407-g-[poly(ILM-TFMSI)-b-poly(MPC)] showed an antibacterial effect only against the *Staphylococci* strains, although with more than double-fold concentrations. This shows the importance of the poly(AETAC) block for a better antibacterial effect. No significant differences on the MIC and MBC of the polymer pre-prepared in DMSO (preparation A) and water (preparation B) were detected (**table 3.2**). The similar values may be due to the extreme hydrophilic non-interacting poly(MPC) block. One interesting observation is, that the IC_{50} of NHP407-g-[poly(ILM-TFMSI)-b-poly(AETAC)] is lower than the IC_{50} of NHP407-g-[poly(ILM-TFMSI)-b-poly(MPC)]. Hence, when the block copolymer is constituted by poly(MPC), it is more cytocompatible to fibroblasts than the one formed by the hydrophilic polyionic liquid poly(AETAC) (**table 3.2**). This property results from the presence of poly(MPC) in the polymeric system, which is described as a biocompatible polymer due to its cell membrane-like surface (33).

Concerning the PU block copolymers of group 3, the main point to explore was the importance of the counter ion dissociation, also related with the pre-preparation in DMSO or H_2O, for an effective bacteria clearance. The two counter ions under study where $N(CF_3SO_2)_2^-$ (also designated as TFMSI) and Br^-. NHP407-g-Poly(ILM-TFMSI) has hydrophobic anionic counter-ions, the bis(trifluoromethanesulfonyl) imide anions $N(CF_3SO_2)_2^-$. An ionic exchange reaction was induced in order to introduce a more hydrophilic anion, the bromide Br^-. The anion exchanged NHP407-g-Poly(ILM-Br) is more likely to exist as free polycation and anion in aqueous environment due to the hydrophilic counter ions. The exposed positive charge stemming from the quaternary ammonium moiety of the grafted polyionic liquid chain allows a higher probability for a stronger electrostatic interaction with the negative charged surface exposed phospholipid head groups of the bacterial membrane. It should be noted that the rate of ion exchange reaction is not 100%, remaining around 5% of $N(CF_3SO_2)_2^-$ (Purkayastha *et al*., unpublished). These remaining anions contribute to the hydrophobic regions together with the PEO-PPO-PEO main chain in NHP407 that undergoes temperature-induced aggregation phenomena as a result of the hydrophobic nature of poly(propylene oxide) (PPO) segment

when heated from ambient to body temperature 37°C (34). Differences were observed in the antibacterial effect of the polymers NHP407-g-Poly(ILM-TFMSI) and NHP407-g-Poly(ILM-Br) before and after the ionic exchange. NHP407-g-Poly(ILM-TFMSI) prepared in DMSO (preparation A) had a bactericidal effect on the Staphylococcal strains, but when pre-prepared in H_2O (preparation B), it did not induce any toxic result against all strains analysed (**table 3.2**). In the drug discovery field, poorly soluble compounds are a challenge in *in vitro* and *in vivo* studies, and many times fail to be active (35). Dimethylsulfoxide (DMSO) is an organic solvent that is able to dissolve polar and apolar compounds. Also it is miscible in water and most organic solvents (36). Additionally, this solvent is very popular to be used to dissolve hydrophobic components (37). The TFMSI anions of the Poly(ILM-TFMSI) block are hydrophobic counter ions. In DMSO these counter anions are solvent surrounded, getting dissolved, and small amounts of ion pairs are dissociated, making the polycation chain exposed and leads to the possibility of occurring electrostatic interaction with the bacteria's membrane. This is the reason why a pre-prepared NHP407-g-Poly(ILM-TFMSI) in DMSO exerted antibacterial effect to the Staphylococci strains while in water the same antimicrobial activity could not have been observed (**table 3.2**).

NHP407-g-Poly(ILM-Br) induced a bactericidal action against *Staphylococcus aureus*, *Staphylococcus epidermidis* and *Enterococcus faecalis* at low concentrations, for instance in the range of 6.5 to 46.85 µg/mL, when prepared in H_2O (preparation B) (**table 3.2**). As expected, with the polymer pre-prepared in DMSO the dissociation of the polycation and Br^- also occurred, but MIC and MBC are slightly higher. This is due to the preferential interaction energy between the anion of the polyionic liquid block Poly(ILM-Br) with water, than with DMSO, undergoing to a complete dissociation and exist as free polycations and anions, as described in Zhao and collaborators' work (32) (**figure 3.2**).

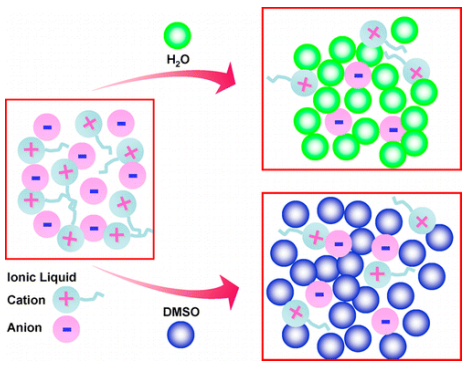

Figure 3.2. Representation of cation and anion dissociation of ionic liquids in water (H_2O) and dimethylsulfoxide (DMSO) (32).

Moreover, with these PU block copolymers pre-stirred in water (preparation B), an antibacterial effect against the Gram-negative *Pseudomonas aeruginosa* was observed at higher concentrations (MIC = 250 and MBC = 500 μg/mL) (**table 3.2**). The higher concentrations needed to produce a bactericidal effect, could be due to the lower permeability through the outer membrane existing on Gram-negative bacteria. To further understand this effect, the antibacterial capacity of NHP407-g-Poly(ILM-Br) (preparation B) on the carbapenem-resistant *P. aeruginosa* was also evaluated with no sign of antibacterial activity (data not shown). Carbapenem-resistant strains have a lower proportion of open functional porins in the outer membrane, reducing the permeability even more (38). Hence, this is one hypothesis for the mechanism to avoid the action of the NHP407-g-Poly(ILM-Br). Nevertheless, the minimal inhibitory concentration (MIC) is much higher than the half maximal inhibitory concentration on fibroblasts (IC_{50}), making it an unsafe polymer for treating *P. aeruginosa* infections (**table 3.2**).

Table 3.2. Inhibition parameters (MIC and MBC) on drug-sensitive bacterial strains and cytocompatibility on L929 fibroblasts of the different newly synthesized amphipathic polyurethanes and its common backbone NHP407.

Polymer	Bacteria spp.	MIC (μg/mL)	MBC (μg/mL)	IC_{50} on L929 (μg/mL)	SI (IC_{50}/MIC)
NHP 407	*S. aureus*	NI	NA	4328.9 ± 988.1	NA
	S. epidermidis	NI	NA		NA
	E. faecalis	NI	NA		NA
	E. coli	NI	NA		NA
	P. aeruginosa	NI	NA		NA
	K. pneumoniae	NI	NA		NA
NHP407-g-[poly(NIPAM)-b-poly(AETAC)]	*S. aureus*	15.6 ± 0	62.5 ± 0	79.6 ± 13.9	5.1
	S. epidermidis	7.3 ± 2.14	14.6 ± 4.25		10.9
	E. faecalis	500 ± 0	NF		0.16
	E. coli	NI	NA		NA
	P. aeruginosa	500 ± 0	NF		0.16
	K. pneumoniae	15.6 ± 0	NF		5.1
NHP407-g-[poly(NIPAM)-b-poly(MPC)]	*S. aureus*	NI	NA	8476.42 ± 2220.1	NA
	S. epidermidis	NI	NA		NA
	E. faecalis	NI	NA		NA
	E. coli	NI	NA		NA
	P. aeruginosa	NI	NA		NA
	K. pneumoniae	NI	NA		NA

NHP407-g-[poly(ILM-TFMSI)-b-poly(AETAC)] (Preparation A)	*S. aureus*	15.62 ± 0	15.62 ± 0	44.38 ± 3.4	2.84
	S. epidermidis	3.91 ± 0	3.91 ± 0		11.35
	E. faecalis	NI	NA		NA
	E. coli	NI	NA		NA
	P. aeruginosa	NI	NA		NA
	K. pneumoniae	NI	NA		NA
NHP407-g-[poly(ILM-TFMSI)-b-poly(AETAC)] (Preparation B)	*S. aureus*	13 ± 3.68	28.64 ± 5.83	26.79 ± 2.35	2.06
	S. epidermidis	3.91 ± 0	3.91 ± 0		6.85
	E. faecalis	NI	NA		NA
	E. coli	NI	NA		NA
	P. aeruginosa	NI	NA		NA
	K. pneumoniae	NI	NA		NA
NHP407-g-[poly(ILM-TFMSI)-b-poly(MPC)] (Preparation A)	*S. aureus*	62.5 ± 0	62.5 ± 0	107.15 ± 8.73	1.71
	S. epidermidis	7.81 ± 0	15.6 ± 0		13.7
	E. faecalis	NI	NA		NA
	E. coli	NI	NA		NA
	P. aeruginosa	NI	NA		NA
	K. pneumoniae	NI	NA		NA
NHP407-g-[poly(ILM-TFMSI)-b-poly(MPC)] (Preparation B)	*S. aureus*	31.25 ± 0	62.5 ± 0	106.84 ± 8.49	3.42
	S. epidermidis	7.81 ± 0	31.25 ± 0		13.68
	E. faecalis	NI	NA		NA
	E. coli	NI	NA		NA
	P. aeruginosa	NI	NA		NA
	K. pneumoniae	NI	NA		NA
NHP407-g-Poly(ILM-TFMSI) (Preparation A)	*S. aureus*	20.8 ± 7.35	46.85 ± 15.6	55.98 ± 8.73	2.69
	S. epidermidis	11.7 ± 3.9	15.6 ± 0		4.78
	E. faecalis	NI	NA		NA
	E. coli	NI	NA		NA
	P. aeruginosa	NI	NA		NA
	K. pneumoniae	NI	NA		NA
NHP407-g-Poly(ILM-TFMSI) (Preparation B)	*S. aureus*	NI	NA	61.77 ± 5.61	NA
	S. epidermidis	Slight inhibition ≥ 250	NF		NA
	E. faecalis	NI	NA		NA
	E. coli	NI	NA		NA
	P. aeruginosa	NI	NA		NA
	K. pneumoniae	NI	NA		NA

NHP407-g-Poly(ILM-Br) (Preparation A)	*S. aureus*	15.6 ± 0	15.6 ± 0	29.6 ± 1.22	1.89
	S. epidermidis	7.8 ± 0	7.8 ± 0		3.79
	E. faecalis	62.5 ± 0	62.5 ± 0		0.47
	E. coli	NI	NA		NA
	P. aeruginosa	NI	NA		NA
	K. pneumoniae	NI	NA		NA
NHP407-g-Poly(ILM-Br) (Preparation B)	*S. aureus*	10.4 ± 3.7	10.4 ± 3.7	35.21 ± 2.51	3.39
	S. epidermidis	6.5 ± 1.8	6.5 ± 1.8		5.42
	E. faecalis	31.2 ± 0	46.85 ± 15.6		1.13
	E. coli	NI	NA		NA
	P. aeruginosa	250 ± 0	500 ± 0		0.14
	K. pneumoniae	Slight inhibition ≥ 500	NF		NA

MIC – Minimum inhibitory concentration, MBC – Minimum bactericidal concentration, IC_{50} – Half maximal inhibitory concentration, SI – Selectivity index = IC_{50} mammalian cells/MIC on bacteria, NA – not applicable, NF – not found starting with a maximum concentration of 2 mg/mL, NI – no inhibition observed starting with a maximum concentration of 2 mg/mL, Preparation A – in DMSO, Preparation B – in H_2O

Table 3.3. Antibacterial effect of the monomers and lithium bromide used to synthesize the different groups of polymers on drug-sensitive strains and its respective cytocompatibility on L929 fibroblasts.

Monomer	**Bacteria spp.**	**MIC (mg/mL)**	**IC_{50} on L929 (mg/mL)**	**SI (IC_{50}/MIC)**
NIPAM	*S. aureus*	50 ± 0	10.68 ± 0.52	0.21
	S. epidermidis	50 ± 0		0.21
	E. coli	25 ± 0		0.43
	P. aeruginosa	12.5± 0		0.85
ILM-TFMSI	*S. aureus*	NI	4.25 ± 0.35	NA
	S. epidermidis	NI		NA
	E. coli	Slight inhibition ≥ 25		NA
	P. aeruginosa	Slight inhibition ≥ 25		NA
AETAC	*S. aureus*	5.62 ± 1.87	0.809 ± 0.14	0.14
	S. epidermidis	3.75 ± 0		0.22
	E. coli	15 ± 0		0.05
	P. aeruginosa	15 ± 0		0.05
MPC	*S. aureus*	NI	> 50	NA
	S. epidermidis	NI		NA
	E. coli	NI		NA
	P. aeruginosa	NI		NA

Lithium Bromide	*S. aureus*	NI	0.141 ± 0.01	NA
	S. epidermidis	NI		NA
	E. coli	NI		NA
	P. aeruginosa	NI		NA

MIC – Minimum inhibitory concentration, IC_{50} – Half maximal inhibitory concentration, SI – Selectivity index = IC_{50} mammalian cells/MIC on bacteria, NA – not applicable, NI – no inhibition observed starting with a maximum concentration of 2 mg/mL

Lithium bromide was used for the ionic exchange reaction to finally obtain NHP407-g-Poly(ILM-Br). It is a salt that dissociates in water, therefore forming Li^+ cations and Br^- anions. After synthesis, the polymer was dialysed and the lithium ions were removed, leaving only the bromide anions as counter ions (Purkayastha *et al*., unpublished). The lithium bromide alone did not induce any toxic activity against bacteria, meaning that the bactericidal effect of NHP407-g-Poly(ILM-Br) comes from the polymer itself and not from the bromide anions (**table 3.3**). However, the ions alone decreased the fibroblast population *in vitro* to 50% when a concentration of 141 μg/mL was added (**table 3.3**). This means that there is a possibility that the reduction in cell viability observed with NHP407-g-Poly(ILM-Br) might have been aggravated due to the presence of bromide anions in the aqueous dispersion.

In general, the newly synthesized polyurethane systems were bactericidal to Gram-positive and inert to Gram-negative bacteria. It is well-known that Gram-positive and -negative bacteria have completely different cell wall structures (**figure 3.3**).

The Gram-positive cell wall is mainly composed by peptidoglycan, teichoic acid and lipoteichoic acid, and presents one periplasmic space between the peptidoglycan layer and the plasma membrane. Wall teichoic acids - covalently linked to the peptidoglycan - and membrane lipoteichoic acids - anchored to the lipid plasma membrane - are polyanionic polymers in the envelope of Gram-positive bacteria that contribute to the negative charge of the cell wall (39,40). These teichoic acids exposed on the cell surface provide optimal binding sites for cationic polymers. For the newly synthesized polyurethanes under study, it is essential that an initial binding to the bacterial surface occurs, involving a strong electrostatic interaction between the polycation and bacteria's surface, to induce its antibacterial activity. The absence of these wall teichoic acids in Gram-negative species might be a reasonable explanation for the inefficient antimicrobial action of the new amphipathic block copolymers in this project.

Moreover, the cell wall of Gram-negative bacteria is more complex. Besides the plasma membrane and peptidoglycan membrane, it is also constituted by lipopolysaccharide, lipoproteins and protein channels (porins) on the outer phospholipidic membrane. Between the

three membranes, there are two periplasmic spaces. Hence, any active compound has a great challenge to impact Gram-negative bacteria survival since it must first cross the hydrophilic highly charged lipopolysaccharide layer of the outer cell envelope (41). The most successful molecules against Gram-negative bacteria are small hydrophilic ones that are able to enter the membrane by the non-selective process of passive diffusion, which is facilitated by the presence of porins (42). It seems, that the polyurethane systems lack or have a very reduced capacity of penetration through the outer membrane, and it is probably due to its large size (for example, NHP407-g-Poly(ILM-TFMSI) has a molecular weight of 80,000 g/mol and 40 repeating units) (Purkayastha *et. al*, unpublished).

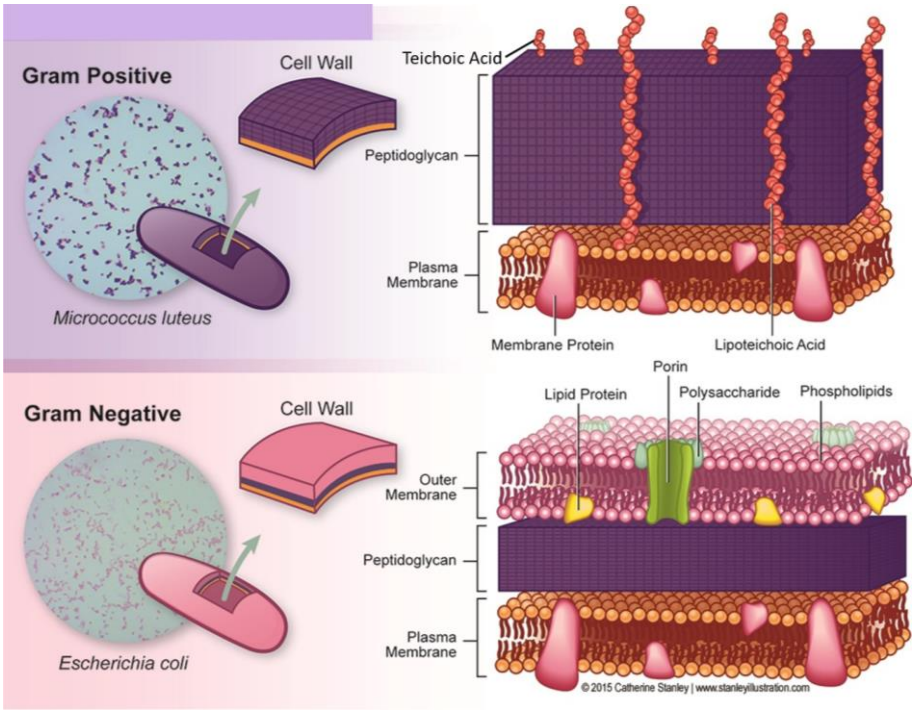

Figure 3.3. Constitution of Gram-positive and Gram-negative bacteria cell walls (43).

3.3.2. Antibacterial efficiency of the antimicrobial amphipathic polyurethanes on multidrug-resistant Gram-positive pathogens

One of the main challenges to be overcome with the utilisation of these polymeric systems, is to combat the emergence and spread of the most relevant clinically isolated multidrug-resistant bacterial strains from chronic wounds. Unfortunately, the loss of skin integrity provides a temperate and humid nutritious region, optimal for adherence, growth and colony establishment of potentially pathogenic bacteria (44). The emergence of antibiotic resistant strains in such environments is a serious issue and has been reported worldwide to be an urgent problem (45,46). This poses the necessity of entering a post antibiotic era.

Antimicrobial resistant (AMR) Gram-positive pathogens are a severe obstacle on chronic wounds that should not be ignored (47). The *Staphylococcus* and *Enterococcus* genera are among the most common bacterial causes of registered clinical infections (48).

Methicillin-resistant *Staphylococcus aureus* (MRSA) is possibly the most known example of hospital-acquired or community-associated infectious organism. The term MRSA persisted even though methicillin is no longer clinically produced or used. Nowadays, this term refers to the resistance of *S. aureus* to all β-lactams antibiotics, such as penicillin and carbapenems with the exception of novel cephalosporin β-lactams (49). The resistance mechanism is usually associated with the expression of the penicillin-binding protein 2A (PBP2A), which is encoded by the mecA gene. PBPA2 has drastically lower affinity for β-lactams, consequently the cell-wall biosynthesis still proceeds in the presence of this antibiotic (49). Just as a reference, the MIC of the narrow-spectrum β-lactam antibiotic oxacillin on MRSA is generally around 15.6 to 1000 μg/mL, while 125 ng/mL to 100 μg/mL are enough to obtain a bacterial inhibition consequence against a sensitive-strain of *S. aureus* (50).

In addition to MRSA, Vancomycin-resistant Enterococci (VRE) is another healthcare-associated pathogen that is a huge burden. Vancomycin is a glycopeptide antibiotic. The origin of the resistance to this antibiotic in *Enterococcus* spp is moderated by the existence of the vancomycin resistance (Van) operons, not previously existing in Enterococci. Van gene operons present various AMR phenotypes due to their constantly evolving genetic variability (51). Among Van genes, VanA is most commonly associated with *Enterococcus faecalis* and *E. faecium* and it is plasmid borne. It confers a high-level of resistance to vancomycin (more than 256 μg/mL has to be applied to obtain the MIC) (52). VanA is mediated by the transposon Tn1546 that encodes a dehydrogenase (VanH) able to reduce pyruvate to D-Lac, and the VanA ligase that catalyses the establishment of an ester bond between D-Ala and D-Lac. Therefore, the usual D-Ala-D-Ala dipeptide in peptidoglycan synthesis is substituted by the D-Ala-D-Lac depsipeptide, to which glycopeptides (e.g. vancomycin) have reduced affinity (53,54).

Mainly the two previously described AMR strains are a major issue in the health-care setting. Taking this into consideration, antibacterial tests were performed on drug-resistant *Staphylococcus* spp and *Enterococcus* spp (**table 3.4**). The latter was assessed only on the PU system, which showed antibacterial activity on its correspondent drug-sensitive strain.

NHP407-g-[poly(NIPAM)-b-poly(AETAC)] was antibacterial against methicillin-resistant *S. aureus* (MRSA) and the antibiotic-resistant *S. epidermidis* (ARSE) (**table 3.4**). However, the concentrations needed to induce a bactericidal effect are considerably superior to the minimal

bactericidal concentration (MBC) on the drug-sensitive cells (4-fold more in case of *S. aureus* and 8.6-fold for *S. epidermidis*) (**table 3.2 and 3.4**).

From group 2 of amphipathic polyurethanes, NHP407-g-[poly(ILM-TFMSI)-b-poly(AETAC)] acted against both drug-resistant Staphylococcal strains, regardless of its previous preparation in DMSO (prep. A) or water (prep. B). However, once again the MBC was higher than the MBC measured in case of the correspondent drug-sensitive bacteria (**table 3.2. and 3.4**). It was interesting to observe that the preparation B of this polymer had a better bactericidal action on MRSA than preparation A, which make us believe that the higher dissociation of polycation and anion chloride (Cl^-) of the poly(AETAC) block in water, was responsible for this outcome. For the other polymer of this group – NHP407-g-[poly(ILM-TFMSI)-b-poly(MPC)] – the antibacterial results showed that it was only efficient against ARSE. Nevertheless, the MBC with both preparations A and B is 2 to 5 times higher than the one detected on *S. epidermidis* ATCC® 12228™ (**table 3.2 and 3.4**).

Table 3.4. Drug-resistant clinically isolated Gram-positive bacteria sensitivity to the newly synthesized antibacterial polyurethanes and its effect on the mammalian cell line L929 fibroblasts.

Polymer	Bacteria clinical isolate	MIC (µg/mL)	MBC (µg/mL)	IC_{50} on L929 (µg/mL)	SI (IC_{50}/MIC)
NHP407-g-[poly(NIPAM)-b-poly(AETAC)]	MRSA	83.3 ± 19.4	250 ± 0	79.6 ± 13.9	0.95
	ARSE	31.25 ± 0	125 ± 0		2.54
NHP407-g-[poly(ILM-TFMSI)-b-poly(AETAC)] (Preparation A)	MRSA	62.5 ± 0	250 ± 0	44.38 ± 3.4	0.71
	ARSE	15.6 ± 0	31.25 ± 0		2.84
NHP407-g-[poly(ILM-TFMSI)-b-poly(AETAC)] (Preparation B)	MRSA	31.25 ± 0	50 ± 5.3	26.79 ± 2.35	0.85
	ARSE	23.42 ± 3.8	31.25 ± 0		1.14

NHP407-g-[poly(ILM-TFMSI)-b-poly(MPC)] (Preparation A)	MRSA	NI	NI	107.15 ± 8.73	NA
	ARSE	31.25 ± 0	83.3 ± 29.5		3.43
NHP407-g-[poly(ILM-TFMSI)-b-poly(MPC)] (Preparation B)	MRSA	NI	NI	106.84 ± 8.49	NA
	ARSE	46.87 ± 15.6	62.5 ± 0		2.28
NHP407-g-Poly(ILM-Br) (Preparation B)	MRSA	13 ± 3.68	13 ± 3.68	35.21 ± 2.51	2.7
	ARSE	13 ± 3.68	18.2 ± 9.73		2.7
	VRE	31.2 ± 0	62.5 ± 0		1.13

MIC – Minimum inhibitory concentration, MBC – Minimum bactericidal concentration, IC_{50} – Half maximal inhibitory concentration, SI – Selectivity index = IC_{50} mammalian cells/MIC on bacteria, NA – not applicable, NI – no inhibition observed starting with a maximum concentration of 2 mg/mL, MRSA – Methicillin-resistant *Staphylococcus aureus*, ARSE - Antibiotic-Resistant *Staphylococcus epidermidis*, VRE – Vancomycin-resistant Enterococci, Preparation A – in DMSO, Preparation B – in H_2O

The most extraordinary case was the NHP407-g-Poly(ILM-Br). This polymer was able to kill MRSA, ARSE and VRE at very low concentrations – 13 to 62.5 µg/mL. It is important to consider that NHP407-g-Poly(ILM-Br) polymer was not cytotoxic to fibroblasts at these concentrations (SI > 1 for all cases) (**table 3.4**). It is worth noticing, moreover, that the MBC on two of the most commonly found AMR species (MRSA and VRE) is very similar to the MBC on the ATCC® drug-sensitive strains (**table 3.2 and 3.4**). In fact, for MRSA only ~2.6 µg/mL more is necessary to induce a 99.9% killing rate, in relation to the sensitive *S. aureus* ($MBC_{S.aureus}$= 10.4 µg/mL and MBC_{MRSA}= 13 µg/mL). For VRE, only a 1.3-fold of $MBC_{E.faecalis}$ is sufficient to reduce its survival to 0 CFU/mL. Usually, the concentration of clinically used antibiotics have to be augmented to induce the desired antibacterial outcome on AMR pathogens (55,56). However, with NHP407-g-Poly(ILM-Br) a bactericidal effect on antibiotic-resistant bacteria was obtained to the same extent as drug-sensitive *Staphylococcus aureus* and *Enterococcus faecalis*. This observation clearly shows that the antimicrobial resistance mechanisms of action, evolutionarily gained in MRSA and VRE, do not seem to impede the significant antibacterial potential of NHP407-g-Poly(ILM-Br).

Considering the results described so far, NHP407-g-Poly(ILM-Br) was selected for further antibacterial and cytocompatibility evaluations. However, NHP407-g-[poly(NIPAM)-b-poly(MPC)] showed excellent cytocompatibility, for instance a better cytocompatibility on L929 fibroblasts than its backbone polymer NHP407 (**table 3.2**). In the following point, further investigation of this behaviour is described.

3.3.3. Assessment of cytocompatibility features of NHP407-g-[poly(NIPAM)-b-poly(MPC)] versus its backbone NHP407: A comparative study

In point 3.3.1, after analysing L929 fibroblasts' cell viability by the CellTiter-Blue® assay, the IC_{50} calculated for NHP407-g-[poly(NIPAM)-b-poly(MPC)] was higher than for NHP407. This captured our attention for understanding more about the cytocompatibility characteristics of this amphipathic polymer.

First, a simple experiment was set in which bright field images of the growth of fibroblasts during 0, 2, 4 and 24 hours in the presence of 5 mg/mL of NHP407 or NHP407-g-[poly(NIPAM)-b-poly(MPC)] were obtained (**figure 3.4**). Our presumption was, that visual differences in cell proliferation rate are detected mainly in the first hours. 5 mg/mL was selected because with 4.33 ± 0.99 mg/mL it was determined a cell viability reduction of 50% with NHP407, but in the same concentration NHP407-g-[poly(NIPAM)-b-poly(MPC)] only induced a reduction of viability of ~30% (**table 3.2 and figure 3.5**). Hence, it was predicted that differences in cell confluency would be observable with 5 mg/mL. However, no major differences were registered with this method (**figure 3.4**). Only it seems that there was less confluency of fibroblasts on the wells with NHP407 or NHP407-g-[poly(NIPAM)-b-poly(MPC)] at the time point of 4 hours when compared to the optimal growth, that corresponds to images of L929 cells grown in RPMI complete medium without any addition of polymers (**figure 3.4**).

To proceed with the analysis of the cytocompatibility of this polymer, another immortalized cell line was added to the study, HaCaT human keratinocytes. These cells are a predominant population on skin and the importance of the crosstalk between fibroblasts and keratinocytes in restoring the barrier function in wounded skin has been reported (57). Herein, a comparative study of cell viability by measuring the conversion of resazurin into the fluorescent resorufin by dehydrogenase enzymes of living cells and cytotoxicity by quantifying the lactate dehydrogenase – LDH - released from damaged cells between a serial dilution of NHP407 and NHP407-g-[poly(NIPAM)-b-poly(MPC)] on L929 fibroblasts and HaCaT keratinocytes were

performed (**figure 3.5**). The analysis of the graphs of both NHP407 and NHP407-g-[poly(NIPAM)-b-poly(MPC)] shows that with the increase of concentration of polymers, the cell viability decreases while the cytotoxicity increases. Overall, the findings show that the tested polymers induced a higher toxic effect on L929 mouse fibroblast cells from the subcutaneous connective tissue than on HaCaT keratinocytes from adult human skin at concentrations of 5 and 10 mg/mL. Moreover, 5 mg/mL of NHP407 on L929 cells (fibroblasts) induced the decrease of viability to ~50%. Respectively, the viable cells percentage with NHP407-g-[poly(NIPAM)-b-poly(MPC)] is around 70% which is still considered as a cytocompatible result by ISO 10993-5 (≥ 70% viable cells) (26). In case of HaCaT cells (keratinocytes) all the polyurethane concentrations tested were not harmful (**figure 3.5**). The cytotoxicity evaluation (LDH release %) confirms the observed results of the cell viability evaluation. In fact, in the presence of NHP407 both cell populations released more LDH to the supernatant than when exposed to NHP407-g-[poly(NIPAM)-b-poly(MPC)] for 24 hours (**figure 3.5**).

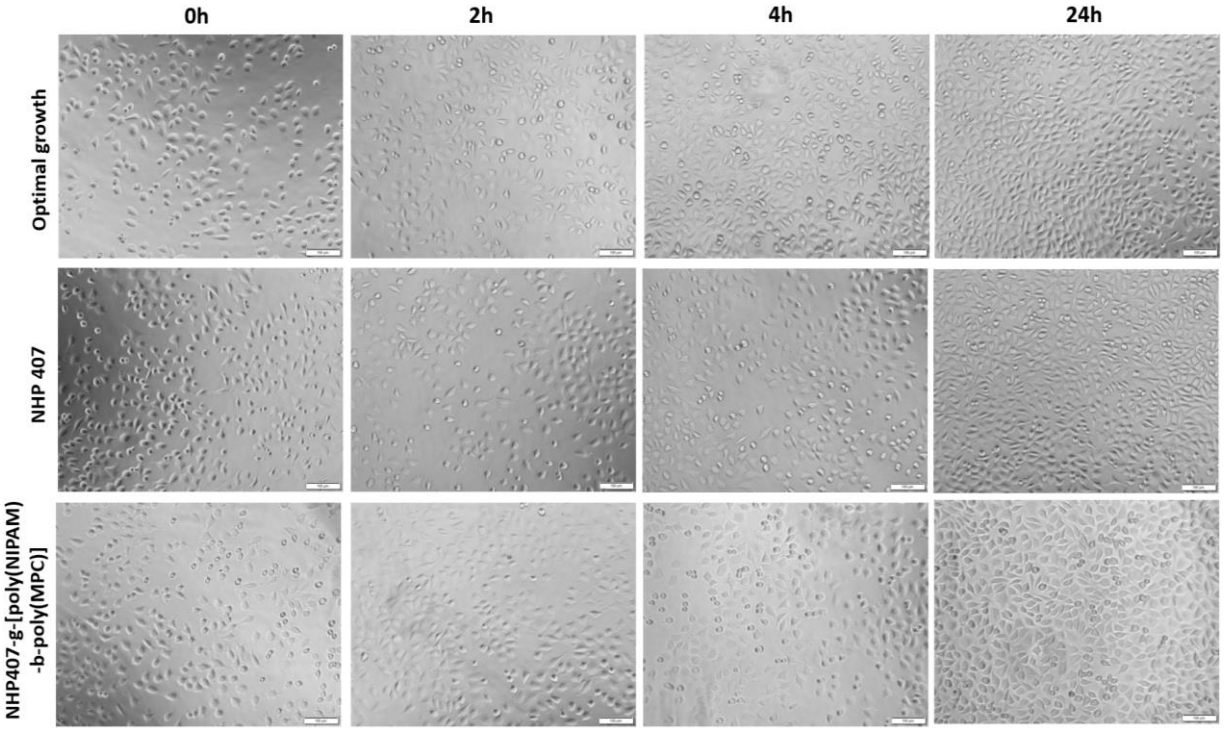

Figure 3.4. Representative bright field microscopic images of L929 fibroblasts in the presence of 5 mg/mL of NHP407 or NHP407-g-[poly(NIPAM)-b-poly(MPC)] during time (0, 2, 4 and 24 hours). White bar represents 100 μm.

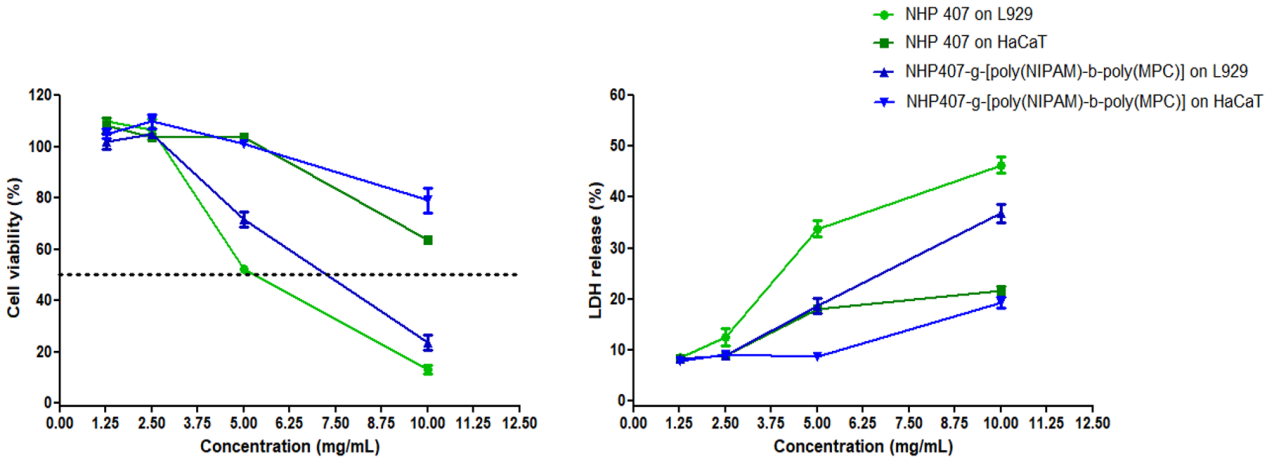

Figure 3.5. Percentage of L929 fibroblasts and HaCaT keratinocytes viability (left graph) and lactate dehydrogenase (LDH) release (right graph) in the presence of increasing concentrations of NHP407 and NHP407-g-[poly(NIPAM)-b-poly(MPC)]. Evaluation performed after 24 hours of incubation. Dashed line represents 50% cell viability.

To obtain a full picture of cell viability and toxicity in the presence of both polymers, a Live/Dead staining assay was executed. This assay employs two probes at the same time, that will detect intracellular esterase activity in living cells with calcein-AM and compromised plasma membrane integrity with ethidium homodimer III, that will be shown as green and red colors, under fluorescence microscopy. Microscopic images were acquired with concentrations of 1.25, 2.5, 5 and 10 mg/mL for both polymers on L929 and HaCaT (**figure 3.6. and 3.7**).

As expected, more dead and/or dying cells (in red) were noticed with the increase of concentration of both PUs (**figure 3.6. and 3.7**). On L929 cells, pronounced differences of the normal cell shape and the confluency of cells were observed at concentrations higher than 2.5 mg/mL. With NHP407, the confluence on the bottom of the well is lower, which suggests that the cells finally detached under the influence of 5 or 10 mg/mL of this backbone PU (**figure 3.6**). Especially with 10 mg/mL NHP407, L929 cells lost their typical elongated shape and adopted a smaller rounded shape which correlates with the low cell viability and high cytotoxicity determined beforehand (**figure 3.5 and 3.6**). After the treatment with 5 mg/mL NHP407-g-[poly(NIPAM)-b-poly(MPC)] for 24 hours, the presence of dying fibroblasts (red) is clearly observable, but the usual fibroblasts shape of the living cells is still intact (green). Similar results were observed at 10 mg/mL of NHP407-g-[poly(NIPAM)-b-poly(MPC)] concentration, with the difference of more open spaces exist between the cells (**figure 3.6**).

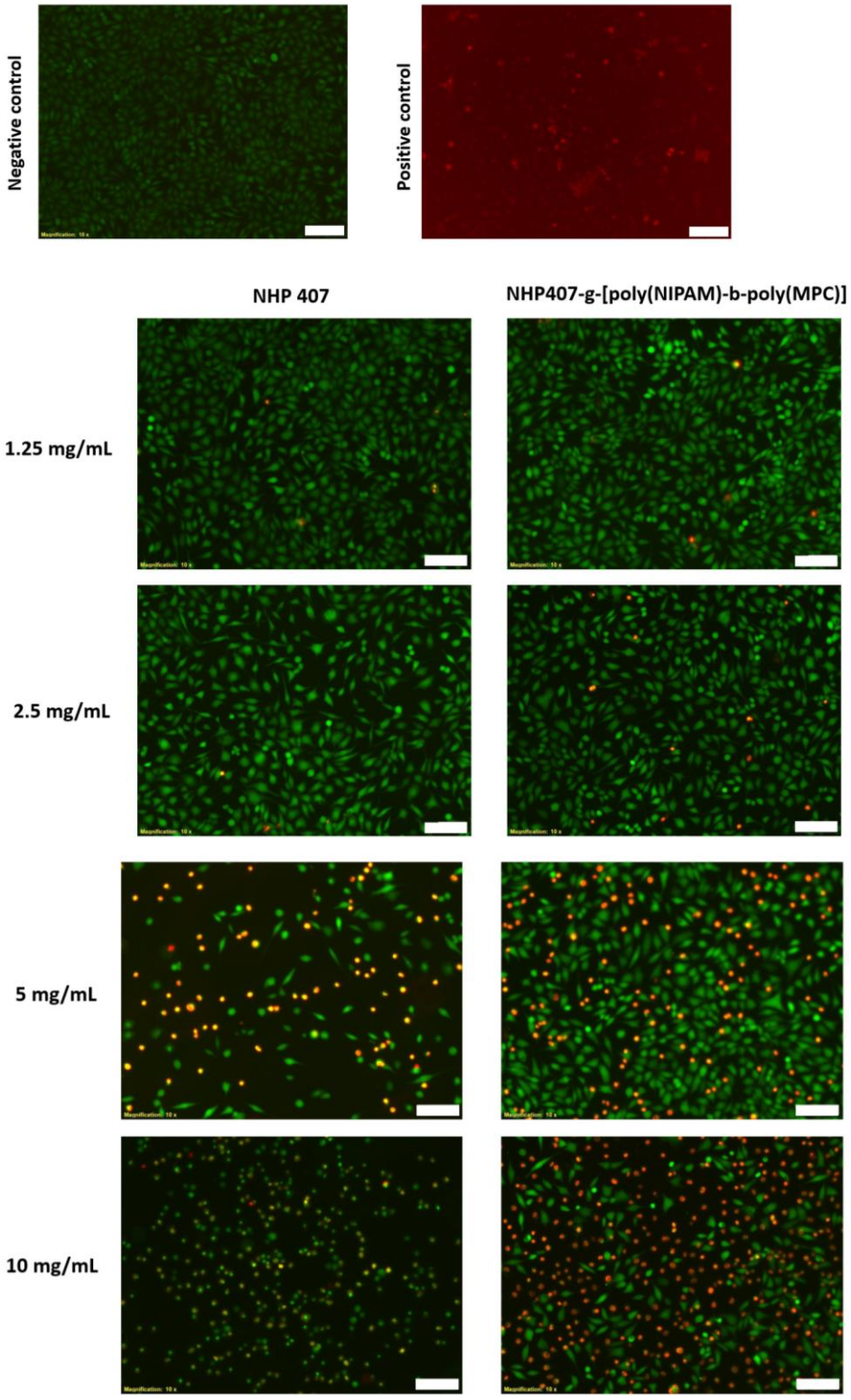

Figure 3.6. Live/dead staining fluorescence microscopic images of fibroblasts (L929) after 24 hours of exposition to 1.25, 2.5, 5 or 10 mg/mL of NHP407 (left side) or NHP407-g-[poly(NIPAM)-b-poly(MPC)] (right side). White bar represents 100 μm. Negative control – L929 cells only, Positive control – L929 cell lysis (2 μL 9% Triton® X-100 lysis buffer).

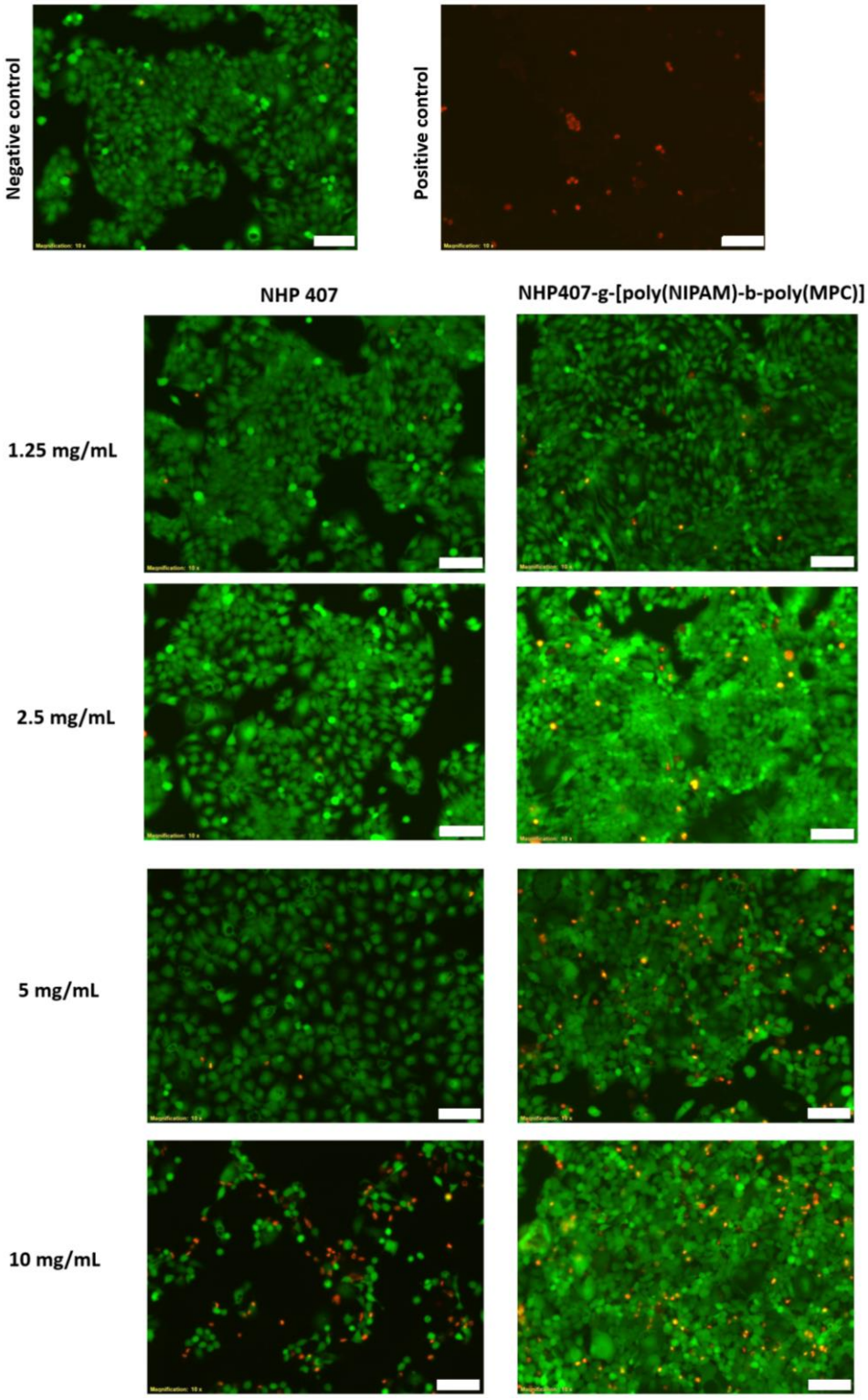

Figure 3.7. Live/dead staining fluorescence microscopic images of keratinocytes (HaCaT) after 24 hours of exposition to 1.25, 2.5, 5 or 10 mg/mL of NHP407 (left side) or NHP407-g-[poly(NIPAM)-b-poly(MPC)] (right side). White bar represents 100 μm. Negative control – L929 cells only, Positive control – L929 cell lysis (2 μL 9% Triton® X-100 lysis buffer).

On HaCaT cells, NHP407-g-[poly(NIPAM)-b-poly(MPC)] does not negatively impact the dense layer formed by multiplying keratinocytes with all concentrations tested, although more dying cells are noticed with the increase of concentration (**figure 3.7**).
On the other hand, with 10 mg/mL of NHP407, a significant difference is visualized. Less cells are adhered to the bottom of the well, with the ethidium homodimer III entering many of the remaining attached cells, showing that these cells have an altered membrane permeability resulting in cell-death (**figure 3.7**).

All these complementary biological assays, including those obtained with the keratinocyte cell line, give support to the higher IC_{50} value on fibroblasts exposed to NHP407-g-[poly(NIPAM)-b-poly(MPC)] than to the NHP407 PU backbone. Therefore, NHP407-g-[poly(NIPAM)-b-poly(MPC)] has shown better cytocompatibility than NHP407 most probably due to the presence of poly(MPC) groups in the polyurethane structure, which have a long history of being highly biocompatible (58).

3.3.4. Further investigation of NHP407-g-Poly(ILM-Br) antimicrobial properties and compatibility with selected skin cell populations

In this point, the focus lies on NHP407-g-Poly(ILM-Br), which has previously shown the most promising properties to combat non- and drug-resistant Gram-positive pathogens.
After observing the significant bactericidal action with low concentrations, the question was, if this bactericidal activity is occurring in a short period of time. For that evaluation, *S. aureus*, MRSA, *S. epidermidis*, ARSE, *E. faecalis* and VRE were exposed to 3 different concentrations related with the MBC (0.5×MBC, 1×MBC, 2×MBC) for 30 and 90 minutes only. After those short periods of contact with the PU, the reduction of CFU/mL was determined for each Gram-positive strain (**figure 3.8**).
It was pleasant to observe that the profile of bacterial reduction with the three different concentrations was very similar between the drug-sensitive *S. aureus* and MRSA. It seems that NHP407-g-Poly(ILM-Br) has the capacity to kill *S. aureus* bacteria after only 30 and 90 minutes, regardless of their multidrug-resistance. By applying the minimal inhibitory concentration, the CFU/mL was immediately reduced from ~50 to 60% after 30 minutes of exposure. With 2×MBC, after both short time periods, almost a complete annihilation of the non- and methicillin-resistant *S. aureus* populations was registered (**figure 3.8**).
S. epidermidis and ARSE were both inhibited at the same percentage with 2×MBC after 30 and 90 minutes of exposure. Remarkably NHP407-g-Poly(ILM-Br) seems to be more efficient in

reducing the bacterial burden against the antibiotic-resistant *S. epidermidis* on its minimal bactericidal concentration (1×MBC) after 90 minutes of action. However, it is necessary to take into consideration that an inconsistent variability of the results (calculated standard deviation from 3 independent experiments is quite high) under this concentration was detected (**figure 3.8**).

In a short period of contact, the polymer had a stronger antibacterial effect on vancomycin-resistant Enterococci (VRE) than on *E. faecalis* drug-sensitive strain (**figure 3.8**). As explained before in this chapter, vancomycin is a drug that binds to the peptidoglycan ending of D-Alanyl-D-Alanine. In the case of this VRE strain, the VanA gene is expressed which results in the synthesis of abnormal peptidoglycan precursors terminating in D-Alanyl-D-Lactate, instead of D-Alanyl-D-Alanine (54). Hence, vancomycin drug binds with much less affinity to D-Alanyl-D-Lactate, and its mechanism of antibacterial action is no longer induced. Possibly, this abnormality is advantageous to the PU antimicrobial activity, attracting them more to the bacterial surface and paving a way for their anti-Enterococci action after only 30 and 90 minutes of time.

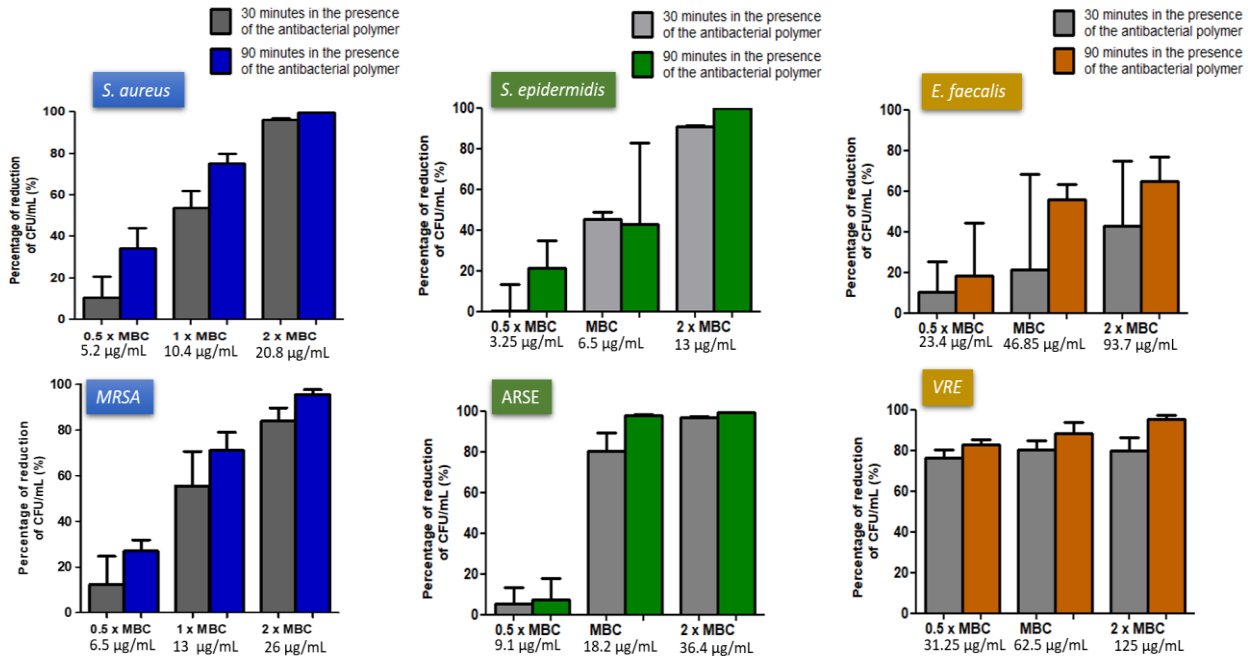

Figure 3.8. Bactericidal effect of NHP407-g-Poly(ILM-Br) on a range of drug-sensitive and -resistant Gram-positive pathogens in a short period of contact (30 and 90 minutes). MBC – Minimal bactericidal concentration.

The next step in unveiling the antibacterial properties of NHP407-g-Poly(ILM-Br) was to perform a dose-dependent growth inhibition of bacteria treated with this polymer through a

broth microdilution assay. The Gram-positive strains had 4 to 6 hours of lag phase (phase in which bacteria adapt themselves to the growth conditions) which preceded detectable bacterial turbidity. Exposing the Gram-positive strains to increasing concentrations of NHP407-g-(ILM-Br) enhanced the bacterial inhibition (**figure 3.9**). Therefore, in all conditions, inhibition of bacterial growth was dose-dependent. The growth was completely inhibited above 31 µg/mL in case of methicillin-sensitive and resistant *S. aureus*, 15 µg/mL for *S. epidermidis* and macrolide-lincosamide-streptogramin B and methicillin (MLS Mec A+) antibiotic-resistant *Staphylococcus epidermidis* (ARSE), and 62.5 µg/mL in case of the sensitive and vancomycin-resistant Enterococci species (**figure 3.9**). Herein, the similar profile of bacterial inhibition between the drug-sensitive and its correspondent drug-resistant bacterial clinical isolate should also be highlighted.

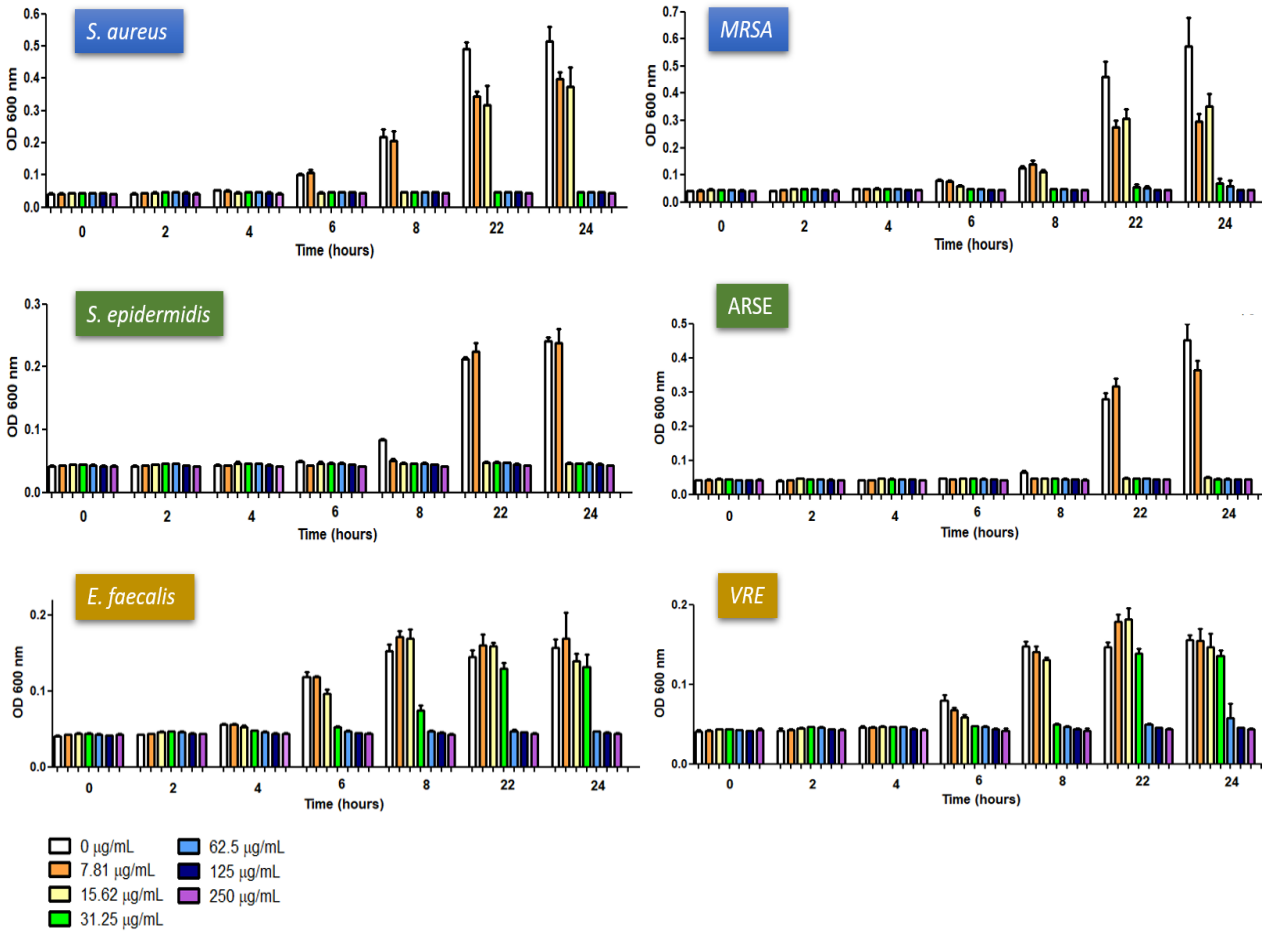

Figure 3.9. Dose-dependent growth inhibition of a range of non- and drug-resistant Gram-positive bacteria in the presence of NHP407-g-Poly(ILM-Br) (broth microdilution assay). Measurements were made at optical density 600nm after 0, 2, 4, 6, 8, 22 and 24 hours of contact between the polymer and Staphylococcal or Enterococcal bacteria.

Besides the susceptibility to infection of acute and chronic wounds by sensitive and multi-antibiotic resistant bacteria as planktonic form, these bacterial cells are able to attach to the wound bed and establish organized microbial communities, referred to as biofilms (4). Biofilms completely diverge from planktonic bacteria in many aspects, including gene expression, structure and antibiotic resistance (29). The most prominent characteristics responsible for increasing antibiotic tolerance are: slow growth rate, adaptative stress responses, stable communication between bacteria, nutrient limitation and a reduced antibiotic penetration (59). Consideration should be given in utilizing a therapy that also prevents the formation of biofilm communities. With this in mind, the capacity of NHP407-g-Poly(ILM-Br) aqueous dispersion in preventing bacterial adhesion and further biofilm formation on favourable surfaces (tissue-culture treated plates) was assessed. For this assay, our interest was to understand the possible outcome for different Gram-positive bacteria genera, hence its efficiency on one Staphylococci strain and one Enterococci spp., including their respective drug-resistant counterparts, was directly compared.

In the first 72 hours of treatment, concentrations above 7.8 μg/mL were able to significantly reduce the biofilm biomass against methicillin-sensitive *S. aureus*. On MRSA, 31.25 μg/mL and higher quantities were extremely efficient in preventing biofilm formation (**figure 3.10**).

On *Enterococcus faecalis*, biofilm formation was significantly reduced with all concentrations in the first 48 hours. At 72h, it was observed that in the presence of 15.6 and 7.8 μg/mL, the enterococci was able to establish a biofilm on the well surface with the same biomass as the non-treated control. NHP407-g-Poly(ILM-Br) had the ability to inhibit an establishment of a fully formed biofilm of VRE until 72 hours, with concentrations above 15.6 μg/mL (**figure 3.10**).

Therefore, above concentration of 15.6 μg/mL, the NHP407-g-Poly(ILM-Br) polymeric system has the capacity to interfere with the bacterial growth and adhesion to surfaces, preventing biofilm formation until a prolonged period of three days.

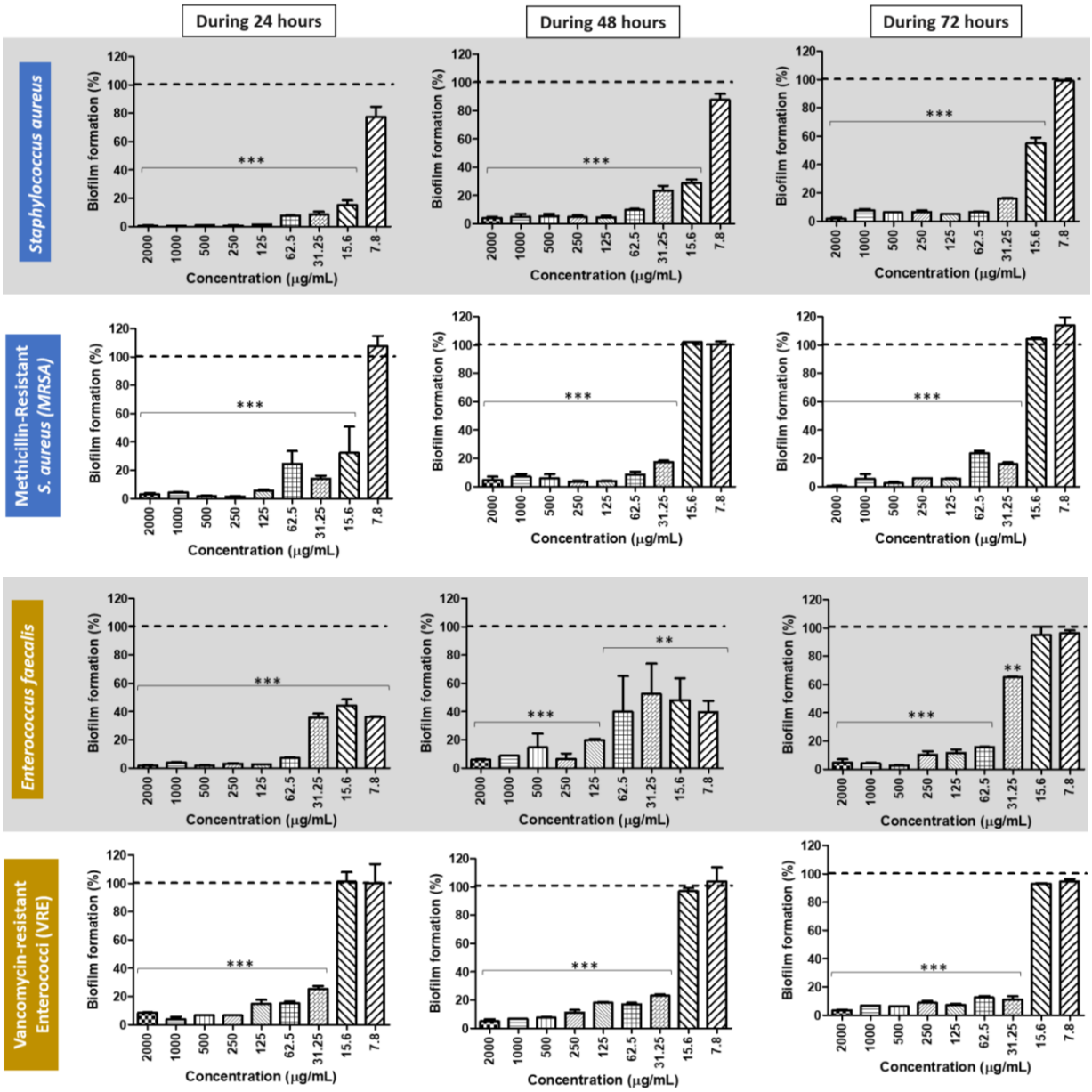

Figure 3.10. Prevention of biofilm formation after 24, 48 and 72 hours in the presence of NHP407-g-Poly(ILM-Br) on a range of pathogenic strains. p values were determined for all groups versus 100% biofilm formation. Statistical significance is presented as following * $p \leq 0.05$, ** $p \leq 0.01$ and *** $p \leq 0.001$.

After obtaining the information that this selected PU dispersion is impeding the development of biofilm structures of *Staphylococcus* and *Enterococcus* spp., its effectiveness on pre-formed biofilms was investigated, taking in consideration that there have been reported cases of specific situations, in which bacteria in sessile life have a 10-fold higher survival rate when exposed to antibiotics than planktonic cells (29,60).

To understand if the maturity of a biofilm influences the antibacterial performance, the experimental set involved biofilms formed during 24, 48 and 72 hours (**figure 3.11**). Usually,

older biofilms are more resistant to antibiotics, proven on diverse approaches: a mouse chronic wound model, a drip-flow biofilm model, a clinical longitudinal debridement study and a porcine skin punch biopsy *ex vivo* model (61). In the same study, the four models showed that a biofilm formed for 24 hours was more susceptible to the selected currently-used antibiotics (e.g. gentamicin) and became increasingly tolerant after maturing for 48 hours.

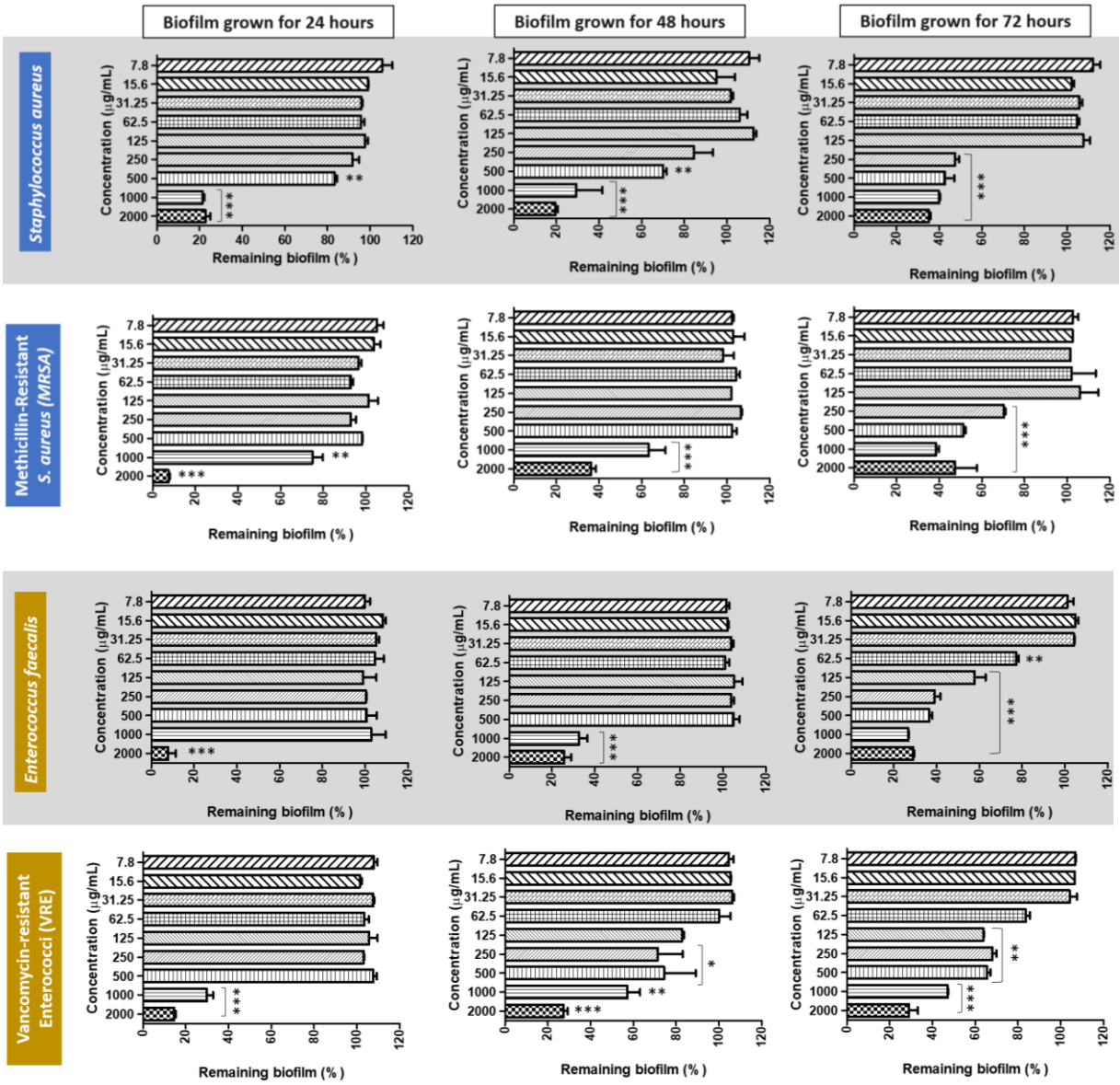

Figure 3.11. Disruption of pre-formed biofilm during 24, 48 and 72 hours of Staphylococcal and Enterococcal strains in the presence of NHP407-g-Poly(ILM-Br) for one day. p values were determined for all groups against 100% remaining biofilm. Statistical significance is presented as * $p \leq 0.05$, ** $p \leq 0.01$ and *** $p \leq 0.001$.

Overall, NHP407-g-Poly(ILM-Br) lacked the capacity to induce a significant impact on the pre-established biofilms with very low concentrations. However, an intriguing outcome was

noticed. It seems that the PU-based antibacterial system was able to reduce more biomass of biofilms grown for 72 hours. This effect is only significantly observable with concentrations equal or above 250 µg/mL against methicillin-sensitive *S. aureus* and MRSA, above 31.25 µg/mL on *Enterococcus faecalis* and higher than 62.5 µg/mL in case of VRE (**figure 3.11**). It seems that the disruptive action of NHP407-g-Poly(ILM-Br) on Gram-positive biofilms is more efficient on cells with a slower growth rate. Recently, it was reported that slow-growing biofilm bacteria present a more rigid and organized bacterial cytoplasmic membrane than actively-replicating bacteria which might facilitate the initial electrostatic interaction from NHP407-g-Poly(ILM-Br) with the bacterial surface (62).

Since the beforementioned AMP-biomimetic amphipathic PUs were designed with view on their perspective biomedical application, L929 murine fibroblasts, HaCaT human keratinocytes and THP-1 monocyte-derived human macrophages were used to perform a comparative cell viability evaluation by the CellTiter-Blue® assay (**figure 3.12**). During wound healing, macrophages exert numerous functions such as overcoming inflammation, elimination of apoptotic cells, stimulation of cell proliferation and host defence, making them a very important cell population in skin (63).

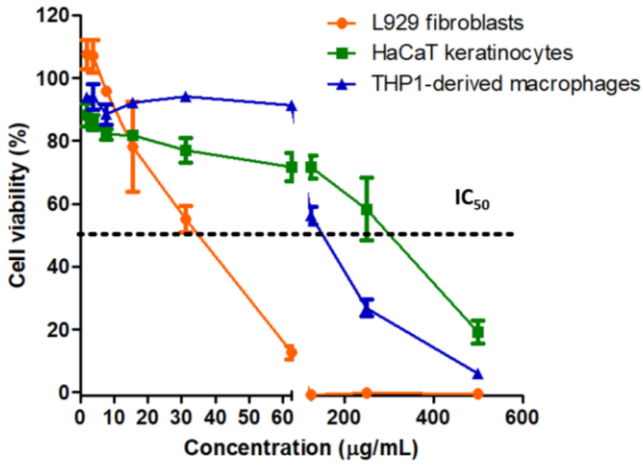

Skin cell populations	MIC MRSA and ARSE (µg/mL)	IC_{50} (µg/mL)	SI (IC_{50}/MIC)
L929 fibroblasts	13	35.21	2.71
HaCaT keratinocytes		278	21.4
THP1-derived macrophages		151.69	11.7

Skin cell populations	MIC VRE (µg/mL)	IC_{50} (µg/mL)	SI (IC_{50}/MIC)
L929 fibroblasts	31.2	35.21	1.13
HaCaT keratinocytes		278	8.91
THP1-derived macrophages		151.69	4.86

MIC - Minimal inhibitory concentration on resistant bacteria;
IC_{50} - Half maximal inhibitory concentration on mammalian cells;
SI – Selectivity index

Figure 3.12. Cytocompatibility of NHP407-g-Poly(ILM-Br) for 1 day on fibroblasts (L929), keratinocytes (HaCaT) and monocyte-derived macrophages (THP-1-derived macrophages) on the graph at the left. The half maximal inhibitory concentration for each cell population and the minimal inhibitory concentration for each Gram-positive drug-resistant pathogen are shown in the tables.

All cell lines show an optimal viability in the presence of the lower NHP407-g-Poly(ILM-Br) concentrations tested after 24 hours (**figure 3.12**). This viability starts to decrease with the increment of dose. Furthermore, the cell lines at the frontline defence HaCaT keratinocytes and THP-1 derived macrophages seem to be more tolerant to the PU dispersion.
Nevertheless, these concentrations that induced a reduction of cell viability to less than 70% are still higher than the minimal inhibitory concentrations (MIC) determined on clinically isolated antibiotic-resistant strains, showing positive selectivity indexes, resulting in the polymers' higher selectivity towards bacteria over eukaryotic cells (**figure 3.12**).

3.4. Conclusion

New therapeutic polymers were analysed to combat drug-resistant bacterial strains in planktonic and sessile forms, as often found in chronic wounds. The polyurethane NHP407 was the main chain for the library of newly designed AMP-biomimetic amphipathic polyurethanes dispersions with intrinsic antibacterial properties. NHP407 is a recently developed reverse thermoresponsive amphiphilic polyurethane based on the FDA approved poloxamer 407, that showed good cytocompatibility with mammalian cells in form of hydrogel (24). Even in the present work, it was determined that NHP407 dispersion in water is cytocompatible to L929 fibroblasts up to a high concentration of 2.5 mg/mL. Out of the AMP-mimicking PU library, NHP407-g-[poly(NIPAM)-b-poly(MPC)] showed the better cytocompatibility results on L929 fibroblasts. In overall, the complementary biological assays, including the biological analysis on the keratinocyte cell line HaCaT, gave support to the fact that cells exposed to NHP407-g-[poly(NIPAM)-b-poly(MPC)] have a superior viability than cells in the presence of NHP407 polyurethane backbone. Hence, the polymerization with poly(MPC) blocks improved the NHP407 cytocompatibility.
The most potential antibacterial AMP-biomimetic polyurethane tested was NHP407-g-Poly(ILM-Br). It was synthesized by grafting a hydrophobic liquid monomer from the amphiphilic NHP407 main chain and subsequently exchanging the hydrophobic anions to hydrophilic bromide anions (Br^-). NHP407-g-Poly(ILM-Br) was able to act on *S. aureus, S. epidermidis* and *E. faecalis*, in their drug-sensitive or drug-resistant strains at very low concentrations from 13 to 62.5 µg/mL, which are still considered safe by the evaluation of the selectivity index (SI) on L929 fibroblasts (SI > 1). Moreover, the minimal bactericidal concentration (MBC) on the most commonly found AMR Gram-positive pathogens (MRSA

and VRE) is very similar to the MBC of antibiotic-sensitive strains. This means that the evolutionarily gained mechanisms of resistance by *S. aureus* (MRSA) and *E. faecalis* (VRE) do not interfere with the bactericidal activity of NHP407-g-Poly(ILM-Br). In addition, the very similar dose-dependent inhibitory effect between drug-sensitive and its correspondent drug-resistant bacterial clinical isolate supports the described hypothesis. NHP407-g-Poly(ILM-Br) induces a rapid bactericidal effect on planktonic Gram-positive bacteria and it is able to prevent biofilm formation for a long period of time (72 hours). This AMP-biomimetic polymer was able to disrupt Gram-positive mature biofilms with concentrations higher than 250 μg/mL against methicillin-sensitive *S. aureus* and MRSA, and above 31.25 μg/mL on *Enterococcus faecalis* and higher than 62.5 μg/mL in case of VRE. On L929 murine fibroblasts, HaCaT human keratinocytes and THP-1 Monocyte-derived human macrophages, the cell viability was optimal in the presence of the lower concentrations that are active against bacteria. Therefore, NHP407-g-Poly(ILM-Br) shows a positive selectivity index on all skin cell populations tested, indicating that this polymer dispersion has a higher selectivity towards bacteria over mammalian eukaryotic cells.

In conclusion, a promising therapeutic AMP-biomimetic amphipathic polyurethane was identified to overcome Gram-positive infections, that could be used as an easy to handle product, being directly applied to a wound bed.

References

1. Ventola C. The antibiotic resistance crisis: part 1: causes and threats. PT. 2015;40(4):277–83.
2. Filius PMG, Gyssens IC. Impact of increasing antimicrobial resistance on wound management. Am J Clin Dermatol. 2002;3(1):1–7.
3. Edwards R, Harding KG. Bacteria and wound healing. Curr Opin Infect Dis. 2004;17(2):91–6.
4. Percival SL, Hill KE, Williams DW, Hooper SJ, Thomas DW, Costerton JW. A review of the scientific evidence for biofilms in wounds. Wound Repair Regen. 2012;20(5):647–57.
5. Attinger C, Wolcott R. Clinically Addressing Biofilm in Chronic Wounds. Adv Wound Care. 2012;1(3):127–32.
6. Stacy A, McNally L, Darch SE, Brown SP, Whiteley M. The biogeography of polymicrobial infection. Nat Rev Microbiol. 2015;14(2):93–105.
7. Thanni LOA, Osinupebi OA, Deji-agboola M. Prevalence of bacterial pathogens in infected wounds in a tertiary hospital, 1995-2001: Any change in trend? J Natl Med Assoc. 2003;95(12):1189–95.
8. Bessa LJ, Fazii P, Di Giulio M, Cellini L. Bacterial isolates from infected wounds and their antibiotic susceptibility pattern: Some remarks about wound infection. Int Wound J. 2015;12(1):47–52.
9. Mowery BP, Lee SE, Kissounko DA, Epand RF, Epand RM, Weisblum B, et al. Mimicry of Antimicrobial Host-Defense Peptides by Random Copolymers. J Am Chem Soc. 2007;129(50):15474–6.
10. Takahashi H, Nadres ET, Kuroda K. Cationic Amphiphilic Polymers with Antimicrobial Activity for Oral Care Applications: Eradication of S. mutans Biofilm. Biomacromolecules. 2017;18(1):257–65.
11. Bansal R, Pathak R, Kumar B, Gautam HK, Kumar P. Enhanced antimicrobial activity of amphiphilic cationic polymers against a broad range of bacterial strains and skin microbes. Colloid Polym Sci. 2017;295(7):1177–85.
12. Zasloff M. Antimicrobial peptides of multicellular organisms. Nature. 2002;415(6870):389–95.
13. Brogden KA. Antimicrobial peptides: Pore formers or metabolic inhibitors in bacteria? Nat Rev Microbiol. 2005;3(3):238–50.
14. Easton DM, Nijnik A, Mayer ML, Hancock REW. Potential of immunomodulatory host defense peptides as novel anti-infectives. Trends Biotechnol. 2009;27(10):582–90.
15. Yount NY, Bayer AS, Xiong YQ, Yeaman MR. Advances in antimicrobial peptide immunobiology. Biopolym - Pept Sci Sect. 2006;84(5):435–58.
16. Song A, Walker SG, Parker KA, Sampson NS. Antibacterial studies of cationic polymers with alternating, random, and uniform backbones. ACS Chem Biol. 2011;6(6):590–9.

17. Joo HS, Fu CI, Otto M. Bacterial strategies of resistance to antimicrobial peptides. Philos Trans R Soc B Biol Sci. 2016;371(1695).

18. Zheng Z, Xu Q, Guo J, Qin J, Mao H, Wang B, et al. Structure-Antibacterial Activity Relationships of Imidazolium-Type Ionic Liquid Monomers, Poly(ionic liquids) and Poly(ionic liquid) Membranes: Effect of Alkyl Chain Length and Cations. ACS Appl Mater Interfaces. 2016;8(20):12684–92.

19. Lam SJ, O'Brien-Simpson NM, Pantarat N, Sulistio A, Wong EHH, Chen YY, et al. Combating multidrug-resistant Gram-negative bacteria with structurally nanoengineered antimicrobial peptide polymers. Nat Microbiol. 2016;1(11):16162.

20. Takahashi H, Caputo GA, Vemparala S, Kuroda K. Synthetic Random Copolymers as a Molecular Platform to Mimic Host-Defense Antimicrobial Peptides. Bioconjug Chem. 2017;28(5):1340–50.

21. Muñoz-Bonilla A, Fernández-García M. Poly(ionic liquid)s as antimicrobial materials. Eur Polym J. 2018;105:135–49.

22. Dumortier G, Grossiord JL, Agnely F, Chaumeil JC. A review of poloxamer 407 pharmaceutical and pharmacological characteristics. Pharm Res. 2006;23(12):2709–28.

23. Fakhari A, Corcoran M, Schwarz A. Thermogelling properties of purified poloxamer 407. Heliyon. 2017;3(8):e00390.

24. Boffito M, Gioffredi E, Chiono V, Calzone S, Ranzato E, Martinotti S, et al. Novel polyurethane-based thermosensitive hydrogels as drug release and tissue engineering platforms: Design and in vitro characterization. Polym Int. 2016;65(7):756–69.

25. Ommen P, Zobek N, Meyer RL. Quantification of biofilm biomass by staining: Non-toxic safranin can replace the popular crystal violet. J Microbiol Methods. 2017;141:87–9.

26. International Organization for Standardization. ISO 10993-5 Biological evaluation of medical devices - Part 5: Tests for in vitro cytotoxicity. International Standard. 2009.

27. Goda T, Ishihara K, Miyahara Y. Critical update on 2-methacryloyloxyethyl phosphorylcholine (MPC) polymer science. J Appl Polym Sci. 2015;132(16).

28. Ueda T, Oshida H, Kurita K, Ishihara K, Nakabayashi N. Perparation of 2-Methacryloyloxyethyl Phosphorylcholine Copolymers with Alkyl Methacrylates and Their Blood Compatibility. Polym J. 1992;24(11):1259–69.

29. Zhao G, Usui ML, Lippman SI, James GA, Stewart PS, Fleckman P, et al. Biofilms and Inflammation in Chronic Wounds. Adv Wound Care. 2013;2(7):389–99.

30. Reddy M, Gill SS, Wu W, Kalkar SR, Rochon PA. Does this patient have an infection of a chronic wound? JAMA - J Am Med Assoc. 2012;307(6):605–11.

31. Shireesh A. The counter ion: expanding excipient functionality. J Excipients Food Chem. 2011;2(2):26–7.

32. Zhao Y, Wang J, Wang H, Li Z, Liu X, Zhang S. Is there any preferential interaction of ions of ionic liquids with DMSO and H2O? A comparative study from MD simulation. J Phys Chem B. 2015;119(22):6686–95.

33. Ishihara K, Ueda T, Nakabayashi N. Preparation of Phospholipid Polylners and Their

Properties as Polymer Hydrogel Membranes. Polym J. 2005;22(5):355–60.

34. Alexandridis P. Poly(ethylene oxide)/poly(propylene oxide) block copolymer surfactants. Curr Opin Colloid Interface Sci. 1997;2(5):478–89.

35. Kennedy T. Managing the drug discovery/development interface. Drug Discov Today. 1997;2(10):436–44.

36. Choulis NH. Miscellaneous drugs, materials, medical devices and techniques. Side Eff Drugs Annu. 2014;36:725–46.

37. Papaneophytou CP, Mettou AK, Rinotas V, Douni E, Kontopidis GA. Solvent selection for insoluble ligands, a challenge for biological assay development: A TNF-α/SPD304 study. ACS Med Chem Lett. 2013;4(1):137–41.

38. Chatterjee M, Anju CP, Biswas L, Anil Kumar V, Gopi Mohan C, Biswas R. Antibiotic resistance in Pseudomonas aeruginosa and alternative therapeutic options. Vol. 306, International Journal of Medical Microbiology. 2016. p. 48–58.

39. Neuhaus FC, Baddiley J. A Continuum of Anionic Charge: Structures and Functions of D-Alanyl-Teichoic Acids in Gram-Positive Bacteria. Microbiol Mol Biol Rev. 2003;67(4):686–723.

40. Koprivnjak T, Weidenmaier C, Peschel A, Weiss JP. Wall Teichoic Acid Deficiency in Staphylococcus aureus Confers Selective Resistance to Mammalian Group IIA Phospholipase A2 and Human β-Defensin 3 ∇. Infect Immun. 2008;76(5):2169–76.

41. Winterhalter M, Ceccarelli M. Physical methods to quantify small antibiotic molecules uptake into Gram-negative bacteria. Eur J Pharm Biopharm. 2015;95:63–7.

42. Nikaido H, Vaara M. Molecular basis of bacterial outer membrane permeability. Microbiol Rev. 1985;49(1):1–32.

43. Stanley C. Bacterial Gram Stains: Gram Positive vs Gram Negative [Internet]. Illustration: Scientific and Medical Illustration. 2015 [cited 2018 Dec 20]. Available from: http://stanleyillustration.com/latest-work/2015/2/8/ngoo8tdfmqo4tyh0vksu37vqroxnvs

44. Hailu D, Derbie A, Mekonnen D, Zenebe Y, Adem Y, Worku S, et al. Drug resistance patterns of bacterial isolates from infected wounds at Bahir Dar Regional Health Research Laboratory Center, Northwest Ethiopia. Ethiop J Heal Dev. 2016;30(3):112–7.

45. World health organization W-H-O. Combating antimicrobial resistance, including antibiotic resistance. Institutional repository for information sharing. 2014.

46. Howard SJ, Catchpole M, Watson J, Davies SC. Antibiotic resistance: global response needed. Lancet Infect Dis. 2013;13:1001–3.

47. Doernberg SB, Lodise TP, Thaden JT, Munita JM, Cosgrove SE, Arias CA, et al. Gram-positive bacterial infections: Research priorities, accomplishments, and future directions of the Antibacterial Resistance Leadership Group. Clin Infect Dis. 2017;64:S24–9.

48. Menichetti F. Current and emerging serious Gram-positive infections. Clin Microbiol Infect. 2005;11:22–8.

49. Peacock SJ, Paterson GK. Mechanisms of Methicillin Resistance in *Staphylococcus aureus*. Annu Rev Biochem. 2015;84(1):577–601.

50. Domaracki BE, Evans AM, Venezia RA. Vancomycin and oxacillin synergy for methicillin-resistant staphylococci. Antimicrob Agents Chemother. 2000;44(5):1394–6.

51. Ahmed MO, Baptiste KE. Vancomycin-Resistant Enterococci: A Review of Antimicrobial Resistance Mechanisms and Perspectives of Human and Animal Health. Microb Drug Resist. 2018;24(5):590–606.

52. Faron ML, Ledeboer NA, Buchan BW. Resistance mechanisms, epidemiology, and approaches to screening for vancomycin-resistant Enterococcus in the health care setting. J Clin Microbiol. 2016;54(10):2436–47.

53. Arthur M, Reynolds PE, Depardieu F, Evers S, Dutka-Malen S, Quintiliani R, et al. Mechanisms of glycopeptide resistance in enterococci. J Infect. 1996;32(1):11–6.

54. Courvalin P. Vancomycin Resistance in Gram-Positive Cocci. Clin Infect Dis. 2006;42(S1):S25–34.

55. Opatowski L, Mandel J, Varon E, Boëlle PY, Temime L, Guillemot D. Antibiotic dose impact on resistance selection in the community: A mathematical model of β-lactams and streptococcus pneumoniae dynamics. Antimicrob Agents Chemother. 2010;54(6):2330–7.

56. Ball P. Conclusions: the future of antimicrobial therapy - Augmentin® and beyond. Int J Antimicrob Agents. 2007;30(S2):139–41.

57. Werner S, Krieg T, Smola H. Keratinocyte-fibroblast interactions in wound healing. J Invest Dermatol. 2007;127(5):998–1008.

58. Lewis A, Tang Y, Brocchini S, Choi JW, Godwin A. Poly(2-methacryloyloxyethyl phosphorylcholine) for protein conjugation. Bioconjug Chem. 2008;19(11):2144–55.

59. Stewart PS. Mechanisms of antibiotic resistance in bacterial biofilms. Int J Med Microbiol. 2002;292(2):107–13.

60. Spiliopoulou AI, Kolonitsiou F, Krevvata MI, Leontsinidis M, Wilkinson TS, Mack D, et al. Bacterial adhesion, intracellular survival and cytokine induction upon stimulation of mononuclear cells with planktonic or biofilm phase Staphylococcus epidermidis. FEMS Microbiol Lett. 2012;330(1):56–65.

61. Wolcott RD, Rumbaugh KP, James G, Schultz G, Phillips P, Yang Q, et al. Biofilm maturity studies indicate sharp debridement opens a time-dependent therapeutic window. J Wound Care. 2010;19(8):320–8.

62. Dubois-Brissonnet F, Trotier E, Briandet R. The biofilm lifestyle involves an increase in bacterial membrane saturated fatty acids. Front Microbiol. 2016;7:1673.

63. Das A, Sinha M, Datta S, Abas M, Chaffee S, Sen CK, et al. Monocyte and Macrophage Plasticity in Tissue Repair and Regeneration. Am J Pathol. 2015;185(10):2596–606.

CHAPTER FOUR

‘Exploration of the mechanism of action of the novel antimicrobial peptide-biomimetic amphipathic polyurethane NHP407-g-Poly(ILM-Br)’

Graphical abstract

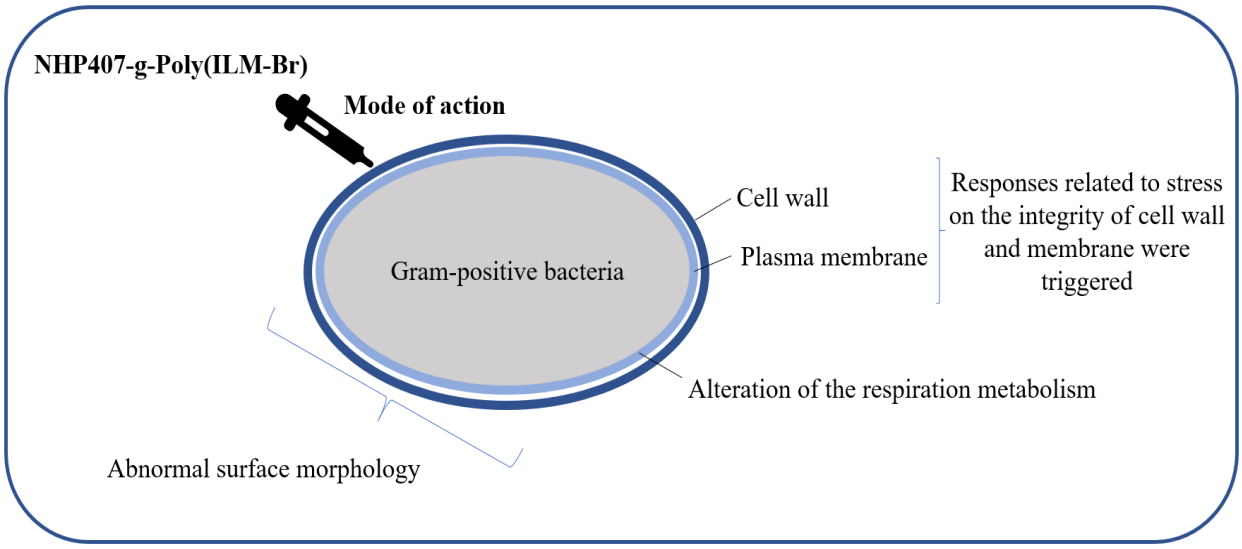

Abstract

Antimicrobial-resistance and polymicrobial biofilm tolerance in infected chronic wounds is a major problem in healthcare settings. The Gram-positive *Staphylococcus aureus* is the most frequent isolated species from chronic wounds, making methicillin-resistant *Staphylococcus aureus* (MRSA) a number one priority issue to be tackled on infected tissues. In the previous chapter, a family of new antimicrobial peptide-mimicking amphipathic polyurethanes has been tested, showing their potential as an innovative formulation against pathogenic bacteria. For instance, one of the amphipathic polyurethanes tested – NHP407-g-Poly(ILM-Br) - emerged as a very effective antibacterial system with bactericidal properties and able to inhibit biofilm formation of *S. aureus* and MRSA. To initiate exploring the mechanism of action of NHP407-g-Poly(ILM-Br), morphological characterization by scanning electron microscopy (SEM) and a combination of 2D gel-based and liquid chromatography–mass spectrometry (LC-MS)–based approaches were performed.

Alterations on the surface of *S. aureus* bacteria were clearly observed after short contact with the polymer dispersion for 5 and 30 minutes. The bacteria's coccal morphology became extremely smooth and some points of the cell envelope show signs of possible collapse. 13 marker proteins showed to be upregulated after the treatment with NHP407-g-Poly(ILM-Br). After analysing the function of each identified upregulated protein, it was determined that the electrostatic interaction and subsequent integration into the bacterial cell envelope of AMP-biomimetic polyurethane colloidal particles induces a strategic stress response on *B. subtilis,* mainly acting on the membrane and cell wall. This led to an alteration of the membrane and cell wall integrity, and an impairment of the respiration metabolism by limiting the energy within the bacteria.

Hence, through this study it was possible to obtain accurate indications that the main mechanism of action of NHP407-g-Poly(ILM-Br) is similar to the most common mode of action of antimicrobial peptides – cell membrane damage.

4.1. Introduction

The interest in synthetic amphipathic cationic antimicrobial peptides with a novel composition and structure as antibacterial agents that do not generate drug-resistance is rising (1–3). The central reason underlining this, is the fact that although antimicrobial peptides (AMPs) naturally occur in all living organisms for millions of years as a hosts' defence tactic, relatively low risk

of mutations leading to AMP-resistance mechanisms within bacteria have been reported until current days (4,5). This results from the common antibacterial mechanism found in most AMPs: a preference to attack the bacterial cell membrane, through binding to the anionic bacterial surface with the electrostatic interaction coming from the cationic region of the AMPs, followed by an integration of the hydrophobic region into the cytoplasmic membrane (6–8). In fact, only when an antimicrobial agent targets specific proteins, the possibility for genetical mutations leading to bacterial resistance is higher (6). Moreover, AMPs are very attractive for clinical applications due to their broad-spectrum of antimicrobial activity relying on their selective antibacterial action on the bacterial membrane. The same bactericidal mode of action is an advantage in treating infections by slow-growing bacteria, such as the ones existing in biofilm communities, due to their more organized and rigid bacterial membrane that facilitates the initial interaction between AMPs and bacteria surface (5,9). Moreover, AMPs usually have more than one mechanism, besides cell membrane damage, such as interference with enzymatic activity, inhibition of DNA and RNA synthesis, and stimulation of the immune system (10).

Antimicrobial-resistance and polymicrobial biofilm tolerance in infected chronic wounds are major problems in the healthcare setting (11). The Gram-positive *Staphylococcus aureus* is still one of the most common isolated species from chronic wounds, making Methicillin-resistant *Staphylococcus aureus* (MRSA) a number one priority issue to be tackled on infected tissue (12,13). The outer monolayer of the phospholipidic bilayer of Gram-positive bacteria is mostly constituted by acidic phospholipids, that have negative head groups. Additionally they have wall teichoic acids which are also negatively charged increasing the chances of AMPs initial electrostatic contact and subsequent antibacterial activity (14). The application of AMP-mimicking agents is a potential therapeutic strategy to overcome such infections.

In a first approach, a library of AMP-biomimetic amphipathic polyurethanes (PUs) was under study. The design rational of these PUs was to mimic the fundamental structure of AMPs (amphipathic cationic structure) to reproduce the membrane-disruptive mechanism. The great antibacterial efficacy of AMP-mimicking polyurethanes on sensitive and drug-resistant Gram-positive bacteria was shown in Chapter 3. One of the amphipathic polyurethanes – NHP407-g-Poly(ILM-Br) - emerged as a very effective antibacterial system with bactericidal properties, able to inhibit biofilm formation and to disrupt pre-stablished biofilms of *S. aureus* and MRSA. In cryogenic-transmission electron microscopy (cryo-TEM), it was observed that this polymeric formulation is aqueous dispersion appears as colloidal particles that show a layered morphology, self-organized hydrophobic patches and cationic hydrophilic regions, created by the dissociation between the anion and polycation (Purkayastha *et al.*, unpublished). This

supports its successful synthesis as a system that mimics the cationic amphiphilic structural organization of antimicrobial peptides.

In the present chapter, morphological characterization by scanning electron microscopy (SEM) and a combination of 2D gel-based and liquid chromatography–mass spectrometry (LC-MS)–based approaches were used to obtain a preliminary and accurate indicative mechanism of action(s) of NHP407-g-Poly(ILM-Br) colloidal particles on Gram-positive bacteria.

4.2. Materials and methods

4.2.1. Chemical/morphologic characteristics and conditions of preparation of NHP407-g-Poly(ILM-Br) for biological assays

The amphipathic polyurethane NHP407 grafted Poly(N,N,N,N-Butyldimethylmethacryloyl-oxyethylammonium) with the hydrophilic anions of bromide as counter-ions [NHP407-g-Poly(ILM-Br)] is a polymer originated after ionic exchange of NHP407-g-Poly(ILM-TFMSI) (**Figure 4.1**).

These polymers were kindly provided by an Early Stage Researcher of the HyMedPoly project, from professor Gianluca Ciardelli's group 'Materials in Biotechnology and Biomedical Lab' from the Politecnico di Torino where it was synthesized by mimicking the amphipathic fundamental structure of antimicrobial peptides (AMPs) (Purkayastha *et al.*, unpublished). NHP407-g-Poly(ILM-Br) are polyurethane-based colloidal particles formed by spatially separate hydrophobic regions and cationic hydrophilic nanodomains in purified water, hence they are denoted as patchy colloidal particles (Purkayastha et al., unpublished).

The stock concentration prepared to be used for biological assays was 50 mg/mL in cold sterile purified H_2O. In the first 5 hours, the solution was stirred at 250-300 rpm with ice surrounding the glass vial. This stirring process was maintained for 7 days at room temperature, to obtain a proper dispersion of the colloidal particles before their usage in biological tests.

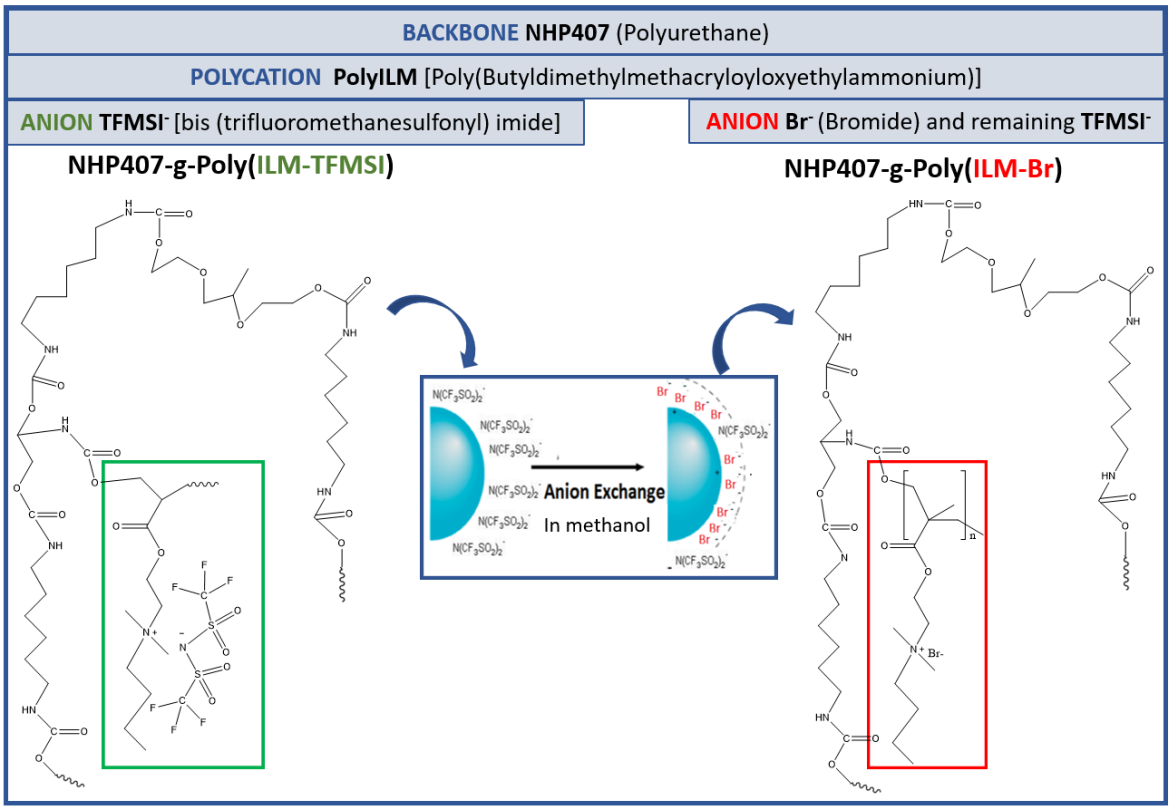

Figure 4.1. Development scheme and final chemical structure of the polyurethane NHP407-g-Poly(ILM-Br).

4.2.2. Antibacterial susceptibility assay against *Staphylococcus aureus* bacteria

Staphylococci bacterial cells were grown at 37°C for 18 hours on blood agar plates (mixture of nutrient agar with 5% sheep blood pH ~7.4). The minimum inhibitory concentration (MIC) and the minimum bactericidal concentration (MBC) were determined for lithium bromide, for monomer ILM-TFMSI and for the different polymers NHP407, NHP407-g-Poly(ILM-TFMSI) and NHP407-g-Poly(ILM-Br) against *Staphylococcus aureus subsp. aureus* Rosenbach (ATCC® 29213™) (MSSA) and its respective drug-resistant clinical isolate methicillin-resistant *Staphylococcus aureus* (MRSA).

First, the MIC was determined by performing the broth microdilution method following ISO 20776-1 standard as recommended by EUCAST. The MIC corresponds to the lowest concentration that inhibits visible bacterial growth (no turbidity). Briefly, pre-inoculated bacterial cells (colonies selected from an overnight culture were inserted in a tube with 2 mL 0.9% NaCl, then turbidity was adjusted to MacFarland 0.5) were diluted in order to have a final concentration in the well of ~3.75×10^5 CFU/mL. A serial dilution of the compounds, monomer and polymers was added in Mueller-Hinton broth (MHB). Then, the 96-well plates were incubated for 18-22h at 37ºC.

After the MIC test, the entire volume of the MIC condition of the 96-well plate and 3 concentrations above were transferred and spread on blood agar plates. The plates were incubated 37ºC for ~18 hours. The MBC value corresponds to the lowest concentration of polymer in which zero colony forming units per millilitre (CFU/mL) were counted (99.9% killing).

4.2.3. Scanning electron microscopy assay

4.2.3.1. Bacteria selected and growth conditions

For scanning electron microscopy (SEM), the selected bacterial strain was *Staphylococcus aureus subsp. aureus* Rosenbach (ATCC® 29213™). This drug-sensitive Gram-positive strain was cultivated at 37°C for 18 hours on blood agar plates (mixture of nutrient agar with 5% sheep blood at pH ~7.4).

4.2.3.2. Sample preparation

To observe *S. aureus*' morphology of untreated and NHP407-g-Poly(ILM-Br)-treated conditions by SEM, the samples were prepared as described in the following paragraphs.

Colonies selected with a swab were inserted in Mueller-Hinton broth (MHB) and the turbidity was adjusted to MacFarland 0.5, corresponding to a cell density of approximately $1.5x10^8$ CFU/mL. Then, the inoculum was diluted to ~$5x10^6$ CFU/mL and divided into different eppendorf microcentrifuge tubes (1 mL/tube). A concentration correspondent to the MBC of NHP407-g-Poly(ILM-Br) colloidal particles was added to these tubes, and incubated at 37°C for 5 and 30 minutes. As controls, a vial with only bacteria and one containing only particles were prepared in parallel. After the established periods of time, the samples were centrifuged at 16 000 × *g* for 3 minutes (Biofuge Pico, rotor 3325, Thermo Scientific-Heraeus). The supernatant was discarded, and the pellet was resuspended in 100 µL of 2.5% glutaraldehyde (Sigma-Aldrich) diluted in PBS (PAN Biotech), with the fixation time of 10 minutes at room temperature. The volume was transferred evenly on the surface of a round glass coverslip and dried under the flow cabinet for at least 4 hours. After this period, the samples were washed 5-times in PBS for 5 minutes each to remove the remaining PBS based glutaraldehyde solution. Next, the remaining water was removed from the samples using ascending percentages of acetone (Merck KGaA, Darmstadt, Germany). The following scheme was taken: 30% acetone during 15 min, 50% for 20 min, 70% for 30 min, 90% for 45 min and 4-times 100% acetone for 30 min each. After that, acetone residuals in the samples were exchanged by super critical

carbon dioxide (CO_2) with the procedure of critical point drying (CPD). This process was repeated 10-times. Finally, samples were sputtered with platinum for 20-30 minutes using a Leica EM ACE600 high vacuum sputter coater. Imaging was recorded using a Crossbeam 340 scanning electron microscope (SEM) equipped with a Zeiss Gemini column with an aperture size set to 30 μm.

Focused ion beam (FIB) technique was also applied on the samples under SEM, to have the chance to visualize the interface between particle-particle and particle-bacterial membrane.

4.2.4. Proteomic approach

4.2.4.1. Bacteria growth conditions

For studying the bacterial adaptation under a stress condition, in this case under the presence of NHP407-g-Poly(ILM-Br)], the Gram-positive *Bacillus subtilis* 168 was chosen since it is an established model organism commonly employed in these type of studies (15–18). Besides, this specie is a Gram-positive bacterium also found on human skin, such as *Staphylococcus aureus* (19). *B. subtilis* was grown under vigorous agitation in Belitsky minimal medium (BMM) at 37 ºC as previously reported (20).

4.2.4.2. Antibacterial susceptibility: Determination of minimal inhibitory concentration against *Bacillus subtilis* 168

The minimal inhibitory concentration (MIC) was evaluated by a tube assay as previously described by Bandow and collaborators (21). Briefly, 10^5 bacteria per millilitre were inoculated in 2 mL of BMM inside glass tubes in the presence of decreasing concentrations of NHP407-g-Poly(ILM-Br). These tubes were incubated for 18 hours at 37 ºC under a rotatory movement. After this period, the MIC was registered as the lowest concentration able to inhibit visible growth (no turbidity).

4.2.4.3. Antibacterial susceptibility: Determination of the optimal stressor concentration for proteomic profiling

In growth experiments, *B. subtilis* was exposed to three different concentrations of NHP407-g-Poly(ILM-Br) close to the determined MIC. The polymer was added during the exponential growth phase, when the culture reached an OD_{500} of 0.35. For proteomic tests, the amphipathic

polymer concentration selected was the one that lead to a reduction in bacterial growth rate of approximately 50 – 70%, in comparison to the untreated control sample.

4.2.4.4. Preparation of cytoplasmic [35S]-L-methionine-labelled protein fractions

The radioactive labelling of newly synthesized proteins under the stress induced by NHP407-g-Poly(ILM-Br) was performed following the previously defined protocol (17,22). Briefly, the optimal stressor concentration of NHP407-g-Poly(ILM-Br) was rapidly added to 5 mL of *B. subtilis* 168 culture in the early exponential growth phase. A flask with bacteria in optimal growth was kept in parallel and was used as control. Bacterial cells were stressed for 10 minutes. Up following to the treatment period, the bacteria were pulse-labelled with the radioactive [35S]-L-methionine (Hartmann Analytic, Germany) for 5 minutes. The radioactive incorporation was discontinued by additing non-radioactive 10 mM L-methionine plus 1 mg/mL of the protein biosynthesis inhibitor chloramphenicol followed by immediate shift of the flask to ice, after a brief shaking. Next, bacterial cells were centrifuged and washed 3-times with 100 mM Tris/1mM EDTA buffer. 10 mM cold Tris buffer containing 1.39 mM of phenylmethylsulfonyl fluoride was used during the bacterial disruption procedure, that was performed by ultra-sonication (Vial Tweeter instrument, Hielscher, Germany). The fraction containing the soluble proteins was separated from the disrupted cells by a centrifugation at 16 000 x *g* for 20 min (4 ºC). Protein quantification was estimated by the Bradford-based Roti® Nanoquant assay with 1:5 Roti®-Nanoquant solution in destillated water (CarlRoth, Germany).

4.2.4.5. 2D-PAGE gels

This procedure was based on a previously published method (22). Soluble proteins were diluted up to 500 µL with rehydration buffer that contains 2 M thiourea, 7 M urea, 6.5 mM 3-[(3-cholamidopropyl)-dimethylammonio]-1-propanesulfonate, 50 mM dithiothreitol (DTT), 0.5% Triton X-100 and 1.04% Pharmalyte 3-10 (GE Healthcare, Uppsala, Sweden). For radioactive gels 55 µg of proteins were loaded and for gels that have been used for protein identification by mass spectrometry (non-radioactive gels) the loading was performed with 300 µg of cytosolic proteins. These proteins were first separated in a first dimension by isoelectric focusing (Multiphor II apparatus, GE Heathcare) into 24-cm immobilized pH gradient (IPG) strips (pH 4 – 7, Immobiline DryStrip, GE Heathcare) by passive rehydration for 18 hours. The applied gradient was 0 – 500 V for 1 kVh, 500 V for 0.01 kVh, 500 – 3500 V for 3 kVh, 3500 V for 57 kVh and 60 V for 0.1 kVh. Then, the IPG strips were placed in an equilibration buffer for 20

minutes that contained 6 M urea, 50 mM Tris (pH 8.8), 30% glycerol and 2% SDS supplemented with 2.5% iodoacetamine and 1%DTT.

Afterwards, these proteins were separated in a second dimension on 12.5% SDS-Polyacrilamide gels. These gels were formed by 0.375 M Tris/HCl (pH 8.8), 0.1% SDS, 0.0138% TEMED (N,N,N′,N′-Tetramethylethylenediamine), 0.05% ammonium persulfate and acrylamide/ bisacrylamide. The IPG strips were positioned on top of the 12.5% SDS-PAGE gels and 0.5% of agarose was added. Next, the running buffer constituted by 25 mM Tris, 192 mM glycine and 0.1% SDS was added to the Ettan DALTwelve system (GE Healthcare). Electrophoresis started with 0.5 W for 1 hour, allowing passage of proteins from the strip to the gel, then run at 10 W per gel for 5 hours for protein separation.

When the gel electrophoresis was completed, the proteins in the gels were fixated in a mixture of 40% ethanol, 53% distilled water and 7% acetic acid for 1 hour, followed by a washing step and finally stained with 0.003% Ruthenium(II) tris(4,7-diphenyl-1,10-phenantrolindisulfonate) (RuBPs) (23). Under a 532 nm excitation/610 nm emission wavelength, SDS-PAGE gels were scanned with a Typhoon Trio variable mode imager system (GE Healthcare). Radioactive gels were additionally dried on Whatman paper and exposed to BAS storage phosphor screens (GE Healthcare). Images of the gels were acquired with the Typhoon Trio variable mode imager system (GE Healthcare) at 633 nm excitation wavelength and 390 nm of emission. Radioactive gel scans were evaluated with the Decodon Delta 2D 4.1 image analysis software (Decodon, Germany) as described by Bandow and co-workers (24). All proteins produced more than 2-fold under stress were reported as marker proteins.

For the 2D-page gels all the chemicals were purchased from Sigma-Aldrich or Carl Roth in electrophoresis grade quality.

4.2.4.6. Identification of marker proteins

The marker proteins were identified as the upregulated proteins synthesized under the stress of NHP407-g-Poly(ILM-Br) in two biological replicates. These marker protein spots were excised from non-radioactive stained 2D gels on a dark reader (non-UV transilluminator, Clare chemical research). The spots were inserted into low-binding vials. First, the spots were destained with 400 µL of washing solution containing 20 mM ammonium bicarbonate in 30% acetonitrile/distilled water. In the next step, the supernatant was removed, and the gel spots were dried in a vacuum centrifuge for 15 minutes. Afterwards, tryptic digestion was performed. For that, approximately 20 µL of trypsin solution (6.25 ng/µL, Promega, USA) was added in order to completely cover the gel spots. The vials were incubated overnight at 37°C. Next,

peptides were eluted for 15 minutes in LC/MS grade water containing 0.1% TFA, inside of an ultrasonic bath.

The samples (~ 2µL) were injected for protein identification in a nanoUPLC column coupled online to a Synapt G2S high definition mass spectrometer (HDMS) equipped with lock spray source for electrospray ionization (ESI) and a ToF detector (Waters, USA). First, the trapping was performed on a nanoACQUITY UPLC trap column Symmetry C18 (Waters, USA) with a length of 20 mm, a pore size of 100 Å and particle size of 5 µm. The applied rate flow was 10 µL/min and 0.5% solvent B (0.1% formic acid in acetonitrile). Then, in a nanoACQUITY-UPLC CSH130 C18 column (length of 100 mm, 75 µm of inner diameter, particle size of 1.7 µm and 130 Å of pore size) the gradient solvent A, constituted by 0.1% formic acid in distilled water, and solvent B (0.1% formic acid in acetonitrile) had a rate flow of 350 nL/min. The experiment was carried out under the following parameters: initial - 0.5% B, 22 min – 50% B, 23 min – 99% B, 26 min – 99% B, 27 min – 0.5% B and 30 min – 0.5% B. For the nanoLockSpray source the capillary voltage was 1.9 kV; sampling cone voltage, 40 V; cone gas flow: 50 l/h; desolvation gas flow was 500 l/h; source temperature was 100°C and desolvation temperature: 150°C. The lock mass capillary voltage was 3 kV and leucine-encephalin was injected through the lock spray channel as lock mass analyte every 60 s to serve as a reference. Proteins were identified using the ProteinLynxGlobalServer 2.5.2 (PLGS; Waters) software. Mass spectra were processed using an automatic chromatographic peak width; automatic MS ToF resolution; 0.25 Da of lock mass window; low energy threshold of 100 counts; an elevated energy threshold of 30 counts and an intensity threshold of 750 counts. For the protein identification, a non-redundant version of the *B. subtilis* 168 database (NCBI Reference Sequence: NC_000964.3) was used. This database contains 4180 protein sequences, including sequences of keratin and trypsin (manually added). The following parameters were applied: automatic peptide tolerance; automatic fragment tolerance; minimal fragment ion matches per peptide of 2; minimal fragment ion matches per protein of 4; minimal peptide matches per protein of 3; a maximum protein mass of 300 kDa; primary digest reagent: trypsin; secondary digest reagent: none; missed cleavages: 1; carbamidomethyl C fixed modification; deamidation N and Q and oxidation M variable modifications; 4 false positive rate.

4.3. Results and discussion

4.3.1. Morphological alteration of *S. aureus* surface after treatment with the colloidal dispersion

4.3.1.1. Antibacterial outcome on MSSA and MRSA

The antimicrobial peptide-biomimetic amphipathic PU colloidal particles NHP407-g-Poly(ILM-Br) are a potent antibacterial agent that induces its bactericidal effect through its fundamental structure. As shown in **table 4.1**, the lithium bromide chemical compound, the monomer ILM-TFMSI, the polymer NHP407 and its origin derivative structure NHP407-g-Poly(ILM-TFMSI) did not induce an inhibitory effect, while the polymer is able to kill Gram-positive staphylococci at very low concentrations in its final structure [NHP407-g-Poly(ILM-Br)]. Moreover, it induces a bactericidal action in the same extent for methicillin-sensitive and -resistant *Staphylococcus aureus* bacteria, observed by similar minimal bactericidal concentrations (MBC_{MSSA}=10.4 μg/mL and MBC_{MRSA}=13 μg/mL) (**table 4.1**). This is an interesting achievement, since the dose of currently-used antibiotics must be increased 2- to 3-fold magnitude to have an efficient antibacterial outcome against different kinds of drug-resistant bacteria, impacting the determined therapeutic window and may consequently lead to toxicity concerns (25,26).

Table 4.1. Minimum inhibitory concentration (MIC) and minimal bactericidal concentration (MBC) of monomers, basis polymer and final polymer structure against drug-sensitive *Staphylococcus aureus* and Methicillin-resistant *S. aureus*. NI – no inhibition observed starting with a maximum concentration of 2 mg/mL.

Most relevant clinical Gram-positive bacterial strains in chronic wounds	Lithium bromide (μg/mL)		Monomer ILM-TFMSI (μg/mL)		NHP407		NHP407-g-Poly (ILM-TFMSI) (μg/mL)		NHP407-g-Poly(ILM-Br) (μg/mL)	
	MIC	MBC	MIC	MBC	MIC	MBC	MIC	MBC	MIC	MBC
***Staphylococcus aureus* ATCC 29213 (MSSA)**	NI		NI		NI		NI		10.4 ± 3.7	10.4 ± 3.7
Methicillin-Resistant Staphylococcus aureus (MRSA)	NI		NI		NI		NI		13 ± 3.68	13 ± 3.68

Average ± Standard Deviation

4.3.1.2. Scanning electron microscopy on *Staphylococcus aureus* after exposition to NHP407-g-Poly(ILM-Br)

Samples of *S. aureus* ATCC® 29213™ were examined by scanning electron microscopy (SEM) to detect any physical changes in the appearance of bacterial cells that were pre-treated with the minimal bactericidal concentration of 13 μg/mL NHP407-g-Poly(ILM-Br) for 5 and 30 minutes. As a control, untreated *S. aureus* was used, in order to have a comparative basis between the normal and abnormal surface morphologies of staphylococci.

Morphologically, in SEM images, *Staphylococcus aureus* cells typically present a rough spherical (coccal morphology) shape (27–29). As observed in **figure 4.2 A**, untreated *S. aureus* cells appear rounded, some appear to be still in the division process and a slightly rough surface is evident. The sample containing only NHP407-g-Poly(ILM-Br) dispersion showed that some particles got associated and formed aggregates (**figure 4.2B**). However, taking the procedure of preparation of samples for SEM into consideration, this association might have occurred due to interactions with 2.5% glutaraldehyde or as a consequence of the centrifugation process.

The exposure of *S. aureus* to 13 μg/mL of NHP407-g-Poly(ILM-Br) for very short-periods of time caused considerable morphological abnormalities (**figure 4.2 C and D**): after 5 or 30 minutes of treatment, the bacteria's surface become very smooth. The images show areas of unstable cell wall, possibly in collapse, which creates a non-uniform surface, in overall (**figure 4.2 C and D**). Similar bacterial surface alteration was reported on *S. aureus* cells following a 3 hours exposure to 3 μg/mL of cloxacillin, a semi-synthetic antibiotic which belongs to the penicillinase-resistant penicillin's group, that acts on inhibiting the third and last stage of bacterial cell wall synthesis (28). Many granular structures are detected in the microscopic images. They appear freely or still associated with the bacteria, which are most probably fragments of the cell wall or cell membrane, indicating the existence of bacterial debris (remnants) after such a short-period of antibacterial action. The appearance of protuberances of different sizes on the surface of some cells is also observable, being more denoted on the bacteria pre-exposed to the colloidal particles for the longer period of 30 minutes (**figure 4.2 C and D**).

One of those protuberance regions was analysed through a cross-sectioning made by focused ion beam-scanning electron microscopy (FIB-SEM), to understand if it was formed by the PU particle, or associated colloidal particles, interacting with the surface of the bacteria (**figure 4.3**). However, this protuberance seems to be continuous with the bacterial membrane, so any point of contact between bacteria and particle(s) or particle-particle was not observed in this

technique so far. Nevertheless, it is observable that the protuberance is an outward deformation of the cell membrane, altering the typical coccal morphology (**figure 4.3**).

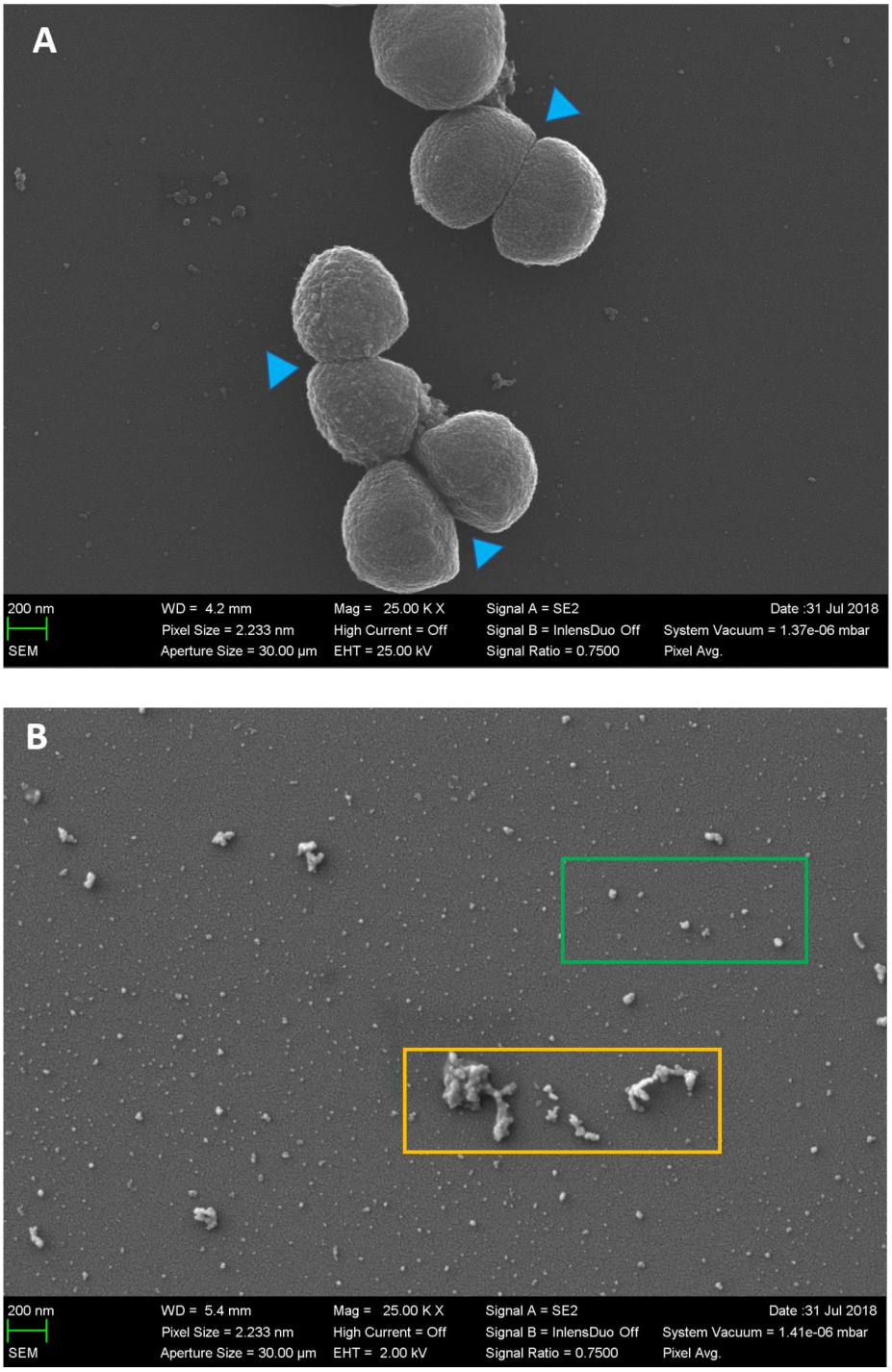

(first part of **figure 4.2.** – description on next page)

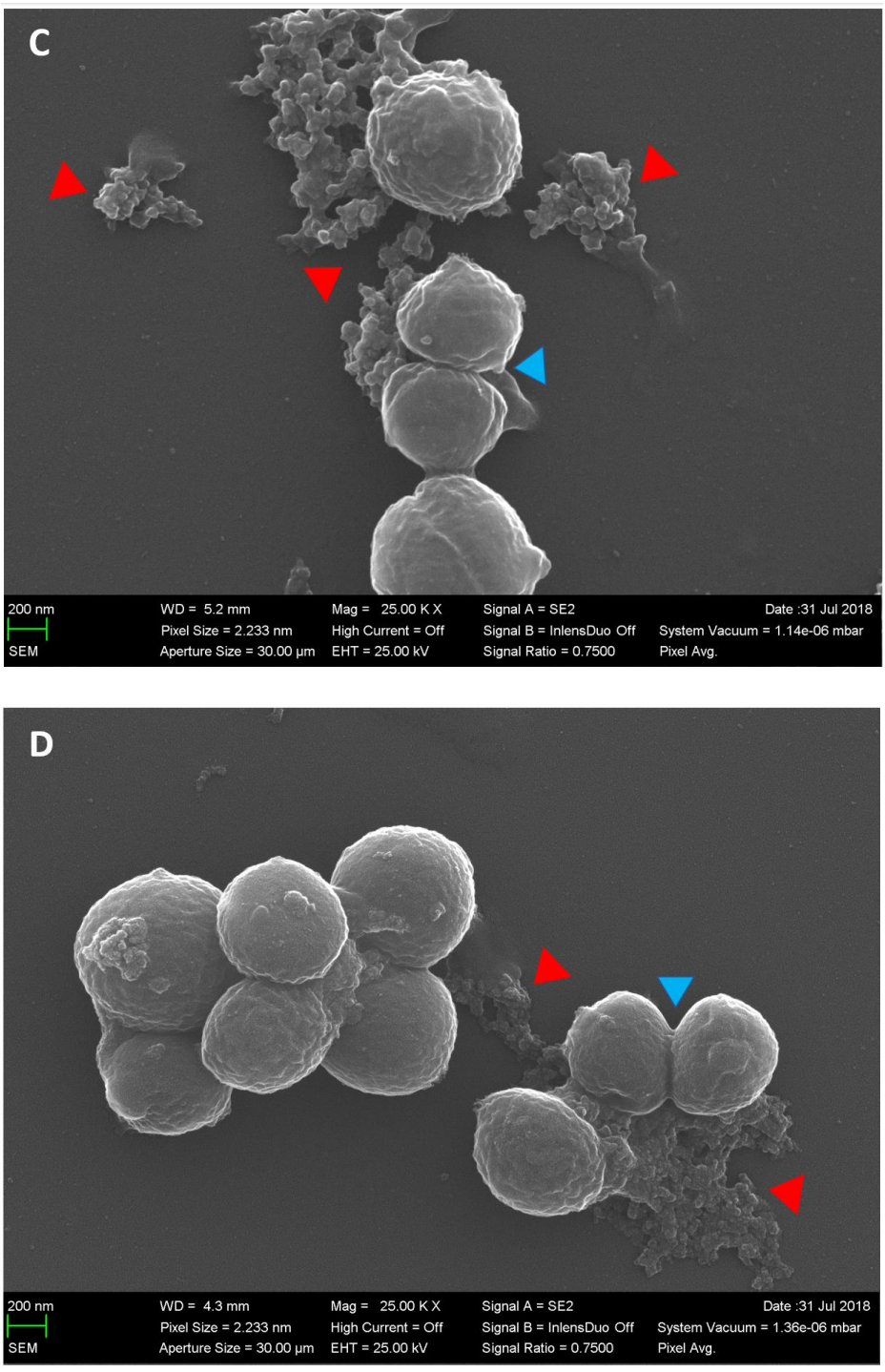

Figure 4.2. Scanning electron microscopy representative images of the influence of NHP407-g-Poly(ILM-Br) on *Staphylococcus aureus*. A – *S. aureus* control (untreated); B – 13 µg/mL NHP407-g-Poly(ILM-Br); C – *S. aureus* + 13 µg/mL NHP407-g-Poly(ILM-Br) for 5 minutes; D - *S. aureus* + 13 µg/mL NHP407-g-Poly(ILM-Br) for 30 minutes. **Blue triangle** – site of bacterial division; **Red triangle** – remnants of destroyed bacteria; **Green square** – distributed colloidal particles; **Yellow square** – associated colloidal particles.

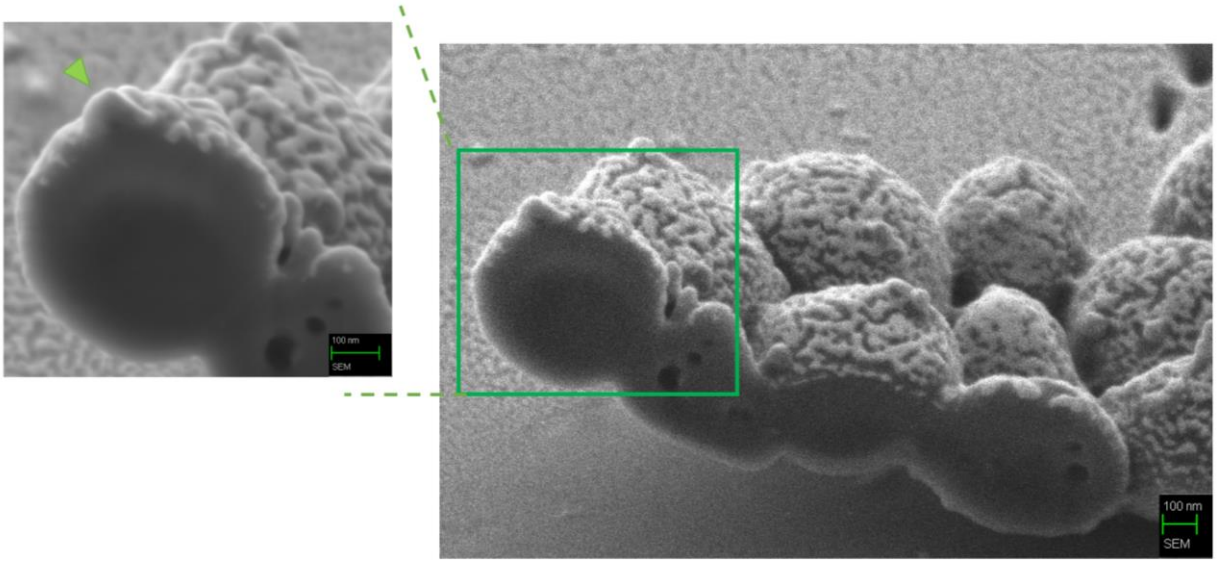

Figure 4.3. Cross-sectioning of a cluster of *S. aureus* previously exposed to 13 µg/mL NHP407-g-Poly(ILM-Br) for 30 minutes by focused ion beam scanning electron microscopy (FIB-SEM). **Green triangle** – protuberance on the bacterial membrane.

4.3.2. Optimization of conditions for proteome analysis

In order to find the appropriate concentration to be used for the determination of specific marker proteins synthesized during the colloidal particles treatment on Gram-positive bacteria, *Bacillus subtilis* 168 was selected as a well-established model (16,17,21). First, the minimal inhibitory concentration (MIC) of the colloidal particles on *B. subtilis* was determined under similar conditions used for the proteome experiment, such as steady agitation in Belitsky minimal medium (BMM) at 37 ºC. Afterwards, based on the determined MIC, bacterial growth experiments were followed to detect the optimal stressor concentration, which is a concentration that induces stress on *B. subtilis* by reducing its growth rate without causing excessive cell lysis or a complete inhibition of their metabolism. Establishing this parameter is crucial for proteomic experiments because protein biosynthesis must continue under this specific stress concentration to permit the identification of the proteomic response to an antibacterial agent.

4.3.2.1. Determination of the minimal inhibitory concentration of NHP407-g-Poly(ILM-Br) on *Bacillus subtilis* 168

The minimal inhibitory concentration (MIC) in broth dilution susceptibility test corresponds to the lowest concentration of an antimicrobial agent that prevents visible growth of a microorganism (30). In order to determine an accurate MIC, *Bacillus subtilis* was subjected to

decreasing concentrations of colloidal particles for 16-18h at 37°C. As observable in **figure 4.4**, the first concentration in which no turbidity is revealed, is 4 μg/mL of NHP407-g-Poly(ILM-Br). The low MIC result shows once again the potent antibacterial action of these AMP-mimicking colloidal particles on Gram-positive bacteria.

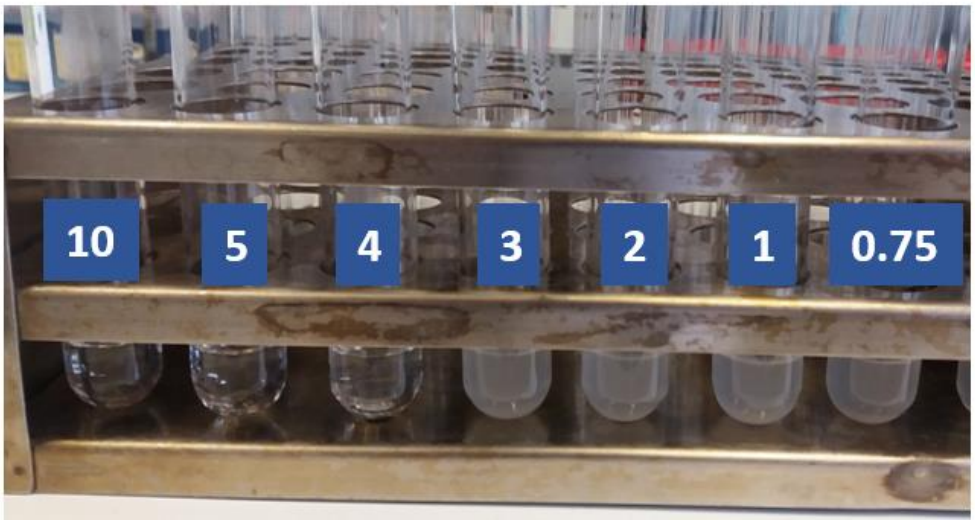

Figure 4.4. Determination of the minimal inhibitory concentration (MIC) of NHP407-g-Poly(ILM-Br) on *Bacillus subtilis* 168 by the macrodilution method. The numbers on the image are decreasing concentrations of NHP407-g-Poly(ILM-Br) in μg/mL units.

4.3.2.2. Identification of the optimal stressor NHP407-g-Poly(ILM-Br) concentration for proteome analysis

Based on the $MIC_{B.subtilis}$= 4 μg/mL, three concentrations of polymer (1, 2 and 4 μg/mL) were tested on *B. subtilis* growth for a total period of approximately 170 minutes, since the antibacterial agent was added at 130 minutes when an early exponential growth was reached. Then, the treatment was stopped when the stationary phase was detected. In parallel, the optical density (OD_{500}) of an untreated culture was also measured in order to have a defined control of the optimal growth rate (**figure 4.5**).

The MIC concentration of 4 μg/mL was selected as the ideal stressor concentration. After its addition, bacteria still grow, but in a lower rate compared to the control condition (**figure 4.5**). Hence, this concentration was selected to study the proteomic response of *B. subtilis* to NHP407-g-Poly(ILM-Br).

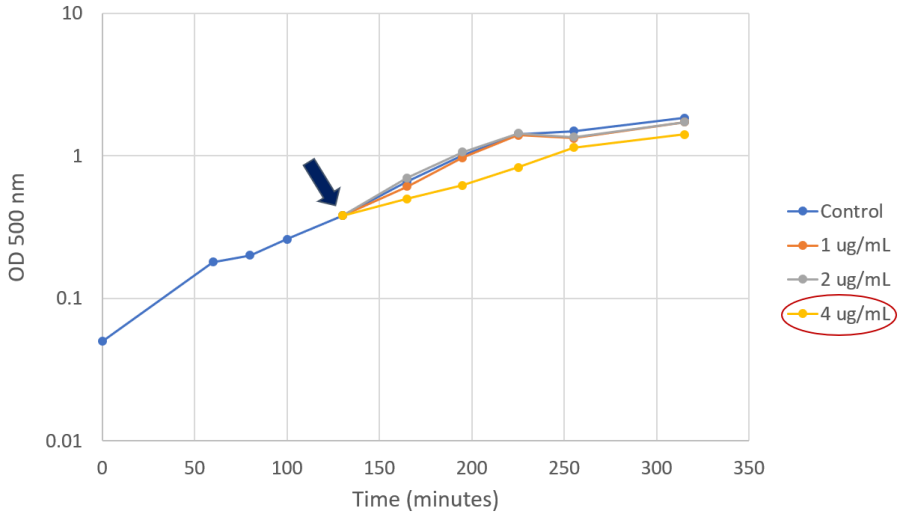

Figure 4.5. *Bacillus subtilis* 168 growth during time under the stress of three different MIC-associated concentrations of NHP407-g-Poly(ILM-Br). Control corresponds to untreated *B. subtilis*. **Red circle** represents the concentration selected for proteomic studies. The arrow is indicating the time point in which the colloidal particles were added (~130 minutes).

4.3.3. Proteomic response of *B. subtilis* to NHP407-g-Poly(ILM-Br)

A well-established platform for expression patterns of protein subsets (proteomic signatures) of *Bacillus subtilis* 168 in different stress conditions was previously developed by Bandow *et al.* with the Gram-positive model (21). Proteomic signatures are strong indicators of which pathways or structures are being targeted by the antimicrobial agent under study (31). The proteomic response reference compendium developed by Bandow and collaborators contains patterns for more than 50 well-known antimicrobial agents. Its efficient use in facilitating the identification of the mechanism of action of newly synthesized compounds has been multiply reported (16,18,21,22,32,33). Its rational design is based on the fact that the bacterial damage caused by an antibiotic reflects closely the antibiotic's mechanism of action (34). Hence, comparative proteome analysis investigates the existence of marker proteins for the antibacterial agent on *B. subtilis* that are newly-synthesized during the period of stress by the optimal stressor concentration. This provides insights of the antibacterial agent's cell targets and is subsequently a link to its mode of action. Most of the identified dysregulated proteins in this method, are predicted to be cytosolic. Nevertheless, these proteins can be associated with a membrane or general cell envelope stress response, cell wall and lipid biosynthesis, and energy metabolism (35). Undoubtedly, it is a great tool to initiate the unravelling of a mechanism of action of completely new antibacterial structures. In this work, it is reported the

first time that this platform was used for the identification of proteomic bacterial signatures under the stress of a polymeric system - the AMP-biomimetic amphipathic polyurethane colloidal particles NHP407-g-Poly(ILM-Br).

In order to initiate the proteomic response experiment, the stressor's optimal concentration of 4 μg/mL NHP407-g-Poly(ILM-Br) was added when the cultured *Bacillus subtilis* 168 attained its early exponential phase. The newly synthesized proteins during the acute bacterial stress response and untreated condition, were selectively pulse labelled with the addition of radioactive [35S]-L-methionine. After recovering the soluble intracellular protein fraction, the protein's concentration was quantified by a Bradford-based assay to normalize the quantities of protein loaded onto 2D-gels. In this step it was noticed that the level of proteins in the NHP407-g-Poly(ILM-Br)-treated *B. subtilis* condition was lower than in the control (untreated *B. subtilis*) (**figure 4.6**). Concomitantly, in the measurement of the radioactivity incorporation rate, it could be observed that the samples previously stressed by NHP407-g-Poly(ILM-Br) showed less than 50% of counts per minute (CPM) and disintegrations per minute (DPM) than the control condition, meaning that in overall the incorporation of [35S]-L-methionine was reduced (**table 4.2**). By combining both results - protein quantification and radioactivity incorporation - it seems that NHP407-g-Poly(ILM-Br) inhibited protein synthesis during the short period of stress, impacting the relative synthesis rate of the Gram-positive model *B. subtilis*.

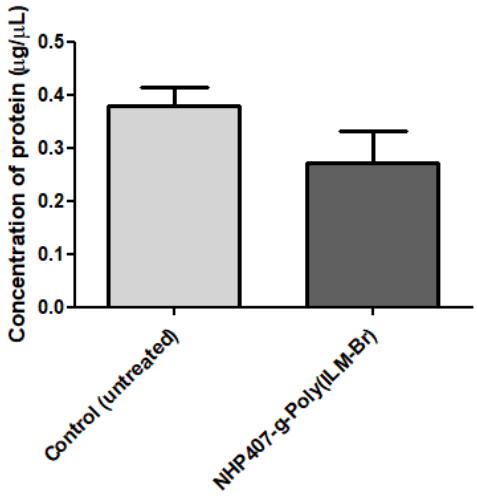

Figure 4.6. Comparison between the quantity of proteins measured in the *B. subtilis* control condition (untreated) and stressed *B. subtilis* by 4 μg/mL of NHP407-g-Poly(ILM-Br) addition, by the Bradford-based Roti® Nanoquant assay.

Table 4.2. Total radioactivity incorporated (by CPM) into the samples and nuclides count (obtained through DPM values) of untreated (control) and NHP407-g-Poly(ILM-Br)-treated *Bacillus subtilis* strains.

Condition	Counts per minute (CPM)	Disintegrations per minute (DPM)
Control	$3.8 \times 10^4 \pm 4.2 \times 10^3$	$4.13 \times 10^4 \pm 4.5 \times 10^3$
NHP407-g-Poly(ILM-Br)	$1.6 \times 10^4 \pm 6.9 \times 10^3$	$1.72 \times 10^4 \pm 7.4 \times 10^3$

Average ± Standard deviation

Afterwards, the soluble protein fraction was separated by 2D-PAGE depending on its isoelectric point (PI) from 4 to 7 and its molecular mass (kDa) from highest to lowest weight. In **figure 4.7**, representative autoradiographs show the proteome expression profiles of untreated- and NHP407-g-Poly(ILM-Br)-treated *Bacillus subtilis*. It can be noticed that in the 2D-gel ran with proteins obtained from the stressed *B. subtilis* culture, the biosynthesis was substantially diminished, represented by the less protein spots (**figure 4.7**). This observation proves once again the protein inhibition capacity of NHP407-g-Poly(ILM-Br).

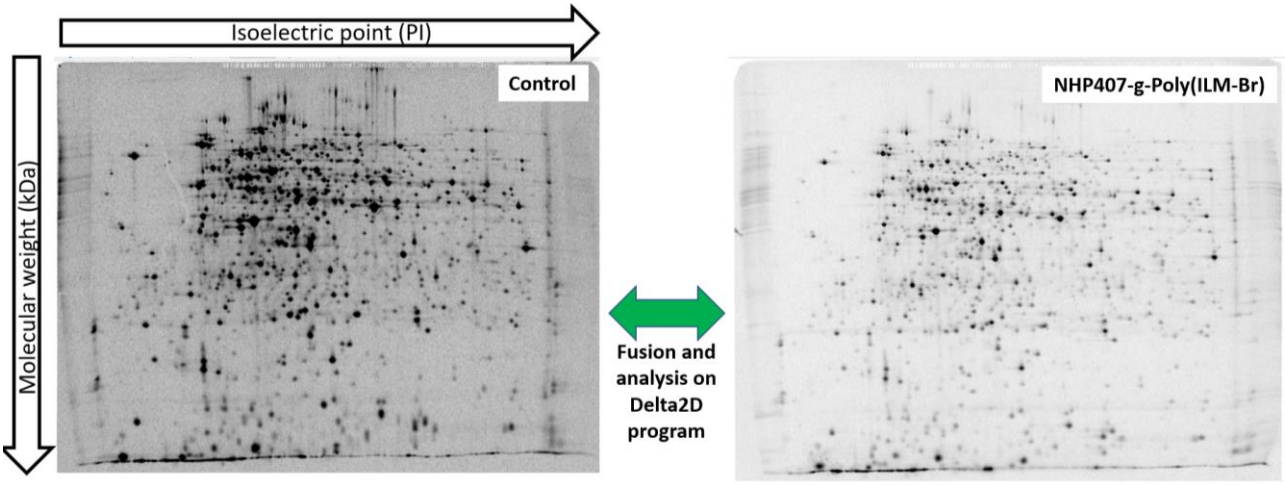

Figure 4.7. 2D-gels of the separated radioactive-labelled cytosolic protein extracts obtained from untreated *B. subtilis* (Control) and treated with 4 µg/mL of colloidal particles [NHP407-g-Poly(ILM-Br)]. The proteins were first separated in a first dimension by its isoelectric point (PI) from 4 to 7, and then by a second dimension by SDS-PAGE from higher to lower molecular weight (kDa). Gel images of untreated and treated conditions were overlaid for merged 2D-gel based proteome analysis on the Delta2D program.

The 2D-gel scans of control and colloidal particles-treated samples were merged in a 2D-gel based proteome analysis program, Delta2D, to recognize marker proteins which are proteins

overexpressed more than 2-fold than the reference gel (control 2D-gel) (**figure 4.8 and table 4.3**). These newly synthesized proteins rate reflects which stress events the bacteria are trying to overcome and give valuable hints for exploring the amphipathic PU colloidal particles' mechanism of action.

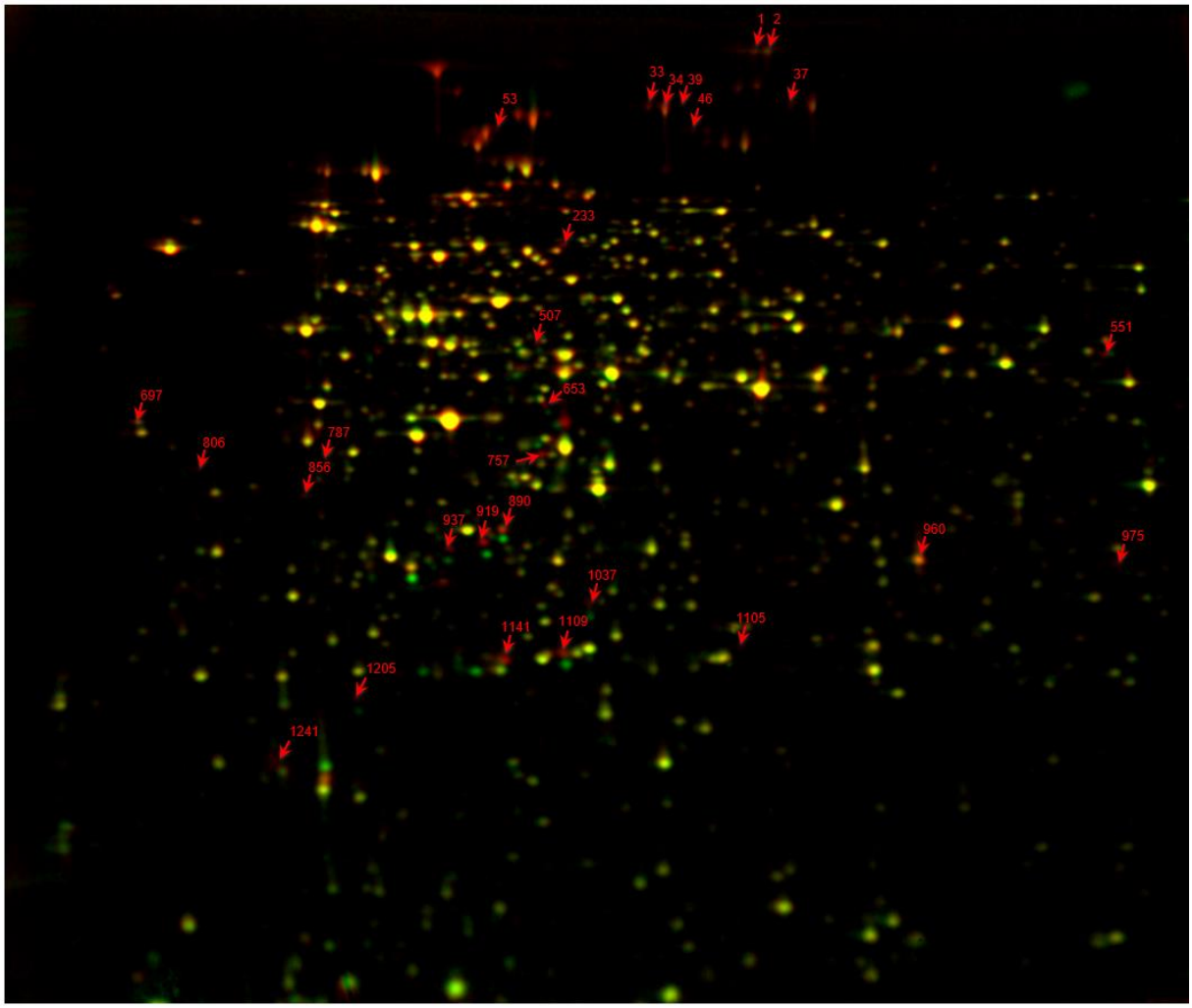

Figure 4.8. 2D gel-based proteome analysis of *Bacillus subtilis* treated with 4 µg/mL NHP407-g-Poly(ILM-Br) colloidal particles in comparison with untreated (control) based on radioactive labelling with [35S]-methionine. **False-coloured in red**: synthesis rate of proteins from extracts of treated-*B. subtilis*; **false-coloured in green**: untreated bacteria protein synthesis rate; **false-coloured in yellow**: proteins expressed at similar rates.

In **figure 4.8**, a 2D gel-based proteome analysis based on radioactive labelling with [35S]-methionine of *Bacillus subtilis* treated with 4 µg/mL NHP407-g-Poly(ILM-Br) colloidal particles in comparison with the untreated condition (control) is displayed. By the false-red coloured spots, the up-regulated proteins induced by the presence of NHP407-g-Poly(ILM-Br) are recognized (also known as marker proteins). These had a ratio of protein overexpression of

more than 2-fold than the control proteins (**table 4.3**). The ratio is proportional to the biosynthesis rate, and in **table 4.3**, one can observe that some proteins were more expressed under the stress of the antibacterial agent than others. In total, 28 spots were categorized as marker proteins induced by treatment with the colloidal particles (**figure 4.8 and table 4.3**). Non-radioactive stained 2D-gels with proteins extracted from treated-*Bacillus subtilis* were developed and by visual comparison with the respective radioactive-gel scan, the spots were excised from the gel on a dark non-UV transilluminator reader. Unfortunately, the spots 46, 233 and 1109 were not found on the non-radioactive 2D-PAGE. This could have occurred due to biological or technical variability (36). The rest of the gel spots were prepared to be identified by mass-spectrometry.

Table 4.3. Ratio score of intensity for each marker protein spot of NHP407-g-Poly(ILM-Br)-treated *B. subtilis* versus untreated-bacterial cells radioactive 2D-gels.

Spot label	Ratio NHP407-g-Poly(ILM-Br)/Control
1	2.487
2	2.006
33	4.640
34	2.982
37	6.142
39	11.239
46	3.338
53	2.070
233	2.477
507	3.113
551	3.388
653	3.635
697	3.674
757	4.823
787	4.942
806	7.927
856	2.799
890	2.681
919	24.094
937	9.784
960	4.418

975	3.736
1037	11.311
1105	3.822
1109	11.053
1141	7.006
1205	17.358
1241	16.135

Out of the excised protein spots, 13 marker target proteins were identified by mass-spectrometry-based approach (**table 4.4**).

The unidentified protein spots were evidently and reproducibly visualized on the radiographs, proving the existence of a specific protein production by the Gram-positive microorganism model in response to the colloidal particle's exposure, but were insufficient for an accurate protein identification by this procedure. It is worth mentioning that even though no assumptions from these protein spots can be discussed, they remain as NHP407-g-Poly(ILM-Br)-specific markers.

Concerning the identified marker proteins, it was detected that the polymeric system is affecting different pathways or structures in *B. subtilis*, namely: membrane and cell wall integrity (3 proteins – PspA, LiaH and RacX), energy metabolism (2 proteins – PdhA and YuJ), amino acids biosynthesis (3 proteins – GltA, YhdR and YxjG), translation process (2 proteins – IleS and PheT), nucleotide synthesis (1 protein - PupG) and sulfur metabolism (CysC) (**table 4.3 and 4.4**).

Primarily, NHP407-g-Poly(ILM-Br) particles seem to inhibit Gram-positive bacteria growth by influencing cell wall biosynthesis/integrity and respiration, which is demonstrated by the upregulation of proteins associated with membrane and cell wall and proteins required for the energy process on the proteome stress response (**table 4.4**).

Phage shock protein A (PspA) upregulation is one of the compensation strategies taken by bacteria to overcome cell envelope stress. It has been reported that this protective membrane-binding protein has the function to stabilize membrane integrity under non-favourable conditions, preventing leakage and loss of membrane potential (16,37–39). Hence, if an antibacterial agent is impairing membrane integrity, it is no surprise that this protein is overexpressed, such as shown by the stress response of *B. subtilis* to the AMP-biomimetic colloidal particles under study (**table 4.3 and 4.4**). Expression of the pspA gene is controlled

by the regulator sigma factor σ^W to adapt membrane composition in response to envelope stress (16,40). Moreover, the modulator of liaIHGFSR operon expression LiaH, which is a homologue of PspA, also appeared upregulated on the proteome extract of treated-*B. subtilis* (**table 4.3 and 4.4**). This protein belongs to a two-component system LiaRS and is produced mainly as response to inhibition of cell wall biosynthesis and oxidative stress, having similar stabilizing membrane integrity functions as PspA in *Bacillus subtilis* (15). The two-component system LiaRS in combination with the extracytoplasmic function sigma factors (σ^W, σ^M, σ^X, σ^B) are a first line of protection against bacterial envelope impairment (40,41). Upregulation of both PspA and LiaH strongly indicates NHP407-g-Poly(ILM-Br) is targeting the cell envelope, more specifically by damaging the membrane and inhibiting cell wall biosynthesis.

In accordance to the previous observation, the presence of the amino acid racemase (RacX) to produce non-canonical D-amino acids was similarly augmented (**table 4.3 and 4.4**). The production of non-canonical D-amino acids, specially D-alanine and D-glutamic acid, is a common survival strategy in bacteria (42). These amino acids have been linked with controlling the peptidoglycan layer remodelling, prevention of biofilm formation and biofilm disassembly (43). Therefore, RacX upregulation in the presence of the optimal stressor concentration of NHP407-g-Poly(ILM-Br) shows that the cell wall is under damaging pressure.

The large subunit of glutamate synthase (GltA) that has the function of glutamate biosynthesis was also identified as a marker target protein (**table 4.3 and 4.4**). It has been described that a high production and release of glutamate is an osmoprotectant response of bacteria to a stress factor, and most probably it is induced during membrane adjustments initiated by the contact with an antibacterial agent active on mechanosensitive channels (35). In the same research work, the osmoprotective glutamate release was described as a general response to bacteriolytic antimicrobial peptides (35).

The bacterial cytoplasmic membrane is the basis for many crucial cellular activities, including one of the most important for its continued existence, the respiration process. Disturbance on the respiratory chain, limiting energy, leads to multiple problems for cellular functions that are necessary for their survival, growth and multiplication (44,45). The latter occurs mainly because the resulting electrochemical gradient from the citric acid cycle on the membrane induces adenosine triphosphate (ATP) synthesis, which is absolutely indispensable in almost every intracellular process as an energy supplier in metabolism and enzymatic reactions, besides having signalling functions (e.g. RNA biosynthesis, transportation, signal transduction) (14,45,46).

In our study, pyruvate dehydrogenase E1 alpha subunit (PdhA) was upregulated on the comparative proteome analysis (**table 4.3 and 4.4**). This subunit has a participative role in the metabolic pathway of glycolysis, which is the first stage of cellular respiration. Impairment of this process has destructive consequences for bacteria. This compensating upregulation might be associated with a mal-function of the citric acid cycle ATP production (substantial energy limitation), proving again that one of the main targets of these AMP-mimicking particles is the cytoplasmic membrane of Gram-positive bacteria.

Under the external stress of an antibacterial agent, bacteria respond rapidly with modifying protein synthesis (21,22). Predictably, the translation process is increased to produce specific proteins to overcome the antibacterial effect, and in this study, this can be seen in the upregulation of proteins – identified by the 2D gel and mass spectrometry approach – that have a function in translation, i.e. isoleucyl-tRNA synthetase – IleS and phenylalanyl-tRNA synthetase – PheT (**table 4.3 and 4.4**).

Sulfur is an indispensable element in all living species for the synthesis of proteins and co-factors (47). It is assimilated from the inorganic source sulfate in *Bacillus subtilis* by transportation into the cell through the sulfate permease on the membrane (48). A highly dysregulated enzyme (7-fold than the control) involved in the process of sulfate reduction and activation, adenyl-sulfate kinase (CysC), was identified (**table 4.3 and 4.4**). A possible explanation for this expression alteration is that the adenyl-sulfate kinase is increased to finally support more synthesis of proteins.

The most upregulated protein detected in the extract of *Bacillus subtilis* previously exposed to NHP407-g-Poly(ILM-Br) was the purine nucleoside phosphorylase (PupG) (**table 4.3 and 4.4**). It is a key enzyme in purine salvage and interconversion in the nucleoside pathway. The nucleosides can be intracellularly originated by the breakdown of nucleotides or obtained readily from the external environment (growth medium) and metabolized, which is the specific case for *Bacillus subtilis*. The nucleoside-catabolizing process in this Gram-positive model serves as a basis for nucleotide synthesis to be subsequently used in the synthesis of DNA, RNA and enzyme co-factors (49). Assuming that, the antibacterial colloidal particles under study are primarily affecting membrane integrity, the uptake of nucleotides will consequently be impaired. Moreover, it has also been reported that the *de novo* purine nucleotide biosynthesis process in *Bacillus anthracis* is essential for bacterial proliferation in the patients' bloodstream (bacteraemia), hence the authors concluded that the involved enzymes are great antibacterial targets for the treatment of this infection (50). Herein, dysregulation of this pathway induced by the colloidal particles seems to support the previous observation.

Although an immense effort has been done in research to identify all genes and their functions in *Bacillus subtilis*, a complete library of all functions of *Bacillus subtilis* genes is still missing. Unfortunately, the second most upregulated protein – Ytsp – by the presence of NHP407-g-Poly(ILM-Br) colloidal dispersion does not have a suggested role regarding cell physiology yet (51) (**table 4.3 and 4.4**).

Table 4.4. Identified *B. subtilis* 168 cytosolic marker proteins overexpressed in response to treatment with NHP407-g-Poly(ILM-Br) colloidal dispersion.

Spot label	Protein ID	Mass weight (Da)	pI	Peptide count	Protein name	Protein function	Stress category
2	GltA	168666	5.44	29	Large subunit of glutamate synthase	Glutamate biosynthesis	Amino acids
33	IleS	104778	5.19	47	Isoleucyl-tRNA synthetase	Translation	Translation
53	PheT	87891	4.86	35	Phenylalanyl-tRNA synthetase (beta subunit)	Translation	Translation
507	YhdR	43860	5.01	40	Similar to aspartate aminotransferase	Unknown	Amino acids
	YxjG	43137	5.00	14	Putative B12-independent methionine synthase	Unknown	Amino acids
551	YutJ	39579	6.06	35	Putative NADH dehydrogenase	Unknown	Energy
	PdhA	41522	5.83	80	Pyruvate dehydrogenase (E1 alpha subunit)	Glycolysis	Energy
919	PupG	29108	4.86	8	Purine nucleoside phosphorylase	Purine salvage and interconversion	Nucleotide synthesis
960	PspA	25125	5.87	11	Phage shock protein A homologue (homologue of liaH)	Protection against cell envelope stress	Membrane
975	LiaH	25682	6.20	14	Modulator of liaIHGFSR operon expression	Resistance against oxidative stress and cell wall antibiotics	Cell wall

1105	RacX	25270	5.46	3	Amino acid racemase, production of non-canonical D-amino acids	Cell envelope stress	Cell wall
1141	CysC	22530	5.08	51	Adenylyl-sulfate kinase	Sulfate reduction and activation	Sulfur metabolism
1241	YtsP	18057	4.39	9	Unknown	Protein with unknown function	Unknown

After analysing the identified upregulated proteins, it is possible to assume that the electrostatic interaction and subsequent integration into the cell envelope of AMP-biomimetic polyurethane colloidal particles induces a strategic stress response on *B. subtilis* mainly based on the modification of the membrane and cell wall. Thus, probable mechanisms of action of NHP407-g-Poly(ILM-Br) are alteration of the membrane and cell wall integrity and impairment of the respiration metabolism by limiting the energy within the bacteria.

4.4. Conclusion

Antimicrobial peptide-based polymers that mimic the common mechanism of action of targeting the bacterial membrane, are potential therapeutic agents for combating drug-resistant microorganisms.

The antimicrobial peptide-biomimetic amphipathic polyurethane colloidal particles NHP407-g-Poly(ILM-Br) were shown to be a powerful antibacterial agent against Gram-positive bacteria that induces its bactericidal effect through its fundamental structure, acting in similar concentrations on drug-sensitive and -resistant bacteria, observed with the bactericidal action on MSSA and MRSA.

To prove that these particles are indeed mimicking the common bactericidal mode of action of AMPs, first it was studied if there were any alterations on the cell wall of *S. aureus* under the presence of NHP407-g-Poly(ILM-Br) by means of SEM techniques. Then, a detailed proteomic study to identify the proteins being upregulated by *Bacillus subtilis* in order to overcome the effect induced by the colloidal particles-treatment was performed. In combination, both experiments showed clear evidence that the particles are in fact acting on the cell's envelope of Gram-positive bacteria.

After only 5 and 30 minutes of treatment, morphological abnormalities were observed on the surface of *S. aureus* bacteria by SEM, namely an extremely smooth surface. Herein, visualized

points of unstable cell wall were also visualized, perhaps due to disintegration. In this experiment the rapid bactericidal action of these particles was again confirmed again, by the detection of cell debris after a short-period of contact.

In this work, the *B. subtilis* proteomic signatures platform was used to identify marker proteins as a response to a polyurethane system. It was confirmed that this 2D-PAGE and mass spectrometry combination approach was very successful for the mentioned objective.

During the establishment of parameters for the study of the response of *B. subtilis* to the treatment with NHP407-g-Poly(ILM-Br) colloidal particles at the proteome level by combining 2D gel-based and liquid chromatography-mass spectrometry-based approaches, it was registered once again the great bactericidal effect of these particles on another Gram-positive specie (acted with very low concentrations ~ 4 μg/mL on *Bacillus subtilis*). In addition, a protein inhibition consequence was verified.

Relatively to the final findings of the proteomic study, strong indicators of targeted pathways or structures were obtained, since it was identified which proteins were over-expressed to overcome the stressful stimuli provoked by the colloidal particles. The identified marker proteins are related to *Bacillus subtilis* stress responses on the membrane and cell wall integrity, the energy metabolism, the nucleotide synthesis and the sulfur metabolism. Overall, this proteome analysis result leads us to the proposition that the mechanism of action of NHP407-g-Poly(ILM-Br) relies on acting on the cell wall and membrane, and on the respiration metabolism, by limiting the bacteria's available energy. To confirm this theory, additional experiments should be performed such as transmission electron microscopy (mainly to confirm if pores are being formed on the membrane), membrane potential measurements to verify the disturbance of the cytoplasmic bacterial membrane, and ATP concentration measurements in order to corroborate with the described energy impairment.

In conclusion, the initial indications on the bactericidal mode of these newly synthesized antimicrobial peptide-biomimetic amphipathic polyurethane colloidal particles on Gram-positive bacteria indicate an identical mechanism of action shared commonly among most antimicrobial peptides: cell membrane perturbation.

References

1. Hancock RE. Cationic peptides: Effectors in innate immunity and novel antimicrobials. Lancet Infect Dis. 2001;1(3):156–64.
2. Hancock R, Patrzykat A. Clinical Development of Cationic Antimicrobial Peptides: From Natural to Novel Antibiotics. Curr Drug Target -Infectious Disord. 2005;2(1):79–83.
3. Findlay B, Zhanel GG, Schweizer F. Cationic amphiphiles, a new generation of antimicrobials inspired by the natural antimicrobial peptide scaffold. Antimicrob Agents Chemother. 2010;54(10):4049–58.
4. Ganz T. The Role of Antimicrobial Peptides in Innate Immunity. Integr Comp Biol. 2006;43(2):300–4.
5. Joo HS, Fu CI, Otto M. Bacterial strategies of resistance to antimicrobial peptides. Philos Trans R Soc B Biol Sci. 2016;371(1695).
6. Bechinger B, Gorr SU. Antimicrobial Peptides: Mechanisms of Action and Resistance. J Dent Res. 2017;96(3):254–60.
7. Brown KL, Hancock REW. Cationic host defense (antimicrobial) peptides. Curr Opin Immunol. 2006;18(1):24–30.
8. Zasloff M. Antimicrobial peptides of multicellular organisms. Nature. 2002;415(6870):389–95.
9. Dubois-Brissonnet F, Trotier E, Briandet R. The biofilm lifestyle involves an increase in bacterial membrane saturated fatty acids. Front Microbiol. 2016;7:1673.
10. Lewies A, Du Plessis LH, Wentzel JF. Antimicrobial Peptides: the Achilles' Heel of Antibiotic Resistance? Probiotics Antimicrob Proteins. 2018;1–12.
11. Bowler PG. Antibiotic resistance and biofilm tolerance: a combined threat in the treatment of chronic infections. J Wound Care. 2018;27(5):273–7.
12. Kassam NA, Damian DJ, Kajeguka D, Nyombi B, Kibiki GS. Spectrum and antibiogram of bacteria isolated from patients presenting with infected wounds in a Tertiary Hospital, northern Tanzania. BMC Res Notes. 2017;10(1):1–6.
13. Rossi A, Gallelli L, Settimio UF, Amato B, Grande R, Caroleo B, et al. Chronic wound infections: the role of Pseudomonas aeruginosa and Staphylococcus aureus. Expert Rev Anti Infect Ther. 2015;13(5):605–13.
14. Shai Y. Mode of action of membrane active antimicrobial peptides. Biopolym - Pept Sci Sect. 2002;66(4):236–48.
15. Wolf D, Kalamorz F, Wecke T, Juszczak A, Mäder U, Homuth G, et al. In-depth profiling of the LiaR response of bacillus subtilis. J Bacteriol. 2010;192(18):4680–93.
16. Wenzel M, Kohl B, Münch D, Raatschen N, Albada HB, Hamoen L, et al. Proteomic response of Bacillus subtilis to lantibiotics reflects differences in interaction with the cytoplasmic membrane. Antimicrob Agents Chemother. 2012;56(11):5749–57.
17. Wenzel M, Chiriac AI, Otto A, Zweytick D, May C, Schumacher C, et al. Small cationic antimicrobial peptides delocalize peripheral membrane proteins. Proc Natl

Acad Sci USA. 2014;111(14):E1409–18.

18. Müller A, Wenzel M, Strahl H, Grein F, Saaki TN V., Kohl B, et al. Daptomycin inhibits cell envelope synthesis by interfering with fluid membrane microdomains. Proc Natl Acad Sci. 2016;113(45):E7077–86.

19. Gonzalez DJ, Haste NM, Hollands A, Fleming TC, Hamby M, Pogliano K, et al. Microbial competition between Bacillus subtilis and Staphylococcus aureus monitored by imaging mass spectrometry. Microbiology. 2011;157(9):2485–92.

20. Stulke J, Hanschke R, Hecker M. Temporal activation of -glucanase synthesis in Bacillus subtilis is mediated by the GTP pool. J Gen Microbiol. 1993;139(9):2041–5.

21. Bandow JE, Brötz H, Leichert LIO, Labischinski H, Hecker M. Proteomic approach to understanding antibiotic action. Antimicrob Agents Chemother. 2003;47(3):948–55.

22. Wenzel M, Patra M, Albrecht D, Chen DYK, Nicolaou KC, Metzler-Nolte N, et al. Proteomic signature of fatty acid biosynthesis inhibition available for in vivo mechanism-of-action studies. Antimicrob Agents Chemother. 2011;55(6):2590–6.

23. Rabilloud T, Strub JM, Luche S, Van Dorsselaer A, Lunardi J. A comparison between Sypro Ruby and ruthenium ii tris (bathophenanthroline disulfonate) as fluorescent stains for protein detection in gels. Proteomics. 2001;1(5):699–704.

24. Bandow JE, Baker JD, Berth M, Painter C, Sepulveda OJ, Clark KA, et al. Improved image analysis workflow for 2-D gels enables large-scale 2-D gel-based proteomics studies - COPD biomarker discovery study. Proteomics. 2008;8(15):3030–41.

25. Lewis K. Platforms for antibiotic discovery. Vol. 12, Nature Reviews Drug Discovery. 2013. p. 371–87.

26. Fair RJ, Tor Y. Antibiotics and bacterial resistance in the 21st century. Perspect Medicin Chem. 2014;6:25–64.

27. Gnanamani A, Hariharan P, Paul-Satyaseela M. *Staphylococcus aureus*: Overview of Bacteriology, Clinical Diseases, Epidemiology, Antibiotic Resistance and Therapeutic Approach. In: Frontiers in Staphylococcus Aureus. 2017.

28. Greenwood D, O'Grady F. Scanning Electron Microscopy of Staphylococcus aureus Exposed to Some Common Anti-staphylococcal Agents. J Gen Microbiol. 1972;70:263–70.

29. Bailey RG, Turner RD, Mullin N, Clarke N, Foster SJ, Hobbs JK. The interplay between cell wall mechanical properties and the cell cycle in staphylococcus aureus. Biophys J. 2014;107(11):2538–45.

30. Cockerill FR, Wikler MA, Alder J, Dudley MN, Eliopoulos GM, Ferraro MJ, et al. Methods for Dilution Antimicrobial Susceptibility Tests for Bacteria That Grow Aerobically ; Approved Standard — Ninth Edition M07-A9. Methods for Dilution Antimicrobial Susceptibility Tests for Bacteria That Grow Aerobically; Approved Standar- Ninth Edition. 2012.

31. VanBoelen RA, Schiller EE, Thomas JD, Neidhardt FC. Diagnosis of cellular states of microbial organisms using proteomics. From Genome to Proteome Adv Pract Appl Proteomics. 1999;20(11):2149–59.

32. Wenzel M, Bandow JE. Proteomic signatures in antibiotic research. Proteomics.

2011;11(15):3256–68.

33. Bandow JE, Hecker M. Proteomic profiling of cellular stresses in Bacillus subtilis reveals cellular networks and assists in elucidating antibiotic mechanisms of action. Prog Drug Res. 2007;64:79–101.

34. Raatschen N, Bandow JE. 2-D gel-based proteomic approaches to antibiotic drug discovery. Curr Protoc Microbiol. 2012;26(1):1F2.1-1F2.16.

35. Wenzel M, Schriek P, Prochnow P, Albada HB, Metzler-Nolte N, Bandow JE. Influence of lipidation on the mode of action of a small RW-rich antimicrobial peptide. Biochim Biophys Acta - Biomembr. 2016;1858(5):1004–11.

36. Bland AM, Janech MG, Almeida JS, Arthur JM. Sources of variability among replicate samples separated by two-dimensional gel electrophoresis. J Biomol Tech. 2010;21(1):3–8.

37. Kobayashi R, Suzuki T, Yoshida M. Escherichia coli phage-shock protein A (PspA) binds to membrane phospholipids and repairs proton leakage of the damaged membranes. Mol Microbiol. 2007;66(1):100–9.

38. Horstman NK, Darwin AJ. Phage shock proteins B and C prevent lethal cytoplasmic membrane permeability in Yersinia enterocolitica. Mol Microbiol. 2012;85(3):445–60.

39. Vrancken K, Van Mellaert L, Anné J. Characterization of the Streptomyces lividans PspA response. J Bacteriol. 2008;190(10):3475–81.

40. Domínguez-Escobar J, Wolf D, Fritz G, Höfler C, Wedlich-Söldner R, Mascher T. Subcellular localization, interactions and dynamics of the phage-shock protein-like Lia response in Bacillus subtilis. Mol Microbiol. 2014;92(4):716–32.

41. Hecker M, Völker U. General stress response of Bacillus subtilis and other bacteria. Adv Microb Physiol. 2001;44:35–91.

42. Cava F, de Pedro MA, Lam H, Takacs CN, Waldor MK, Oh D-C, et al. D-Amino Acids Govern Stationary Phase Cell Wall Remodeling in Bacteria. Science (80-). 2009;325(5947):1552–5.

43. Miyamoto T, Katane M, Saitoh Y, Sekine M, Homma H. Identification and characterization of novel broad-spectrum amino acid racemases from Escherichia coli and Bacillus subtilis. Amino Acids. 2017;49(11):1885–94.

44. Brötz-Oesterhelt H, Brunner NA. How many modes of action should an antibiotic have? Curr Opin Pharmacol. 2008;8(5):564–73.

45. Mempin R, Tran H, Chen C, Gong H, Kim Ho K, Lu S. Release of extracellular ATP by bacteria during growth. BMC Microbiol. 2013;13(1).

46. Montes De Oca LYJG, Chagolla-López A, De La Vara LG, Cabellos-Avelar T, Gómez-Lojero C, Cirlos EBG. The composition of the bacillus subtilis aerobic respiratory chain supercomplexes. J Bioenerg Biomembr. 2012;44(4):473–86.

47. Burguière P, Fert J, Guillouard I, Auger S, Danchin A, Martin-Verstraete I. Regulation of the Bacillus subtilis ytmI operon, involved in sulfur metabolism. J Bacteriol. 2005;187(17):6019–30.

48. Mansilla MC, De Mendoza D. The Bacillus subtilis cysP gene encodes a novel sulphate

permease related to the inorganic phosphate transporter (Pit) family. Microbiology. 2000;146(4):815–21.

49. Schuch R, Garibian A, Saxild HH, Piggot PJ, Nygaard P. Nucleosides as a carbon source in Bacillus subtilis: Characterization of the drm-pupG operon. Microbiology. 1999;145(10):2957–66.

50. Mankin AS, Cook JL, Samant S, Neyfakh AA, Chen J, Lee H, et al. Nucleotide Biosynthesis Is Critical for Growth of Bacteria in Human Blood. PLoS Pathog. 2008;4(2):e37.

51. Studer R, Eschevins C, Koski P, Schumann W, Ashikaga S, Vagner V, et al. Essential Bacillus subtilis genes. Proc Natl Acad Sci. 2003;100(8):4678–83.

CHAPTER FIVE

‘Final remarks:
General discussion and conclusion’

The present thesis focusses on the biological characterisation of technologies, either available in the market or under development for the treatment of bacterial infections in chronic wounds. Two common pathological events hinder proper wound healing: bacterial infection and perpetuation of inflammation (1–3). Infection can lead to a life-threatening condition, especially if biofilms or antibiotic-resistant bacteria develop as contaminants of the wound (4,5). The constant inflammatory phase at the wound site dysregulates the optimal function of cell populations involved in the complex regulation of the wound healing process, including the wound healing key players: the macrophages (3,6,7). Antibacterial susceptibility, biocompatibility and immunomodulation should be deeply explored to have the most complete information about currently-used and newly synthesized products that are proposed for wound care.

For the first section of the laboratory work (**chapter 2**) the issue tackled was to determine if selected silver incorporating wound dressings present in the market are efficient in reducing bacterial burden. Furthermore, properties of these dressings in immunomodulating the macrophages to an anti-inflammatory state were explored, which is an important feature that has not been evaluated properly for clinically-applied products. Ideally, a wound dressing should stimulate the shift from the inflammatory to the proliferation/remodelling phases of wound healing. Three different clinically applied antimicrobial wound dressings, that contain silver, were selected for this study: Atrauman® Ag, Biatain® Alginate Ag and PolyMem WIC Silver® Non-adhesive. Dressings without silver, Atrauman®, Biatain® Alginate and PolyMem WIC, were also tested for control and comparison purposes. Disk diffusion and broth dilution were performed to evaluate antimicrobial susceptibility on *S. aureus*, *S. epidermidis*, *E. coli* and *P. aeruginosa* bacteria, which are among the most commonly encountered strains on chronic wounds (8,9). Herein, it was observed that two of the products, Atrauman ® Ag and PolyMem WIC Silver® Non-adhesive, induced a better antibacterial effect when surrounded by liquid medium than when placed on agar. This result indicates that for these two silver-containing dressings a moist environment is insufficient to induce the release of their antimicrobial active component(s). The antibacterial effect of Biatain® Alginate Ag was excellent in disk diffusion and broth dilution assays. This result can be ascribed to the highest level of impregnated silver and a probable quicker release of Ag^+ cations among the three dressings. In order to evaluate the cytocompatibility properties of the commercial wound dressings, CellTiter-Blue® assay was performed on 2D cell culture of fibroblasts, keratinocytes and monocyte-derived macrophages. Atrauman®, Atrauman® Ag and Biatain® Alginate showed excellent cytocompatibility results

in vitro. The same outcome was not observed for the remaining tested dressings, that induced a reduction of cell viability to approximately 70% or below.

Combining the antibacterial and cytocompatibility results, it becomes clear that the balance between antibacterial activity and cytotoxicity *in vitro* remains a significant challenge even for commercially-available and clinically-applied products. Experiments to determine macrophage polarization as a response of biomaterial-macrophage interactions within 24 hours were performed by flow cytometry, ELISA and glucose uptake measurements. The common response of M0 macrophages to all silver-impregnated dressings was an increase in the production of the anti-inflammatory cytokine TGF-β that indicates a polarization towards M2-like macrophages, more specifically associated with M2a and M2c subtypes (10). Moreover, the anti-inflammatory effect is certainly attributed to the presence of silver. For example, PolyMem WIC alone stimulates macrophages to have pro-inflammatory properties (non-significant but higher expression of $CD197^{+}$/$HLA\text{-}DR^{+}$ and significantly higher IL-1β concentration than M0) and tissue-healing characteristics, such as high production of IL-10 and TGF-β, leading to a dual effect. In the presence of nanocrystalline silver particles, the values of pro-inflammatory associated membrane markers and inflammatory cytokine were reduced. The anti-inflammatory properties of silver have been described in previous works (11,12).

Overall, main findings described in **chapter 2** were:

1) dressings behave differently depending on the experimental design;
2) macrophages start to change their metabolism and phenotype in response to wound dressings of different composition in a short time (one day);
3) a stronger anti-inflammatory stimulation is associated with the presence of silver;
4) silver-containing dressings trigger the shift to an anti-inflammatory environment.

In the future, it would be interesting to investigate the immunomodulatory effects of these same dressings on macrophages polarized to M1 pro-inflammatory state instead of M0 resting state macrophages, due to the fact, that in the wound environment this macrophage phenotype is predominant. Studies on monocytes isolated from donors' blood would also be a great addition, to have an *in vitro* set closer to human circumstances. Moreover, an experimental set with increasing incubation time – 24, 48, 72 hours and one week – for bacterial and cell culture methods is an option for future research.

In section 2 of the research experiments, from **chapter 3** on, the work was focussed on understanding the efficiency of new biomaterials in tackling drug-resistant bacteria and biofilms that are commonly found in non-healing wounds. The greatest challenge was to understand if these newly synthesized polymers are able to destroy bacteria without the usage of currently-used antibiotics, which is of great importance taking into consideration the antibiotic resistance problem. The hypothesis was that these biomaterials induce a bactericidal effect on antibiotic-resistant bacteria to the same extent as drug-sensitive microorganisms. The materials under scrutiny were new therapeutic polyurethanes which mimic the structural organization of antimicrobial peptides (AMPs). Generally, AMPs induce their antibacterial effect by acting on the bacterial membrane which is an attractive target, since different processes of membrane biogenesis, cell wall biosynthesis, and overall integrity are promising targets that have been described as less predisposed to induce bacterial resistance (13,14). However, AMPs still face a major challenge related to their high production costs, low scalability and complicated manufacturing procedure (15). The development of cationic amphipathic antimicrobial peptides-mimetic polymers is a stimulating alternate strategy to overcome the previously mentioned problems of natural or synthetic AMPs. One major advantage is the versatility offered by polymer chemistry that permits a wider exploration of chemical and structural features in order to optimize the antibacterial potency and biocompatibility properties. Taking all considerations into account, polyurethane (PU) was chosen as the basis for the synthesis of these AMP-biomimetic block copolymers that were built on the essential physiochemical properties of antimicrobial peptides - the cationic amphiphilic structure – which is the basis for the AMPs bactericidal mode of action (Purkayastha *et al*., unpublished). In fact, the structure consisting in the clustering of cationic hydrophilic and hydrophobic segments into distinct domains is responsible for the interaction of AMPs with the bacterial cytoplasmic membrane and further antibacterial activity (16).

Out of a library of newly synthesized AMP-mimicking PUs, the amphipathic polyurethane NHP407 grafted Poly(N,N,N,N-Butyldimethylmethacryloyloxyethylammonium bis(trifluoro-methanesulfonyl)imide with the hydrophilic anions of bromide as counter-ions [NHP407-g-Poly(ILM-Br)] proved to be extremely efficient in combating planktonic and biofilm-associated Gram-positive sensitive and drug-resistant bacteria of *S. aureus*, *S. epidermidis* and *E. faecalis*. The Gram-positive species methicillin-resistant *Staphylococcus aureus* (MRSA) and vancomycin-resistant *Enterococcus* spp. (VRE) were classified as serious threats by the Center for Disease Control and Prevention assessment report of current-antibacterial resistance threats due to the growing number of reported cases of resistance development to many common

antibiotics (17). Moreover, NHP407-g-Poly(ILM-Br) induces a bactericidal action to the same extent for methicillin-sensitive and -resistant *Staphylococcus aureus* bacteria, observed by the very similar minimal bactericidal concentrations (e.g. MBC_{MSSA}=10.4 μg/mL and MBC_{MRSA}=13 μg/mL). This is a very interesting achievement, since the dose of currently-used antibiotics must be increased from 2- to 3-fold magnitude in order to have an efficient antibacterial outcome against some drug-resistant bacteria, reducing the therapeutic window and consequently leading to toxicity concerns (18).

NHP407-g-Poly(ILM-Br) induced a rapid bactericidal effect on planktonic Gram-positive bacteria and it was able to prevent biofilm formation for a long period of time (72 hours). NHP407-g-Poly(ILM-Br) was prepared by anion exchange reaction on the polycation block of NHP407-g-Poly(ILM-TFMSI), which was synthesised by the grafting of ionic liquid monomers (ILM) from the polyurethane backbone (NHP407). Hence, the counter anions TFMSI of the ionic liquid block were exchanged for Br^-. Before ionic exchange, no antibacterial activity was observed in the pre-preparation with H_2O. Hence, it was clear that its antibacterial activity is generated by the ionic exchange from $N(CF_3SO_2)_2^-$ (TFMSI) counter ions to more hydrophilic ones – bromide anions, that dissociate to a higher extent in aqueous medium, exposing the positive charge of the polycation chain and allowing the interaction between the polymer and the bacterial surface. Moreover, it was registered that NHP407-g-Poly(ILM-Br), which forms colloidal particles in aqueous medium, had a better disruptive capacity on longer matured biofilms, showing that they are able to act on slow-growing Gram-positive bacteria. On L929 murine fibroblasts, HaCaT human keratinocytes and THP-1 monocyte-derived human macrophages, the cell viability was optimal in the presence of concentrations that are active against Staphylococcal bacteria (13 μg/mL). These results indicate that NHP407-g-Poly(ILM-Br) colloidal particles dispersion could be developed to a product that is easy to handle, being directly applied on the wound bed and having the potential to overcome the inability of currently-used therapeutics to reach the invading pathogenic bacteria in deep tissue layers.

In summary, main results described in **chapter 3** were:

1) NHP407-g-Poly(ILM-Br) was identified as a promising therapeutic polyurethane to combat Gram-positive bacteria;

2) the newly synthesized polymer is active against both sensitive and drug-resistant Gram-positive isolates at the same extent;

3) the indication that the efficient exposure of bioactive blocks (polycation chains) is extremely important for the antibacterial action;

4) NHP407-g-Poly(ILM-Br) induces its bactericidal action rapidly and is efficient in preventing biofilm formation of staphylococcal and enterococcal species.

Future studies should include scanning electron microscopy images showing the reduction of the biofilm biomass by the preventive and/or disruptive effect originated by the polymers. Also, conduction of skin permeation studies will be essential to determine the capacity of these colloidal particles to reach deeper tissues. These tests could be performed in artificial or reconstructed 3D skin models and *ex vivo* human or animal skin. Another aspect to be assessed is the *in vitro* haemolytic activity. Moreover, concerning biomaterial design, the cytocompatibility of the polymer could be enhanced by controlling the length of individual blocks to have an improved balance between the ability to kill desired bacteria and biocompatibility on eukaryotes. Once this objective is achieved, properly designed assays should be performed to understand if NHP407-g-Poly(ILM-Br) has immunomodulatory properties, similarly to many AMPs. Finally, studies on animal models with non-healing wounds should be carried out to prove their efficacy *in vivo*.

After having selected the most promising newly synthesized material [NHP407-g-Poly(ILM-Br)], the exploration of its mechanism of action was initiated through morphological characterization by scanning electron microscopy (SEM) and a combination of 2D gel-based and liquid chromatography–mass spectrometry (LC-MS)–based approaches (described in **chapter 4**). The polymer being an AMP-mimicking material, the intention of this study was to verify if PU particles are in fact inducing their bactericidal effect in a similar mode as AMPs'. SEM micrographs showed considerable morphological abnormalities of *S. aureus* surface after very short periods of contact with NHP407-g-Poly(ILM-Br) particles. The surface became extremely smooth, in some regions the cell wall seems to be unstable and protuberances were visualized. Remnants of bacteria were detected on the prepared samples, proving once again the rapid bactericidal activity of this PU system. For the first time, a well-established proteomic response reference platform using the Gram-positive model *Bacillus subtilis 168* was used to obtain indicative results concerning the mode of action exerted by NHP407-g-Poly(ILM-Br) block copolymer. This approach was revealed as a promising tool to gain preliminary indications about the mechanism of action of a completely new antibacterial polymer structure. The 13 upregulated marker proteins identified after treatment with NHP407-g-Poly(ILM-Br) were associated with different pathways or structures in *B. subtilis*, specifically: membrane and cell wall integrity (PspA, LiaH and RacX), energy metabolism (PdhA and YuJ), amino acids

biosynthesis (GltA, YhdR and YxjG), translation process (IleS and PheT), nucleotide synthesis (PupG) and sulfur metabolism (CysC). After analysing the function of each upregulated protein, and correlating their functions, it was possible to conclude that the AMP-biomimetic amphipathic polyurethane NHP407-g-Poly(ILM-Br) is inducing an alteration on the membrane and cell wall integrity, and it is impairing the respiration metabolism. The production of energy occurs on the bacterial membrane. Hence, the modification of membrane integrity affected the respiration metabolism.

Major findings described in **chapter 4** were:

1) a proteomic approach with the platform made with *B. subtilis* responses was successful in identifying the upregulated proteins, exposing the mechanisms of action of the cationic amphipathic polyurethane;

2) strong indications were obtained, that NHP407-g-Poly(ILM-Br) has the bacteria cell membrane as a main target, which is one of the most reported mechanism of action of antimicrobial peptides.

Additional experiments should be performed to confirm the mechanism of action of NHP407-g-Poly(ILM-Br). For example, transmission electron microscopy can be used to observe if pores are being formed on the membrane, membrane potential measurements by flow cytometry can be carried out to verify the disturbance of the cytoplasmic bacterial membrane, and ATP concentration measurements can corroborate evidence of the described energy impairment.

In **conclusion**, for an efficient treatment of chronic wounds, products applied should ideally have antibacterial activity against sensitive and drug-resistant strains, antibiofilm properties, rapid mode of action, avoid facilitated evolution of bacterial resistance mechanisms and have an immunomodulatory effect driving the wound environment to proliferation and remodelling stages. The newly synthesized AMP-biomimetic polyurethane NHP407-g-Poly(ILM-Br) turns out to be a promising candidate to fulfil all the described parameters.

References

1. Guo S, Dipietro LA. Factors affecting wound healing. J Dent Res. 2010;89(3):219–29.
2. Nunan R, Harding KG, Martin P. Clinical challenges of chronic wounds: searching for an optimal animal model to recapitulate their complexity. Dis Model Mech. 2014;7(11):1205–13.
3. Varela P, Sartori S, Viebahn R, Salber J, Ciardelli G. Macrophage immunomodulation: An indispensable tool to evaluate the performance of wound dressing biomaterials. J Appl Biomater Funct Mater. 2019;17(1):1–10.
4. Zhao G, Usui ML, Lippman SI, James GA, Stewart PS, Fleckman P, et al. Biofilms and Inflammation in Chronic Wounds. Adv Wound Care. 2013;2(7):389–99.
5. Bowler PG. Antibiotic resistance and biofilm tolerance: a combined threat in the treatment of chronic infections. J Wound Care. 2018;27(5):273–7.
6. Brancato SK, Albina JE. Wound macrophages as key regulators of repair: Origin, phenotype, and function. Am J Pathol. 2011;178(1):19–25.
7. Witherel CE, Graney PL, Freytes DO, Weingarten MS, Spiller KL. Response of human macrophages to wound matrices in vitro. Wound Repair Regen. 2016;24(3):514–24.
8. Gjødsbøl K, Christensen JJ, Karlsmark T, Jørgensen B, Klein BM, Krogfelt KA. Multiple bacterial species reside in chronic wounds: A longitudinal study. Int Wound J. 2006;3(3):225–31.
9. Kirketerp-Møller K, Jensen PØ, Fazli M, Madsen KG, Pedersen J, Moser C, et al. Distribution, Organization, and Ecology of Bacteria in Chronic Wounds. J Clin Microbiol. 2008;46(8):2717–22.
10. Ferrante CJ, Leibovich SJ. Regulation of Macrophage Polarization and Wound Healing. Adv Wound Care. 2012;1(1):10–6.
11. Tsang K-K, Kwong EW-Y, Woo KY, To TS-S, Chung JW-Y, Wong TK-S. The Anti-Inflammatory and Antibacterial Action of Nanocrystalline Silver and Manuka Honey on the Molecular Alternation of Diabetic Foot Ulcer: A Comprehensive Literature Review. Evidence-Based Complement Altern Med. 2015;2015:1–19.
12. Seethalakshmi S AMK. Evaluation of In-vitro Anti-Inflammatory Activity of Silver Nanoparticles Synthesised using Piper Nigrum Extract. J Nanomed Nanotechnol. 2015;6(268).
13. Hurdle JG, O'Neill AJ, Chopra I, Lee RE. Targeting bacterial membrane function: An underexploited mechanism for treating persistent infections. Nat Rev Microbiol. 2011;9(1):62–75.
14. Wenzel M. Bacterial response to membrane - active peptide antibiotics. Ruhr University Bochum; 2013.
15. Kang S-J, Park SJ, Mishig-Ochir T, Lee B-J. Antimicrobial peptides: therapeutic potentials. Expert Rev Anti Infect Ther. 2014;12(12):1477–86.
16. Zasloff M. Antimicrobial peptides of multicellular organisms. Nature. 2002;415(6870):389–95.
17. United States Centers for Disease Control. Antibiotic resistance threats in the United

States, 2013. Current. 2013;

18. Fair RJ, Tor Y. Antibiotics and bacterial resistance in the 21st century. Perspect Medicin Chem. 2014;6:25–64.

APPENDIX

PhD candidate information:
List of publications and communications in conferences

1. PhD CANDIDATE BACKGROUND

PERSONAL INFORMATION	**Name:** Patrícia Varela **Date of birth:** 06/07/1988 **City of birth:** Guimarães **Nationality:** Portuguese	
ACADEMIC FORMATION	**Master's degree in Cell Biology and Biotechnology** Faculty of Sciences – University of Lisbon (2010-2012) **Master's Thesis** Institute for Molecular and Cell Biology (IBMC) 'Drug screening of Bisnaphthalimidopropyl derivatives on *Trypanosoma brucei*' **Bachelor's degree in Biology** University of Trás-os-Montes e Alto Douro (2007-2010) **Bachelor's Thesis** 'Study of phenotypic resistance to antibiotics of Gram-negative bacilli isolated from mackerel (*Trachurus trachurus*)'	
PROFESSIONAL EXPERIENCE	**Internship in Microbiology and Infection Research Domain (January to October 2015)** 'Metabolic reprogramming of Macrophages: Implications on Immunity and Immunotherapeutic approaches'	ICVS Life and Health Sciences Institute
	National Recycling Campaign 'Missão Reciclar' (January to December 2014) Media and door to door campaign to teach the population to recycle and to obtain data for a statistical study.	Sociedade Ponto Verde
	FCT Research fellowship (March to October 2013) 'Development of new drug delivery systems based on bisnaphthalimidopropyl derivative compounds liposomal formulation for pancreatic cancer and leishmaniasis drug therapy'	*Parasite Disease* group; IBMC

2. PUBLICATIONS DURING THE PhD PERIOD

- Varela, P., Sartori, S., Viebahn, R., Salber, J. & Ciardelli, G. (2019) 'Macrophage immunomodulation: An indispensable tool to evaluate the performance of wound dressing biomaterials' Journal of Applied Biomaterials & Functional Materials
  DOI: 10.1177/2280800019830355

- Tonda-Turo, C., Ruini, F., Ceresa, C., Gentile, P., Varela, P., Ferreira, AM., Fracchia, L. & Ciardelli, G. (2018) 'Nanostructured scaffold with biomimetic and antibacterial properties for wound healing produced by 'green electrospinning' Colloids Surface B Biointerfaces DOI: 10.1016/j.colsurfb.2018.08.039

- Varela, P.*, Idrees, A*., Ruini, F.*, Vasquez, J.*, Salber, J., Greiser, U., Wang, W., McMahon, S., Sartori, S., Ciardelli, G. & Chiono, V. (2018) 'Drug-free antibacterial polymers for biomedical applications' Biomedical Science and Engineering
  DOI: 10.4081/bse.2018.39
  *authors contributed equally

3. COMMUNICATIONS IN CONFERENCES DURING THE PhD PERIOD

Oral presentations

- Purkayastha, S., Varela, P., Ranzato, E., Sartori, S. & Ciardelli, G. 'Novel polyurethanes mimics of antimicrobial peptides' Congresso Biomateriali - SIB 2016

- Varela, P., Purkayastha, S., Boffito, M., Sartori, S.; Salber, J. & Ciardelli, G. 'Functional mimetics of antimicrobial peptides: Novel amphipathic polyurethane to combat Gram-positive bacteria' Congresso Biomateriali - SIB 2017

- Purkayastha, S.*, Varela, P.*, Boffito, M., Ceresa, C., Sartori, S., Fracchia, L., Salber, J. & Ciardelli, G. 'Novel amphipathic antimicrobial polyurethanes: Design and development of new biomaterials with intrinsic antimicrobial properties' European Chapter Meeting of the Tissue Engineering and Regenerative Medicine International Society – TERMIS 2017
  *authors contributed equally

- **Varela, P.**, Purkayastha, S., Boffito, M., Marlinghaus, L., Sartori, S., Viebahn, R., Ciardelli, G. & Salber, J. 'Novel Amphipathic Polyurethane based Colloidal Dispersions to Combat Gram-positive bacteria' German Society for Biomaterials - DGBM 2017

- Purkayastha, S., Varela, P., Boffito, M., Viebahn, R., Wang, W., Sartori, S., Salber, J. & Ciardelli, G. 'Polyurethane Colloidal Particles Mimicking Antimicrobial Peptides' Europolymer Conferences - EUPOC 2018

- Purkayastha, S., Varela, P., Boffito, M., Viebahn, R., Wang, W., Sartori, S., Salber, J. & Ciardelli, G. 'Core-shell switchable thermoresponsive polyurethane based colloidal particles with intrinsic antibacterial properties' Europolymer Conferences - EUPOC 2018

- **Varela, P.**, Purkayastha, S., Boffito, M., Sartori, S., Viebahn, R., Ciardelli, G. & Salber, J. 'Biomimetic Nanostructured Polyurethane-based Patchy Colloidal Particles to Combat Biofilm and Planktonic Drug-resistant Bacteria' European Society for Biomaterials - ESB 2018

- Purkayastha, S., Varela, P., Vasquez, J., Idrees, A., Sartori, S., Mcmahon, S., Greiser, U., Viebahn, R., Wang, W., Salber, J., Chiono, V. & Ciardelli, G. 'Antibacterial synthetic polymers' European Society for Biomaterials - ESB 2018

- Purkayastha, S., Varela, P., Vasquez, J., Idrees, A., Sartori, S., Mcmahon, S., Greiser, U., Viebahn, R., Wang, W., Salber, J., Chiono, V. & Ciardelli, G. 'Biomimetic Strategies in the Design of Antibacterial Synthetic Polymers' Drug-Free Antibacterial Technology for Medical Applications - First Cambridge International Conference of HyMedPoly 2018

Poster presentations

- **Varela, P**., Sartori, S., Ranzato, E., Fracchia, L., Salber, J. & Ciardelli, G. 'Antibacterial evaluation of polymers' PhD day of Politecnico di Torino 2016

- **Varela, P.**, Purkayastha, S., Boffito, M., Sartori, S., Viebahn, R., Salber, J. & Ciardelli, G. 'Biological evaluation of Biomimetic Polyurethane-grafted Poly(ionic liquid) Bromide patchy colloidal particles to combat antibiotic-resistant Staphylococci bacteria' ESR 15 European Society for Biomaterials - ESB 2018

- Kaya, S., Idrees, A., Varela, P., Salber, J., Cresswell, M., Sartori, S., Boffito, M., Chiono, V., Ciardelli, G., Goldmann, W. & Boccaccini, A. 'Synthesis and characterization of novel antibacterial mesoporous silicate bioactive glass/polymer films as wound dressings' European Society for Biomaterials - ESB 2018

- Purkayastha, S., Varela, P., Boffito, M., Viebahn, R., Salber, J., Sartori, S., Wang, W. & Ciardelli, G. 'Antimicrobial Peptide Mimetic Polyurethane Grafted Poly(Ionic liquid) Based Patchy Colloidal Particles To Combat Drug Resistant Bacteria ESR 2' European Society for Biomaterials 2018 - ESB 2018

- Kaya, S., Varela, P., Salber, J., Cresswell, M., Boffito, M., Chiono, V., Ciardelli, G. & Boccaccini, A. 'Antibacterial mesoporous bioactive glass poly(ether-urethane) composites for wound healing-ESR7' European Society for Biomaterials - ESB 2018

- **Varela, P.**, Purkayastha, S., Boffito, M., Sartori, S., Viebahn, R., Salber, J. & Ciardelli, G. 'Biological evaluation of Biomimetic Polyurethane-grafted Poly(ionic liquid) Bromide patchy colloidal particles to combat antibiotic-resistant Staphylococci bacteria (ESR 15)' Drug-Free Antibacterial Technology for Medical Applications - First Cambridge International Conference of HyMedPoly 2018

- Purkayastha, S., Varela, P., Boffito, M., Viebahn, R., Salber, J., Sartori, S., Wang, W. & Ciardelli, G. 'Antimicrobial peptide mimetic polyurethane grafted poly(ionic liquid) based patchy colloidal particles to combat drug resistant bacteria (ESR 2)' Drug-Free

Antibacterial Technology for Medical Applications - First Cambridge International Conference of HyMedPoly 2018